

THE PETROGRAPHY, GEOCHEMISTRY,  
AND PETROGENESIS OF TWO GRANITE  
SUITES, CHURCHILL PROVINCE,  
THEKULTHILI LAKE, N.W.T.

THE PETROGRAPHY, GEOCHEMISTRY,  
AND PETROGENESIS OF TWO GRANITE  
SUITES, CHURCHILL PROVINCE,  
THEKULTHILI LAKE, N.W.T.

by

D. Keith MacDonald

A Research Paper  
Submitted to the Department of Geology  
in Partial Fulfillment of the Requirements  
for the Degree  
Honours Bachelor of Science

McMaster University

April, 1980

BACHELOR OF SCIENCE (1980)  
(Geology)

McMASTER UNIVERSITY  
Hamilton, Ontario

TITLE: The Petrography, Geochemistry, and Petrogenesis of two  
Granite Suites, Churchill Province, Thekulthili Lake, N.W.T.

AUTHOR: D. Keith MacDonald

SUPERVISOR: Dr. R. H. McNutt

NUMBER OF PAGES: x; 117

SCOPE AND CONTENTS:

A petrographic and geochemical analysis has been carried out on two granite suites with contrasting morphologies and field relations. Included is a discussion of their age relationships relative to the Nonacho Series supracrustal sequence. The respective petrographic and petrochemical features of the two granitoids is given; followed by a comparison of the two, and a discussion on their modes of petrogenetic evolution. Petrographic descriptions of selected Nonacho supplement the granitoid study.

Analytical methods and a discussion of the results are included.

"There are granites and granites ..."

(Read, 1948 in "The Granite  
Controversy," Murby, London, 1957)

## ACKNOWLEDGEMENTS

The author would initially like to thank PNC (Power reactor and Nuclear fuel Development Corporation) Exploration (Canada) Co. Ltd. for granting permission for the collection of samples on their properties, in the summer of 1979. As well as their financial assistance for sample freight charges was greatly appreciated. I would also like to thank Mr. M. Houle and Mr. H. Miyada (of PNC) for their knowledgeable interpretations and assistance in the collection of samples.

I would particularly like to thank Dr. R. H. McNutt for his invaluable guidance and understanding in the supervision of this thesis. And also Dr. D. Mohr, some of whose interpretations were incorporated into the thesis.

The author also expresses thanks to Mr. L. Zwicker for preparation of thin sections; Mr. O. Mudroch for his instructive assistance in the preparation and running of samples for geochemical analysis; and Mr. J. Whorwood, Ms. D. Hunter and Mr. D. Rees for their assistance in preparation of photomicrographs.

Special thanks go out to my parents for their support and helpfulness in rewriting chaotic first drafts, and especially my sister, Mrs. Charlene Duggan whose striving for perfection in the typing of this manuscript was greatly appreciated.

Last but not least, I wish to thank the graduating geology class of 1980 (i.e. this decades geological future), in particular Mr. E. E. Meszaros, who never at any time let the author take his thesis deadline for granite.

## TABLE OF CONTENTS

	PAGE	
CHAPTER I	INTRODUCTION	1
	1. Location and Accessibility	1
	2. Previous Work	1
	3. Statement of Problem	4
CHAPTER II	REGIONAL TOPOGRAPHY AND GEOLOGY	8
	1. Regional Topography and Vegetation	8
	2. Regional Geology	8
	a) Supracrustal Rocks	10
	b) Basement Rocks	12
	c) Intrusive Granite Pluton	13
	d) Diabase Dykes	14
	3. Structural Geology	15
	4. Age Relationships	17
	5. Method of Sampling	20
CHAPTER III	PETROGRAPHY	25
	1. Introduction	25
	2. Basement Granites	29
	a) Essential Minerals	29
	b) Accessory Minerals	30
	c) Textures	30
	3. Intrusive Plutonic Granite	33
	a) Essential Minerals	33
	b) Accessory Minerals	35
	c) Textures	37
	4. Granite Dykes (Aplites)	40
	a) Sample Al-b (Monzogranite)	42
	b) Sample YD-1 (Syenogranite)	42

	PAGE
5. Argillaceous Nonacho Sediments	44
a) Samples from the Argillite Proper	44
b) Argillite Xenolith (sample ARG-LENS)	47
6. Other Nonacho Series Sediments	48
CHAPTER IV      GEOCHEMISTRY AND PETROGENETIC INTERPRETATIONS	51
1. Analytical Methods	51
2. Chemical Variation Diagrams	52
3. Major Elements	53
a) Linear Variation Diagrams	53
b) Ternary Variation Diagrams	62
4. Trace Elements	69
5. Significance of the migmatite-granite association	80
Anatexis	81
6. Hypersolvus and Subsolvus Granites and the Orthoclase to Microcline Transformation	84
7. Significance of Myrmekite in Basement Granites	86
8. Significance of K-Feldspar megacrysts and Synneusis Relationships in the Younger Granite	87
9. Deuteric Alteration and Metasomatic Relationships of the Younger Granite	89
10. Contact Metamorphism	91
CHAPTER V      CONCLUSIONS	92
REFERENCES	94
APPENDIX A      PETROGRAPHIC DESCRIPTIONS OF TEN NONACHO GROUP SEDIMENTS	99
APPENDIX B      MESONORM TABLES	106

	PAGE
APPENDIX C	
GEOCHEMICAL WHOLE ROCK DATA	108
Accuracy of XRF Determinations	109
1. Major Oxides (Fusion Method)	109
2. Trace Elements (Powder Method)	109

## LIST OF TABLES

TABLE		PAGE
I	Geologic History of the Thekulthili Lake Area	21
II	Salients Petrographic Features of the Granite Suites	41
III	Mesonorms	107
IV	Major Element Whole Rock Analyses	113
V	Trace Element Analyses (P.P.M.)	114
VI	Trace Element Analyses (P.P.M.)	115
VII	Trace Element Analyses (P.P.M.)	116
VIII	Element Ratios Based on P.P.M.	117

## LIST OF FIGURES

FIGURE		PAGE
1	General Location Map	2
2	Expanded Location Map	2
3	Granitic Dyke (Aplite) cutting an argillaceous unit.	6
4	Deformation effects in the argillite	6
5	Argillaceous xenoliths	7
6	Fault contact unconformity	7
7	Regional geology and sample location map	9
8	Expanded sample location map, west shore of Thekulthili Lake	22
9	Expanded sample location map, south-central Thekulthili Lake.	22
10	Expanded sample location map, east shore of Thekulthili Lake	23
11	Quartz-Alkali feldspar-Plagioclase diagram	27
12	Quartz-Total Feldspar-Total Mafic Diagram	28
13	Photomicrograph of unstrained quartz and microcline-micropertthite in basement granite	31
14	Photomicrograph of allotriomorphic granular texture of basement granite.	32
15	Photomicrograph of myrmekitic intergrowths in basement granite	34
16	Photomicrograph of porphyritic texture in the younger granite	36
17	Photomicrograph of biotite and accessory minerals in younger granite	38
18	Photomicrograph showing synneusis structure	38
19	Photomicrograph of aplitic texture in a granite dyke	43
20	Photomicrograph of hornblende in argillite	46
21	Photomicrograph of biotite in argillite	46
22	Photomicrograph of argillaceous xenolith	49
23	Weight % SiO <sub>2</sub> vs alkalinity ratio	55
24	Mafic Index vs Alkalinity Ratio	56
25	Felsic Index vs Mafic Index	57
26	Biotite Mg/Fe percent Ratio vs Mafic Index	59
27	Weight % Ti and P vs Modified Larsen Index	60
28	Weight % Si vs Modified Larsen Index	61
29	K-Na-Ca ternary diagram	63
30	Qtz-Ab-Or ternary diagram	65
31-a	Qtz-Ab-Or ternary diagram with variable Ab/An ratios	68
31-b	An-Ab-Or ternary diagram	68

## FIGURE

## PAGE

32	Rb vs Sr	73
33	Wt.% K vs Rb ppm.	74
34	Ba vs Rb	75
35	Rb-Ba-Sr ternary diagram	77
36	Wt. % Ti vs Zr ppm.	79

CHAPTER I  
INTRODUCTION

1. Location and Accessibility

The study area (Figures 1 and 2) is located near the southern reaches of Thekulthili Lake N.W.T. approximately 100 miles northeast of Fort Smith, at approximately  $61^{\circ}\text{N}$  latitude and  $110^{\circ}\text{W}$  longitude. This region represents the southern most extent of the Nonacho Group sedimentary basin, which lies within the Churchill Province of the Precambrian shield. The region most extensively studied here covers an area of approximately 25 km (east to west) by 10km (north to south), or roughly 250 sq. km. (Figure 2). Four interconnecting Geological Survey of Canada reconnaissance maps cover the study area, these are 1) 75E/1, 2) 75F/4, 3) 75D/16 and 4) 75C/13; authors of these maps are listed in Figure 2.

This region is virtually uninhabited and is accessible only by float equipped airplanes or helicopter.

2. Previous Work

Geological studies in this area were initiated by Henderson in 1937. Following that field season he published the Taltson Lake and Nonacho Lake reconnaissance maps in GSC Preliminary Report 37-2. Subsequently Wilson (1941) mapped the Fort Smith map area, which was followed by mapping of the Hill Island Lake map area in 1954 by Mulligan and Taylor (1969).

Figure 1      General location map. Showing position of thesis area in the Churchill Province of the Precambrian shield. (Base map after Baadsgaard and Godfrey, 1972)

Figure 2      Expanded location map showing latitude-longitude position of thesis area. The four reconnaissance maps which adjoin at Thekulthili Lake are also given.

Map areas:

1. Taltson Lake (Henderson, 1937)
2. Nonacho Lake (Henderson, 1937)
3. Fort Smith (Wilson, 1941)
4. Hill Island Lake (Mulligan and Taylor, 1969)

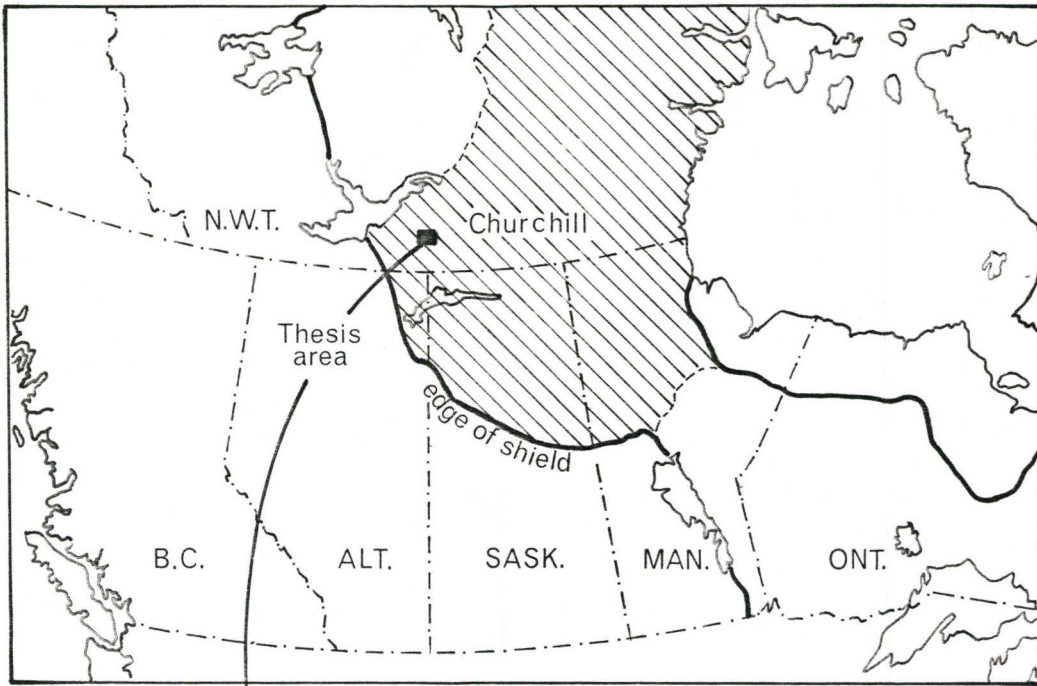


FIGURE 1

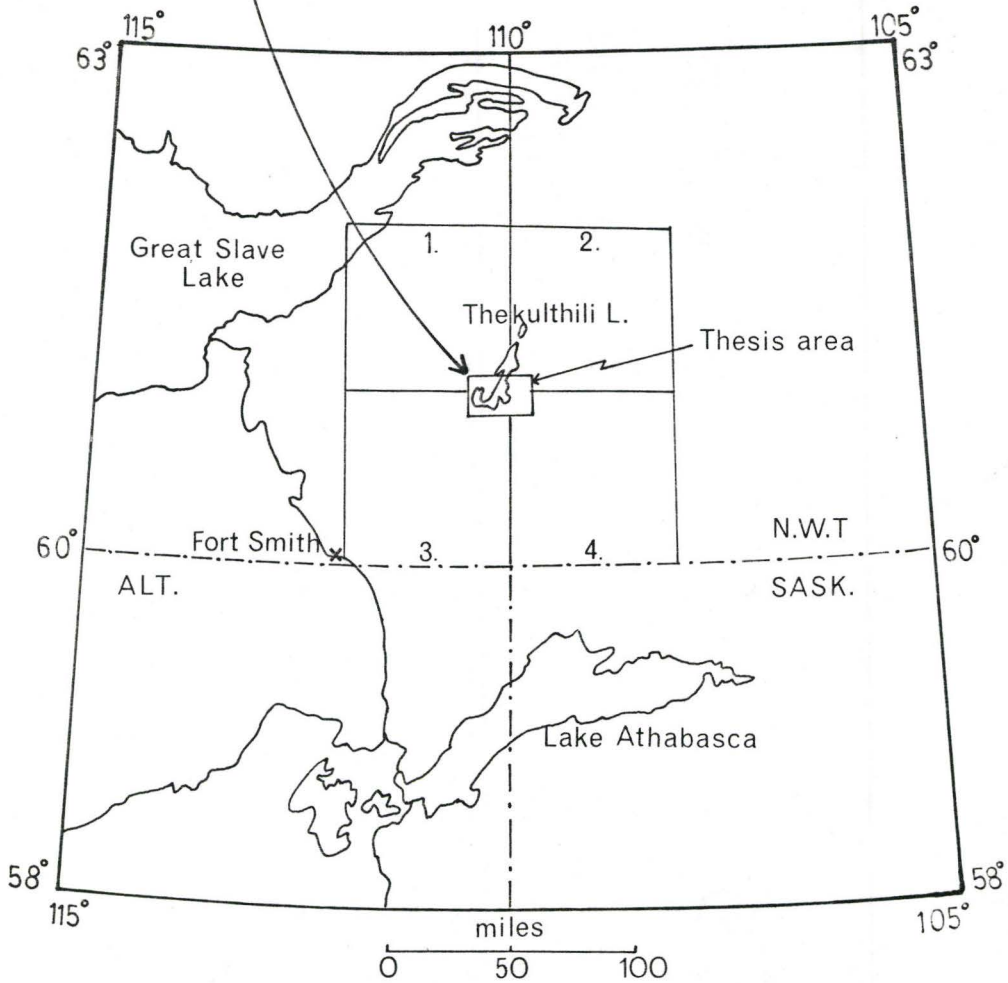


FIGURE 2

Henderson (1937) noted that along the east shore of Thekulthili Lake, Nonacho Gp. sediments showed both unconformable and intrusive relations with "older granitic intrusives" and "younger granitic intrusives" respectively. He concluded that "Nonacho sediments rest unconformably on an older granite and are intruded by a younger granite." Henderson's 1937 map shows the majority of the "younger" granite intrusive outcropping on the west shore of Thekulthili, while the "older" granite intrusive sits on the south and east shores.

In 1958 Burwash (Burwash and Baadsgaard, 1962) traversed the east-shore contact, and sampled the "older" and "younger" granitic rocks previously mapped by Henderson (1937), as well as some Nonacho Gp. sediments for K-Ar dating. Of the six dates obtained, two ages were evident; those for the "younger" granites ranged from 1790-1850 m.y. while the "older" granites had an age between 2260 and 2420 m.y.

More recently (1966-1978) extensive work in the area has been done by McGlynn. His work has concentrated on the geologic mapping and age dating of Nonacho Gp. sediments and their adjacent plutonic rocks. McGlynn (1978) recently completed a reconnaissance mapping of the Nonacho Gp. sedimentary basin, at the scale of 1:50,000. McGlynn's study of the peripheral plutonic rocks led him to a conclusion in opposition to previous authors, McGlynn (1971) states:

Evidence from contact areas on both sides of the basin indicate that all plutonic rocks in contact with Nonacho strata are older and therefore part of the basement in which the

sediments were deposited. Commonly along the western margins of the basin evidence of unconformity has been destroyed or obscured by faulting.

A petrologic study of the Thekulthili Lake area was carried out by Thomas Donaghy (University of Alberta, Msc. thesis) from 1975-1977. Much of Donaghy's thesis area covered the same area studied by the author.

PNC (Power Reactor and Nuclear Fuel Development Corporation) Exploration (Canada) Co. Ltd. has been involved in an ongoing uranium exploration project in the Thekulthili Lake Area since 1977.

### 3. Statement of Problem

In the summer of 1979 the author was employed by PNC Exploration (Canada) and involved with their uranium exploration project. During the survey it became apparent that two morphologically different "basement" granites occur. To the west of the Nonacho basin, granites appear as a massive, homogeneous, coarse grained leucocratic body; while the scattered granite and migmatite bodies to the east are finer grained, weak to moderately foliated and interlayered with other lithologies (particularly amphibolites and paragneisses).

Besides its morphological and spatial differences, it is clear to the author that the leucocratic body west of Thekulthili Lake is an intrusive granite pluton. Field relations verifying this include:

- 1) Several granitic dykes (aplites) seen discordantly trans-

ecting an argillaceous unit in contact with the granite. One such dyke is shown in Figure 3.

- 2) Intense deformation of the incompetent argillaceous unit, particularly at the contact with the pluton. Bedding in the argillite strikes approximately north-south and dips nearly vertical. Figure 4 shows the argillite deformed into a vertical fold.
- 3) Xenoliths of the argillite, found as enclaves within the pluton near the contact (Figure 5).
- 4) The baked appearance of the adjacent argillaceous unit.

None of the above relations are seen to occur between Nonacho sediments and plutonic rocks on the south and east shores of Thekulthili Lake. Contacts there are gradational on the most part, less commonly they are sharp and distinctly unconformable. A sharp contact is shown in Figure 6, and may be the result of basement faulting prior to deposition of Nonacho sediments.

In order to accompany and perhaps further substantiate field relation differences a sample study was undertaken. Approximately thirty samples were collected from both the eastern and western granitic bodies, of these nineteen were selected for a detailed geochemical and petrographic analysis. Furthermore a petrographic analysis of some Nonacho Gp. sediments was initiated to determine differences in metamorphic features, adjacent to the western granite and eastern granites and gneisses respectively (see Figure 7 for sample location map).

Figure 3

Showing a granitic dyke (aplite) cutting across an argillaceous unit on the west shore of Thekulthili. Strike of the argillite is NS (left to right), and the dyke is trending eastward into the lake. Hammer (12" long) for scale.

Figure 4

Showing deformation of the argillite. This is an oblique view of a vertical fold in the unit. Notice the numerous quartz veins and the aplite (above hammer) which are also folded and shear fractured.

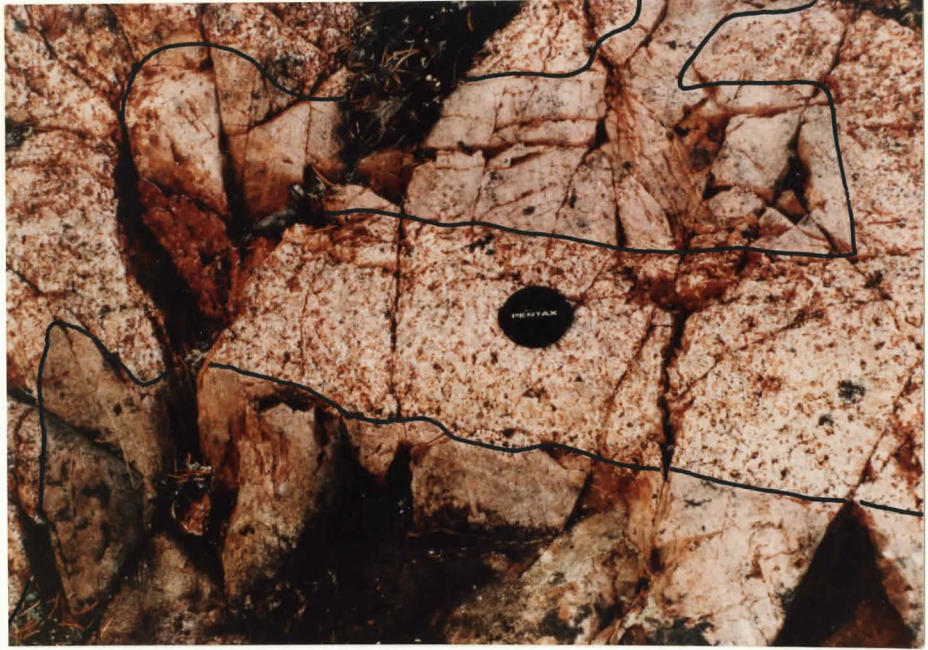


Figure 5

Two argillaceous xenoliths (outlined in black) found in the younger intrusive granite. Lens cap for scale.

Figure 6

Showing a fault contact unconformity from the east shore of Thekulthili Lake. The scintillometer (10" long) sits on the contact which separates an undeformed Nonacho Gp. sandstone (left) from granitic basement rock (right).



CHAPTER II  
REGIONAL TOPOGRAPHY AND GEOLOGY

1. Regional Topography and Vegetation

There is a general gradation in topography from northern Saskatchewan to the Northwest Territories. The trend is towards a more rugged terrain with gently rolling hills and a thin to non-existent regolith. There is a significant increase in the number of lakes and muskeg towards the north. Approximately 40% of the study area is covered by water. Many lakes are enclosed in elongate valleys which are structurally (fault) controlled, and gouged out by glaciation processes. Further evidence for glaciation is denoted by large whale-back forms and Roche Moutonee, which indicate a southward ice flow direction. Glacial Striae on outcrops are quite consistently oriented towards  $220^{\circ}$ .

Subarctic vegetation covers about 60% of the region and is predominated by mosses, lichen and various coniferous trees. Some low lying soil covered valleys contain birch, particularly in areas adjacent to small creeks.

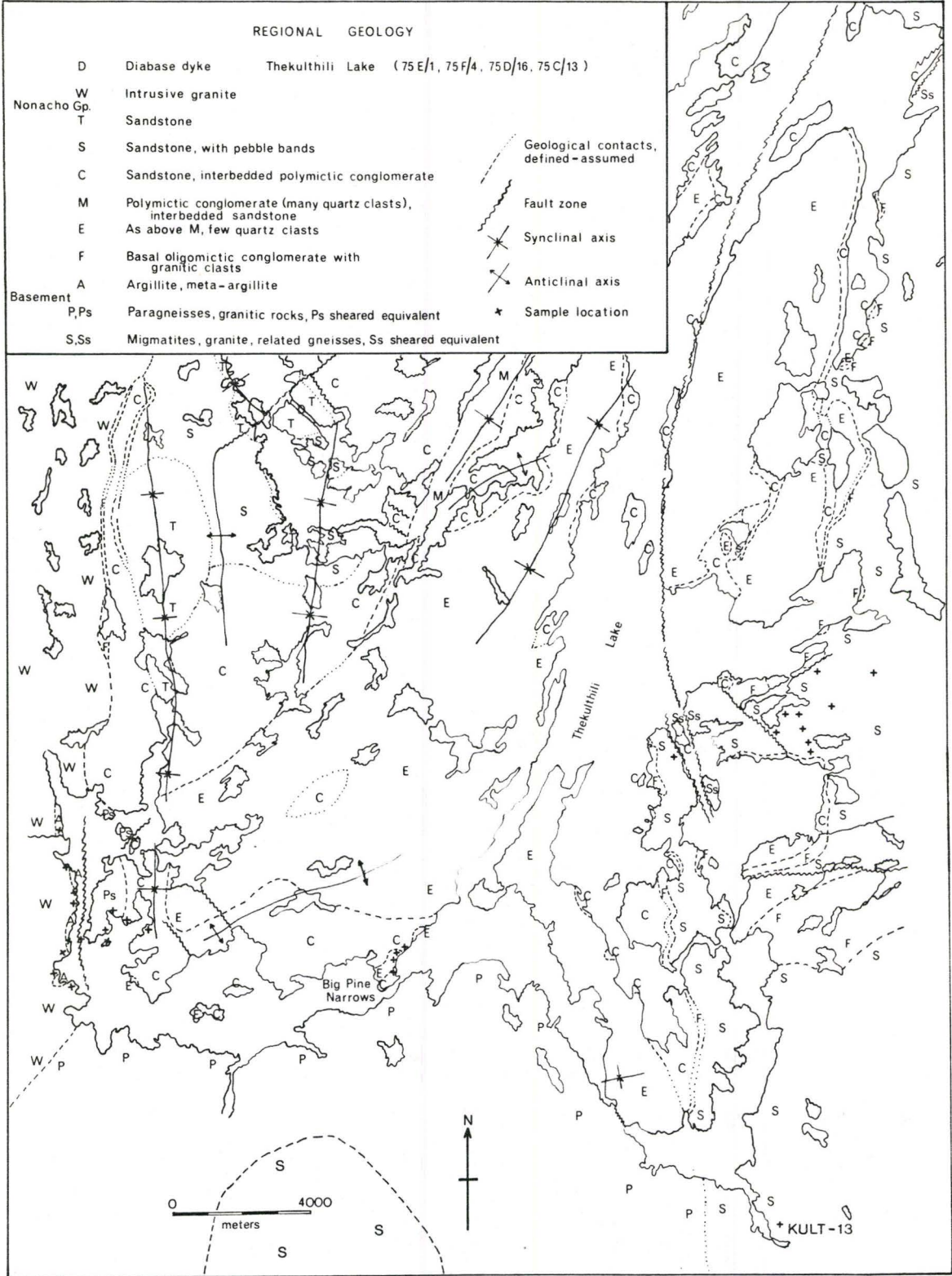
Outcrop exposure in this part of the N.W.T. is approximately 25% with glacially polished hills and ridges having elevations up to 400 feet.

2. Regional Geology

Figure 7 shows the regional geology of the Thekulthili Lake area at the scale of 1:125,000. This map shows the basic geology

Figure 7

Regional geology and sample location map. Showing the geology of the Nonacho Basin in the Thekulthili Lake area, which encompasses portions of the GSC map areas 75E/1, 75F/4, 75D/16, and 75C/13. Geology after J.C. McGlynn (GSC) and G. Crooker (formerly of PNC Exploration) with additions by the author.



as determined by J.C. McGlynn (1978) of the GSC and G. Crooker (1978), formerly of PNC Exploration (Canada) Ltd. Some additions and deletions have been made by the author. The component parts of the geology are discussed below.

a) Supracrustal Rocks

The Nonacho Gp. sedimentary basin has an elongated NE trend. It is approximately 160 Km. long, and has a maximum width of about 30 Km. The Thekulthili Lake study area occupies the southern reaches of the basin. Nonacho Series stratigraphy rests unconformably on Archean igneous and metamorphic rocks, which outcrop to the south and east of the basin. McGlynn (1971) describes the series as a conformable sequence of essentially unmetamorphosed to weakly metamorphosed clastic sediments. Outcrop distribution of Nonacho units is very complex, there are many places where beds pinch out, contacts are obscured by faulting, or portions of the sequence are missing entirely. As a result the overall depositional sequence has never been deciphered conclusively (McGlynn, 1978). However the following unit descriptions are considered to be in at least partial chronologic order, based on the authors knowledge of the basin stratigraphy.

Figure 7 outlines the aerial distribution of Nonacho Gp. sediments in the Thekulthili Lake area, a synthesized field description of each unit is given below.

Unit T:

A grey to pink feldspathic sandstone or greywacke with minor interbeds of siltstones and shales.

Unit S:

Predominantly greywackes or feldspathic sandstones rarely containing thin pebble horizons.

Unit C:

Feldspathic sandstones (or arkoses) and greywackes with interbeds of polymictic conglomerate. May contain oligomictic conglomerate near the base.

Unit M:

Polymictic conglomerate containing many fining-upward cycles, eventually grades into interbedded sandstones near the top. Quartzite clasts predominate in the conglomerate.

Unit E:

Essentially identical to Unit M but other clast lithologies predominate over quartzite clasts. This unit is much more common than Unit M in the Thekulthili Lake area.

Unit F:

This is the most common unit to rest unconformably on Archean basement rocks. It consists of a basal oligomictic conglomerate (or breccia in fault zones) with cobble sized clasts of basement granitic rock (up to 15 cm. and more), grading into a coarse arkosic sandstone.

Unit A:

This unit was described as an argillite in the field due to its dark colour and aphanitic grain size. It was only observed outcropping on the west shore of Thekulthili Lake.

Bedding planes within or between units are often obscured in

this area of the basin, it is presumed that bedding is frequently massive and contacts between facies are often gradational. Missing sections of units, and the great variability in outcrop widths is likely a result of spatial variations in deposition, variations in dip, and differential erosion of the basin. As a result, individual unit thicknesses, and the thickness of the entire sedimentary sequence is very difficult to establish, although Burwash and Baadsgaard (1962) estimate a total thickness of 3,000 M. or more.

b) Basement Rocks

The oldest rocks in the area are the Archean granitic complexes which outcrop south and east of the basin (P and S in Figure 7), and underly the Nonacho Series. This basement complex is composed of paragneiss, granitic gneiss, migmatites, and massive to slightly foliated granitic rocks (McGlynn 1967, 1970, 1971). Bands of amphibolite and metagabbro occur within the granitoid rocks (McGlynn, 1971), less commonly altered mica-schists are found as well. Gneissic banding ranges from 10's of centimeters to several meters or more. Paragneisses occur predominantly south of Thekulthili Lake and grade laterally into other rocks of the basement complex (see Figure 7). Near fault zones brecciated gneiss and porphyroblastic or flaser gneiss occurs (McGlynn, 1971, 1978).

While mapping the Fort Smith, N.W.T. area (area 3, Figure 2), Wilson (1941) described gneissic rocks south of Thekulthili Lake as equivalent to the Tazin Group of NW Saskatchewan. Krupicka and Sassano (1972) describe the Tazin Gp. north of Lake Athabasca, Saskatchewan, as an Archean to Aphebian age complex of amphibolite,

paragneiss, paraschist, and granitic gneiss, containing a high proportion of cataclastic rocks. The Tazin Gp. of high-grade metamorphic rocks (amphibolite facies assemblages) are believed to derive from metamorphism of a supracrustal and minor plutonic igneous rock assemblage (Krupicka and Sassano, 1972; Christie, 1953). Tazin Gp. rocks extend from Saskatchewan to an area east of Thekulthili Lake (Donaghy, 1977).

Baadsgaard and Godfrey (1972) have described and dated similar basement rocks approximately 120 Km. south of Thekulthili Lake in the extreme NE corner of Alberta.

Thus it appears quite viable that basement rocks surrounding Thekulthili Lake are, at least in part, cogenetically related to Archean rocks elsewhere in the Churchill Province.

#### c) Intrusive Granite Pluton

This granitic body is designated as Unit W in Figure 7. It is clearly intrusive in nature with respect to field relations with the adjacent Nonacho stratigraphy (see Chapter I). Consequently the pluton is younger than both the Archean basement rocks and the Nonacho Series sediments.

Henderson (1939) originally mapped the pluton as an elongate body bordering, and partially truncating the western fringes of the Nonacho Basin. It extends 115 Km NE (parallel to the basin) from the SW corner of Thekulthili Lake, gaining a maximum width of 15 Km. Smaller, scattered intrusions outcropping on the eastern margin of the basin are shown on Henderson's 1939 map, although these were not seen during the present study.

The western pluton is composed of massive pink-red, leucocratic,

coarse grained granitic material. Grain sizes approach pegmatite proportions (3 cm. or larger) in some localities. The most abundant mineral is a red potassium feldspar commonly found as megacrysts up to 7 cm. long. Substantial amounts of quartz and plagioclase are also seen in hand specimen. Total feldspar content is 60 to 70%. The only mafic mineral recognized is an altered biotite which occurs in patches throughout the rock. Biotite composes up to 5% of the rock and has trace amounts of pyrite associated with it.

Fine grained granitic dykes (aplites), which emanate from the pluton in an eastward direction, are subvertical and range in thickness from several centimeters to 3M. These dykes are everywhere discordant to Nonacho sediments.

#### d) Diabase Dykes

These basic dykes are the youngest rocks in the area and are discordant to both "granites" (Henderson, 1939), and the Nonacho Series sediments. They are generally narrow (1-6 M wide; McGlynn et al, 1974) but are occasionally wide enough to be mappable units, reaching thicknesses of 125 M. Dykes are most numerous around the margins of the basin. The prevailing strike of the larger dykes is N to NNW and are subvertical (Henderson 1939; McGlynn et al, 1974). They are fine to medium grained, commonly amygdaloidal and often contain wall rock inclusions. Medium grained varieties often display the distinctive ophitic texture defined by laths of plagioclase and pyroxene.

According to McGlynn et al (1974) the dykes are not displaced by faults but are somewhat fractured, indicating they were intruded at about the time of the last minor reactivation of marginal basin

faults. Their  $^{40}\text{Ar}/^{39}\text{Ar}$  studies of the dykes suggest they were emplaced at about 1700 m.y.

### 3. Structural Geology

Nonacho Stratigraphy is folded about steeply dipping axial surfaces which trend NE in the western part of the basin and ENE in the eastern parts (McGlynn, 1970; McGlynn et al, 1974). Folding is symmetrical and open in sandstone and conglomerate lithologies, and is tighter when shales and siltstones are involved (McGlynn, 1971). On the limbs of folds, dips vary generally from  $45^\circ$  to  $60^\circ$  but dips up to  $80^\circ$  are not uncommon (Henderson, 1939). Synformal and antiformal folds plunge gently, usually to the NE (McGlynn, 1970).

Faulting in the area is concentrated along basin margins and about basement "highs" within the basin (McGlynn, 1974). Faults truncate both Nonacho Gp. sediments and basement rocks, often obscuring the unconformable contact. Undoubtedly many of these faults have had multistage movements, some prior to Nonacho deposition and some during or after sedimentation (McGlynn, 1974). Evidence for movement prior to deposition are: clasts of cataclastized basement rocks in the basal conglomerates (McGlynn, 1974), and fault contacts between undeformed Nonacho strata and basement rocks (see Figure 6). Movement after deposition is evidenced by breccia zones within Nonacho Gp. sediments. McGlynn (1970, p. 155) suggests:

These faults probably are boundary faults that formed the original basin and movement on these continued during sedimentation and, at a higher level, after sedimentation both during and after the folding of Nonacho strata.

Figure 7 details Nonacho Basin structure in the Thekulthili Lake area.

Due to the localized nature of this study the only rock seen in contact with, and deformed by the intrusive pluton is the argillaceous unit (Unit A, Figure 7), outcropping on the west shore of Thekulthili Lake. This unit strikes approximately NS and dips sub-vertically. Locally the argillite is vertically folded, shear fractured, and cut by numerous quartz veins and granitic dykes, particularly at the intrusive contact (see Figure 4). Similar features can likely be seen in other lithologies north of the study area.

Regional foliation trends in the basement complex run parallel to the basin, i.e. N-NE. Equivalent trends occur in similar basement rocks described by Baadsgaard and Godfrey (1972) in NE Alberta.

South of Thekulthili Lake a "thermal gneissic dome" has been described by Donaghy (1977). His studies of this structural feature are synthesized in the following discussion.

The southern dome consists of two gneissic components, a mono-metamorphic paragneiss mantle (Unit P, Figure 7) and a polymetamorphic core (Unit S, Figure 7). Paragneisses on the flanks and nose of the dome suggest that the structure plunges north under Nonacho Gp. strata. Donaghy (1977) contends that foliation trends in mantle and core gneisses are distinctly different, such that the change in foliation strike distinguishes a sharp contact between the two gneiss types. Petrographic contrasts further differentiates the two.

Gneissic foliation on the western flank of the dome dips west.

However at the contact with the western intrusive pluton (see Figure 7) there is an abrupt reversal, with foliation there dipping east. Crossing the contact from dome gneisses, to the granitic pluton, rock fabric changes from foliated to massive.

Doming of the southern gneissic dome is considered to have occurred after crystallization of the gneisses.

#### 4. Age Relationships

The relative ages of rock units in and around the Nonacho Basin has been under debate for many years. Discrepancies in part, stem from differences in interpretation of field relations between Nonacho strata and adjacent igneous and metamorphic rocks. Conflicting interpretations between various authors have been outlined in Chapter I.

Prior to 1970, the majority of age dates in the broad area of the Precambrian shield from northern Saskatchewan to Great Slave Lake were obtained using the K-Ar dating technique. This method is notorious for yielding anomalously variable dates from point to point in geologic regions. It is particularly unsatisfactory in such a high-grade metamorphic and igneous terrain, which has been subjected to multiple heating events, since  $^{40}\text{Ar}$  can escape from host minerals at temperatures around  $200^{\circ}\text{C}$  or more. Hence K-Ar dates quoted below should be regarded as minimum dates, and probably reflect uplift and/or the last thermal event.

Burwash and Baadsgaard (1962) dated four basement gneiss samples and two granitic cobbles from the basal oligomictic conglomerate on the east shore of Thekulthili Lake. Using the K-Ar

technique they obtained dates ranging from 1790 m.y. to 2260 m.y.

Similar results were obtained by Wanless et al (1967) from basement rocks in the vicinity of the Nonacho Basin. These gave K-Ar dates ranging from 1735 m.y. to 2175 m.y.

McGlynn (1974) quotes K-Ar ages of basement rock from 1735 m.y. to 2555 m.y., with most between 1735 m.y. and 1900 m.y., for the general region south of Great Slave Lake and north of 60° latitude.

In 1972 Stockwell revised his Precambrian time classification for the Canadian shield, placing the Kenoran Orogeny between 2500 m.y. and 2700 m.y., and the Hudsonian Orogeny between 1700 m.y. and 1950 m.y. Thus from the K-Ar dates given above it appears that the western portion of the Churchill Structural Province was involved in both Kenoran and Hudsonian orogenies.

Burwash and Baadsgaard (1962) and McGlynn (1970) suggest basement complex rocks in this region are in fact Archean (Kenoran), with younger K-Ar ages resulting from "overprinting" by the Hudsonian Orogeny. Thus since dyke emplacement is postulated at 1700 m.y. (McGlynn et al, 1974), Nonacho sedimentation and folding, followed by intrusion of the western granitic pluton must have taken place between 2500 m.y. and 1700 m.y.

To explain the younger K-Ar dates (those younger than 2500 m.y.) found in the basement complex, McGlynn (1974) suggests the Nonacho Basin and adjacent basement rocks were buried many thousands of meters and heated to 100 or 200°C; enough to drive off some <sup>40</sup>Ar yet maintain the unmetamorphosed state of the Nonacho Series. Subsequently, McGlynn (1974) contends the Hudsonian Orogeny mostly

consisted of regional faulting and folding in this area.

However since it is generally accepted that basement rocks around Thekulthili Lake are equivalent to the Tazin Group of NW Saskatchewan, an alternative model is suggested by Krupicka and Sassano (1972). They suggest that isotopic age dating strongly indicates that part of the Tazin is Kenoran, and part is Aphebian. They concur with Burwash's (1969) suggestion that the Hudsonian comprises two distinct orogenic pulses. The first produced the progressive metamorphism of Aphebian supracrustal rocks (Krupicka and Sassano, 1972). Between orogenic events in the Hudsonian, erosion occurred, and the Nonacho Series was deposited in a basement depression. Finally the second stage pulse caused regional folding, faulting, uplift and intrusion of the granitic pluton west of Thekulthili Lake.

This latter model is preferred as it closely parallels the development of the Athapuscow Aulacogen of Great Slave Lake, studied by Hoffman et al (1974). He states that during the Aphebian the Slave and Churchill Provinces occupied a foreland platform to the Coronation Geosyncline-Athapuscow Aulacogen system. Over this platform, sediment was transported to the system from an eroding mountain belt to the east. Deposition within the geosyncline and aulacogen is assumed to have occurred sometime between 2200 m.y. and 1700 m.y. Sometime during this period, presumably in the Hudsonian Orogeny, the Churchill Province was uplifted along its western margin and displaced relative to the Slave Province. At this time K-Ar radiometric clocks were reset in the Churchill

Province basement complex. In the uplift the Churchill was subjected to extensive faulting (mostly in the vertical sense) and minor plutonism; erosion then deposited great volumes of fanglomerate deposits into the intermontane Nonacho Basin and the Athapuscow Aulacogen. The fanglomerate phase of the Athapuscow Aulacogen is a sequence of boulder stone conglomerates and pebbly sandstones, which is analogous to Nonacho Gp. sediments.

A synthesized geologic history and geochronology of the Thekulthili Lake-Nonacho Basin area is given in Table I.

#### 5. Method of Sampling

Sample locations and their corresponding rock units are shown in Figure 7, and in greater detail in Figures 8 to 10.

Having established differences in morphology and age between "younger" and "older" granites in the field, the objective of this sample study is to determine their differences in petrography and chemistry.

Much of the summer was spent by the author in detailed mapping of basement rocks east of Thekulthili Lake. In choosing an area for "older" granite sampling the following criteria was used: 1) the basement complex must not be cataclastized, and 2) the area should contain a high proportion of migmatites and scattered, massive granitic bodies. The area chosen east of Thekulthili Lake (Figure 7 and Figure 10) contained the above characteristics.

Less time was available for sampling the intrusive granite pluton west of Thekulthili Lake (Figure 7 and Figure 8). Consequently, only the margin of the pluton was sampled and studied by

TABLE I

## GEOLOGIC HISTORY, THEKULTHILI LAKE N.W.T.

GEOLOGIC EVENT	TIME	DESCRIPTION OF EVENT
Hypabyssal Intrusions	Paleohelikian (1700 m.y.)	Emplacement of diabase dykes
Late stage plutonism	Upper Hudsonian	Intrusion of western granite pluton.
Folding, Faulting		Nonacho series fold and faulted.
Basement & supracrustal erosion - deposition	Middle Hudsonian (1800 m.y.)	Nonacho Gp. ("Fanglomerate") deposited in a fault controlled basin.
UNCONFORMITY		
Regional uplift, metamorphism, and faulting	Lower Hudsonian (1950)	Basement Reactivation-Churchill Province uplifted along western margin. High level faulting generates an intermontane quasi-graben basin. Progressive metamorphism of Apebian supracrustals (Tazin Equivalent) to upper Amphibolite paragneisses. Doming of gneissic basement south of Thekulthili Lake.
Erosion, Deposition	Lower to Middle Apebian	Deposition of upper Tazin Group supracrustals over Kenoran (lower Tazin Gp.) basement.
Orogenic Uplift, high grade metamorphism	Kenoran (2500 m.y.)	Upper amphibolite-granulite facies metamorphism of Lower Tazin Gp. supracrustals in orogenic core. Uplift of overlying strata.
Deposition	Pre-Kenoran (2700 m.y.)	Deposition of Lower Tazin Gp. supracrustals.

Figure 8

Expanded sample location map, showing sample locations for the younger granite and profile "A" Nonacho sediments along the western margins of Thekulthili Lake. Dashed lines are geologic contacts, irregular lines represent fault zones. Scale is 1:50,000. (see Figure 7 for the geology of this area).

Figure 9

Expanded sample location map, showing sample locations for profile "B" Nonacho sediments in the area of Big Pine Narrows (south central Thekulthili Lake). Dashed lines denote bedding contacts. Scale is 1:50,000.

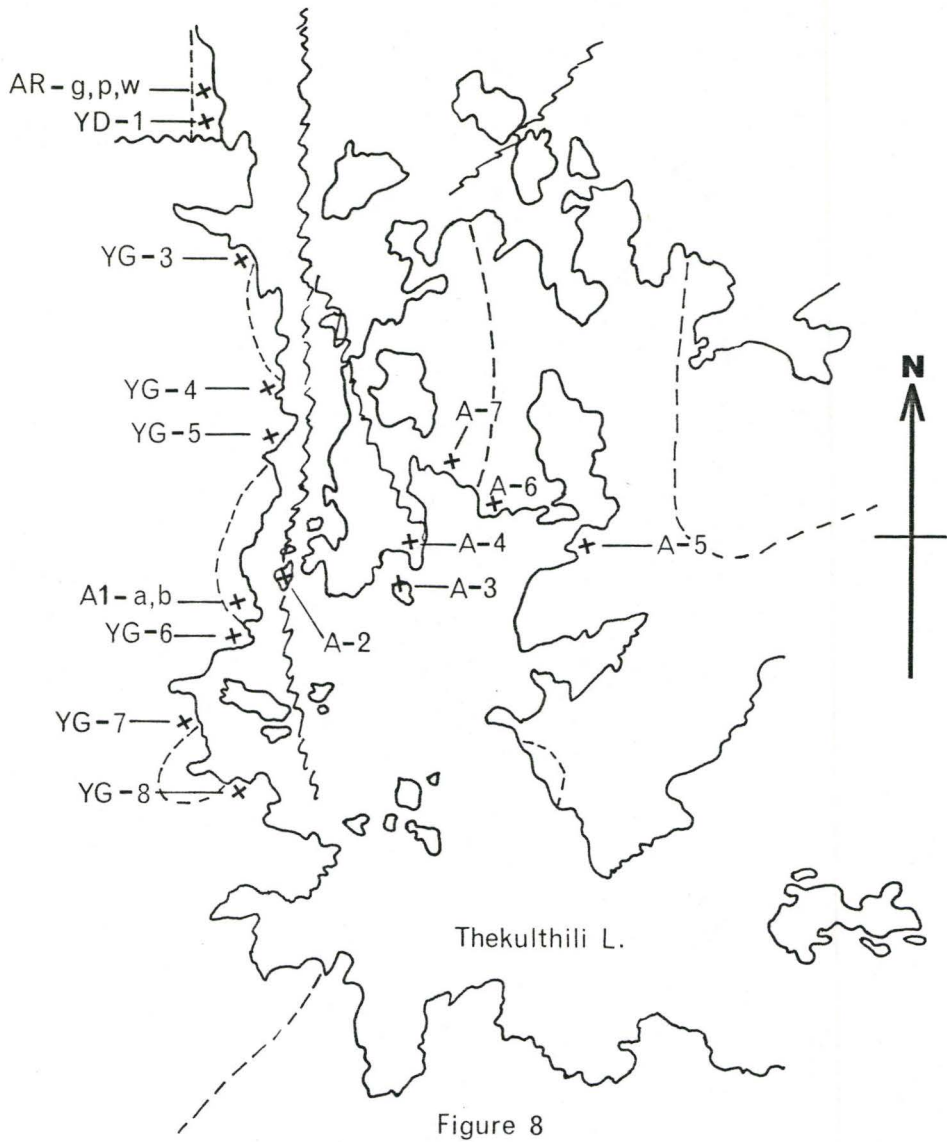


Figure 8

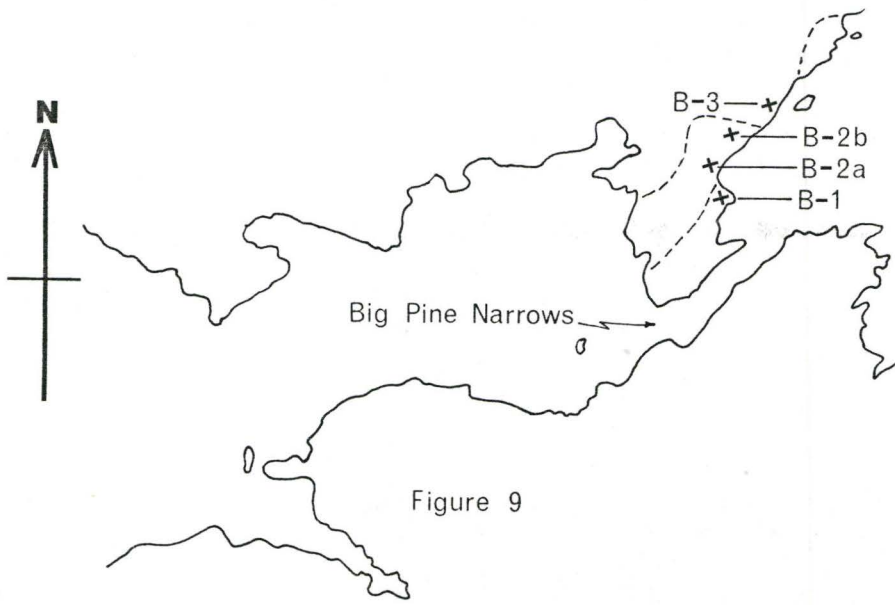


Figure 9

Figure 10

Expanded sample location map, showing sample locations for basement granitic rocks at the eastern margin of Thekulthili Lake. Dashed lines are geologic contacts and irregular lines denote fault zones. Scale is approximately 1:50,000.

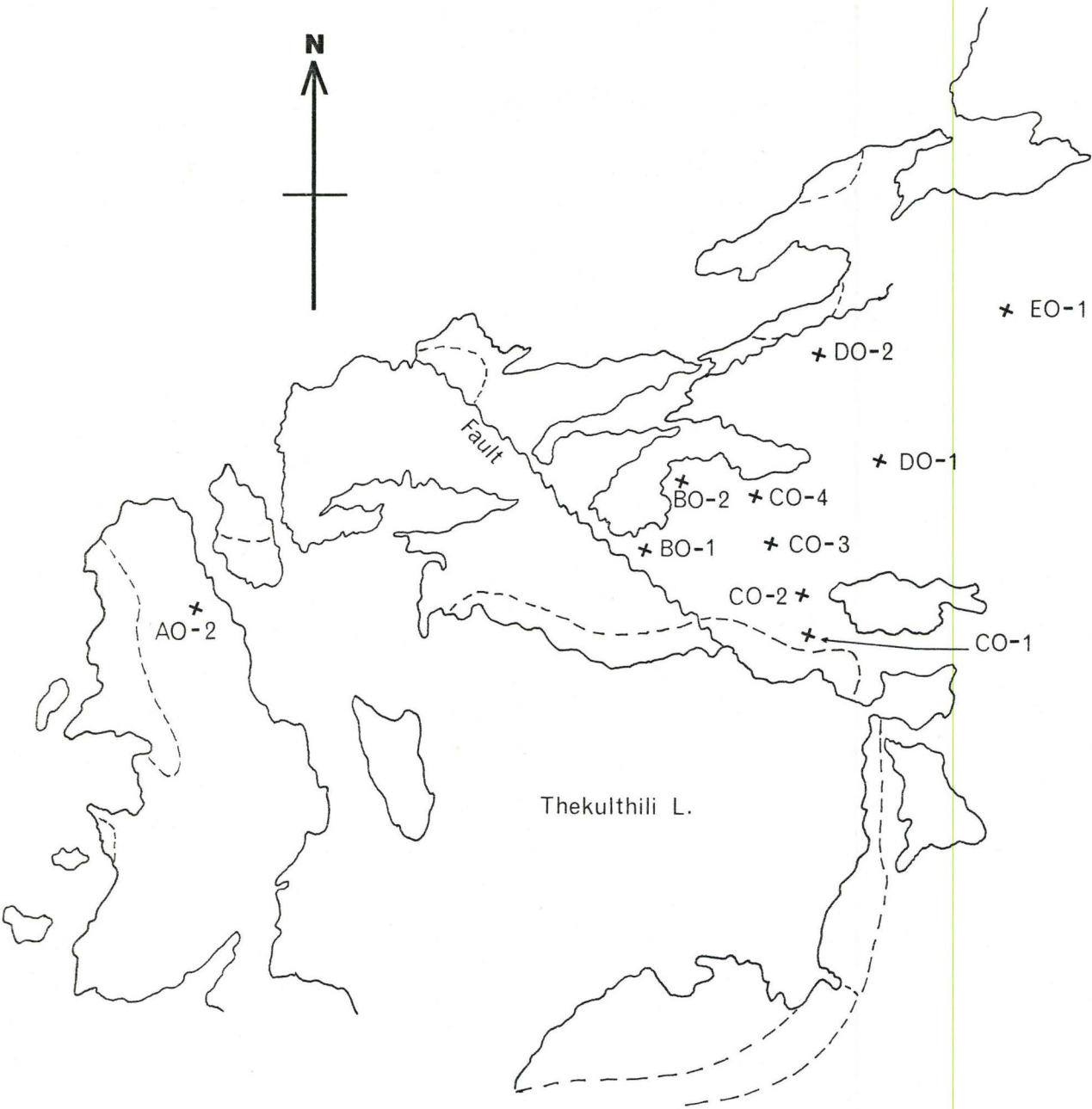


Figure 10

boat in one day. Due to the homogeneity of the younger granite relative to basement granites, fewer samples were deemed necessary to be representative of the former.

Four samples of the argillaceous unit adjacent to the pluton were taken for petrographic analysis, to determine the effects of contact metamorphism. Also an xenolith of what looked to be the same argillite (see Figure 5) was sampled for comparison.

Two profile lines across Nonacho strata were sampled to determine the extent of metamorphism the western pluton imparted on Nonacho sediments. Profile "A" runs 3 km. eastward from the west shore of Thekulthili Lake (Figure 7 and Figure 8). Profile "B" extends north of Big Pine Narrows for 1.5 km. (Figure 7 and Figure 9) and was chosen as a control line, in an area where Nonacho strata appears essentially unmetamorphosed. Both profiles were chosen in zones perviously sampled by Donaghy (1977), in order to compare petrographic analyses.

Sample kult-13 from the extreme SE shore of Thekulthili Lake (Figure 7) was taken from a small, massive granitic body which resembled the western pluton. It was sampled to compare its petrography and chemistry to "younger" and "older" granites.

## CHAPTER III

## PETROGRAPHY

1. Introduction

Over the course of the 1979 summer field season a total of 50 samples were collected, 34 of which were chosen for subsequent analysis. Of these, 19 samples from both granitoid suites were thin sectioned and crushed for geochemical analysis. The remaining 15 samples of Nonacho sediments and metasediments were thin sectioned for petrographic analysis. Detailed petrographic descriptions of the granitoids and some Nonacho sediments are discussed here, the remaining sections of Nonacho sediments (10) are given in Appendix A.

Following a whole rock geochemical assay for major elements using the x-ray fluorescence spectrometer (XRF) technique (see Chapter IV), chemical analyses were recast into a mesonorm computer program (devised by D. Birk, 1978; based on the mesonorm of Barth (1962) as modified by Hutchison and Jeacocke, 1971) to determine the normative mineralogy of the granitoid specimens. Mesonorms are preferred to standard CIPW norms for granitoid rocks (which have mineral assemblages analogous to amphibolite facies metamorphism, Barth 1962), because in the latter hydrated minerals such as hornblende and biotite are represented in the norm by such minerals as diopside, hypersthene, orthoclase and corundum (Nockolds et al, 1978). Consequently, CIPW normative composition can vary widely from the mode, or actual composition of the rock, since siliceous grani-

toid rocks rarely contain pyroxenes or corundum. Furthermore mesonorms, as initially devised by Barth (1959, 1962) for "mesozone" rocks (those centering around amphibolite facies) are computed from cation percentages rather than the oxide weight percentages of the CIPW norm. As a result mesonorm calculations are more compatible with the volume percentages of the mode.

It is found by petrographic analysis that modal compositions of the granitoid samples are essentially identical to the calculated mesonorm compositions (given in Appendix B). As a result a detailed modal analysis based on point counting of stained rock slabs or thin sections was deemed unnecessary. In particular, the mesonorm alleviated the problems associated with modal analysis of granitic fabrics containing myrmekite and perthite (Parslow, 1969).

The only discrepancy between mesonorm and modal compositions is with respect to the relative proportions of orthoclase (Or), albite (Ab), and anorthite (An) components. Mesonorms gave cation percentages of each, and the author estimated by staining techniques the relative proportions of the minerals plagioclase and potassium feldspar, which contain these components, i.e., the albite component is not a separate phase, but is part of both plagioclase and the K-feldspar.

Consequently mineral percentages given in subsequent sections are estimated in part, from normative compositions and from approximated modal abundances in stained rock slabs.

Figure II is a ternary Quartz-Alkali Feldspar-Plagioclase (QAP) plot of granitoid specimens, as recommended by the IUGS Sub-

Figure II

Quartz-Alkali Feldspar-Plagioclase  
Diagram (after IUGS, 1973).

PHASE FIELDS

- 1A Quartzolite
- 1B Quartz-rich granitoids
- 2 Alkali-feldspar granites  
(hypersolvus, one alkali-feldspar granites)
- 3A Syenogranites
- 3B Monzogranites (Normal granites)
- 4 Granodiorite
- 5 Tonalite
- 6 Alkali-feldspar quartz syenites
- 7 Quartz-syenites
- 8 Quartz-monzonites
- 9 Quartz-monzodiorites
- 10 Quartz-diorites

Symbols used for this and subsequent variation diagrams.

- Basement (Old) Granites
- ★ Intrusive (Young) Granite
- ⊙ Granitic Dykes (Aplites)

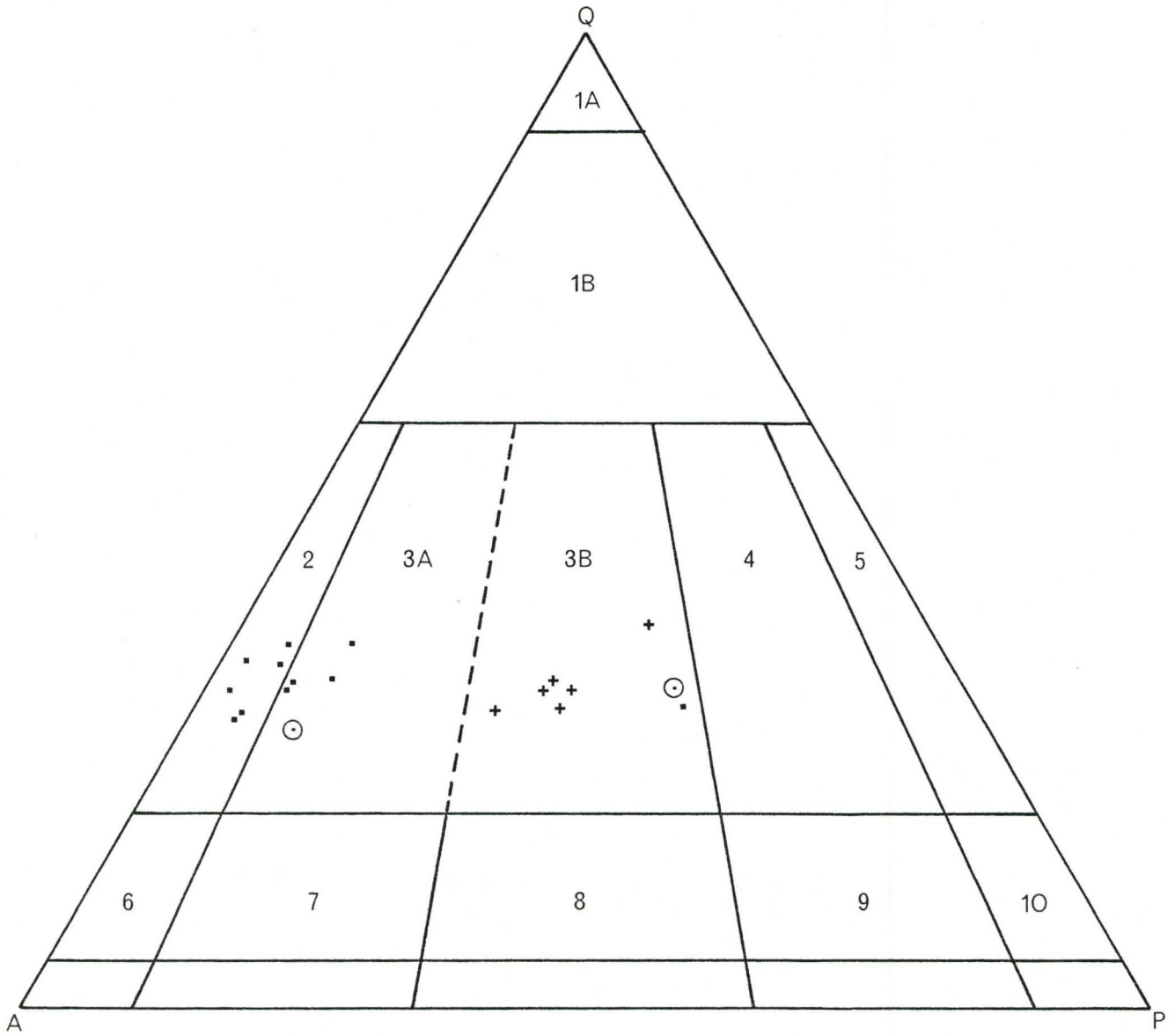
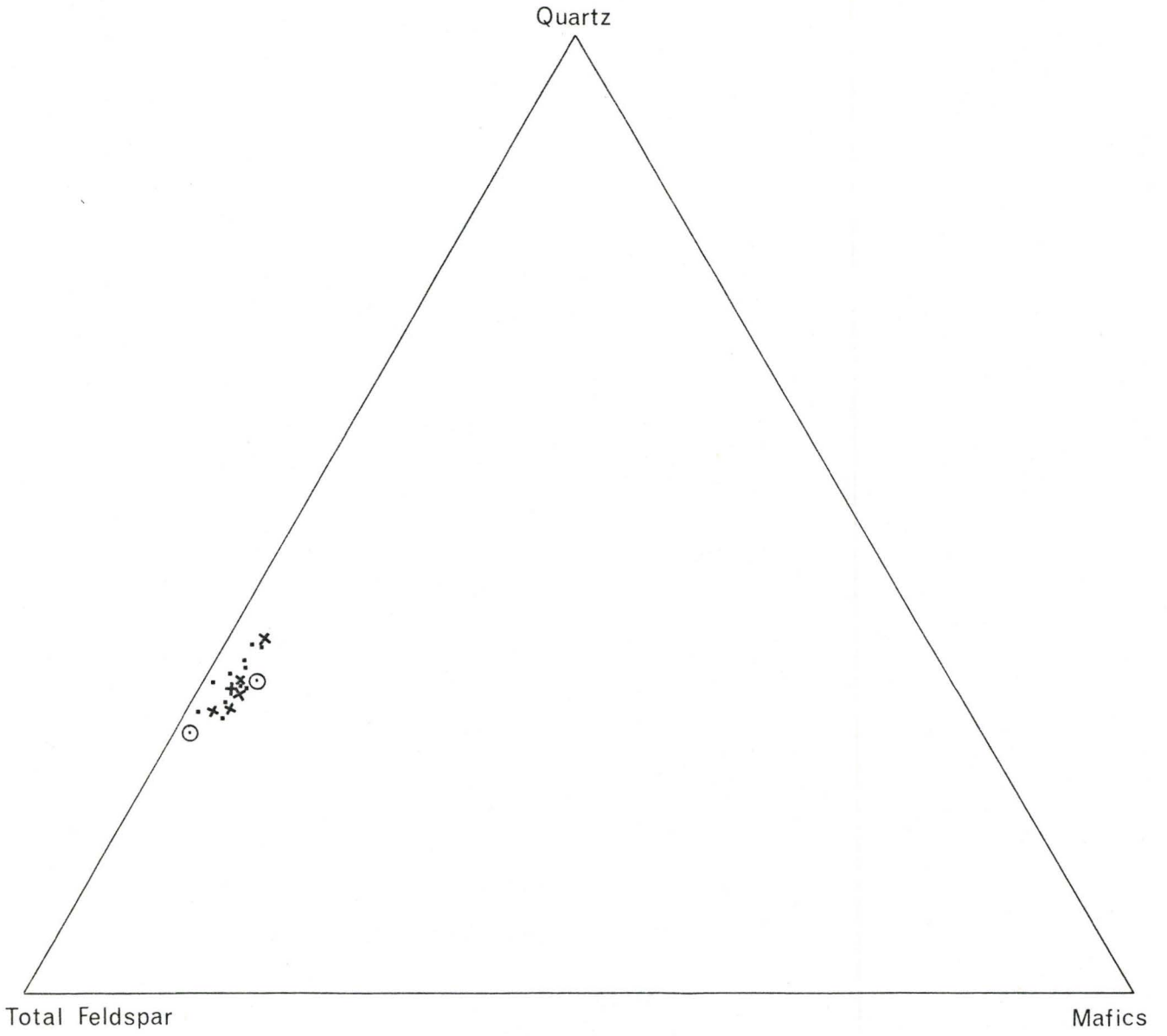


Figure 12

Comparative color index.  
Quartz-Total Feldspar-Total Mafic  
Diagram (after IUGS, 1973).



commission of the Systematics on Plutonic Igneous Rocks (1973). A comparative color index is given by the Quartz-Total Feldspar-Total Mafics (QFM) plot in Figure 12. This figure shows that both granitoids are leucocratic (total mafics less than 5%) and are virtually identical with respect to total Q-F-M content. However, Figure 11 graphically illustrates that the two granites have distinctly different feldspar contents. The intrusive granite (monzogranite) falls near the center of the QAP triangle, which according to Streckeisen (1973) is typical of most granites. Meanwhile basement granites (alkali-feldspar granites and syenogranites) have a much higher alkali-feldspar content with a plagioclase content less than 10% (excluding Kult-13 sample which plots in monzogranite field).

Synthesized petrographic descriptions of intrusive granite, basement granite, and various Nonacho Gp. samples are discussed below.

## 2. Basement Granites

### a) Essential Minerals

In order of abundance the predominating minerals are microcline-microperthite, microcline, and quartz. Occasionally, as in CO-2, orthoclase-microperthite is significant as well. Many or most of the crystals identified as microcline may actually be microcline-microperthite, but were cut such that perthitic relationships cannot be seen. Potassium feldspar content ranges from 54 to 65%, and quartz content is between 28 and 35%.

Microcline and/or microcline-microperthite are anhedral and display characteristic grid twinning (according to combined albite-

pericline twin laws). Perthitic K-feldspar contains both stringer and vein exsolutions. Quartz occurs in two forms, as polycrystalline quartz aggregates in the matrix, and as single anhedral quartz grains up to 4 mm. in size. Undulatory extinction is variable, the larger monocrystalline grains generally being undeformed (Figures 13 and 14).

Plagioclase content is always less than 10% and is usually less than 5%. It generally occurs in minute anhedral, highly altered, masses associated with potassium feldspar. Twinning is rare. A few grains show albite twinning and were found to have an albite ( $An_{0-10}$ ) composition (Michel-Levy method).

#### b) Accessory Minerals

The characterising accessory mineral is biotite, much of which has subsequently altered to chlorite and iron oxides. These minerals constitute 1 to 5% of the mode. Green chlorite is distinguished by its anomalous violet and "Berlin-blue" interference colors. Unaltered biotite has a range of pleochroism from light to dark brown to intermediate light green to dark green-brown.

Trace amounts (less than 1%) of iron oxides (magnetite, ilmenite) are generally found in close association with biotite and chlorite.

#### c) Textures

All samples are holocrystalline and medium to coarse grained, with the majority of crystal being 1-4 mm in size. The texture in most cases is massive and allotriomorphic granular. Sometimes a crude foliation is defined by elongation of quartz and K-feldspar, and subparallel discontinuous stringers of biotite.

Figure 13

Photomicrograph of basement granite showing anhedral, unstrained quartz (Q) and grid twinned microcline-microperthite.

(crossed nicols, magnification 17X).

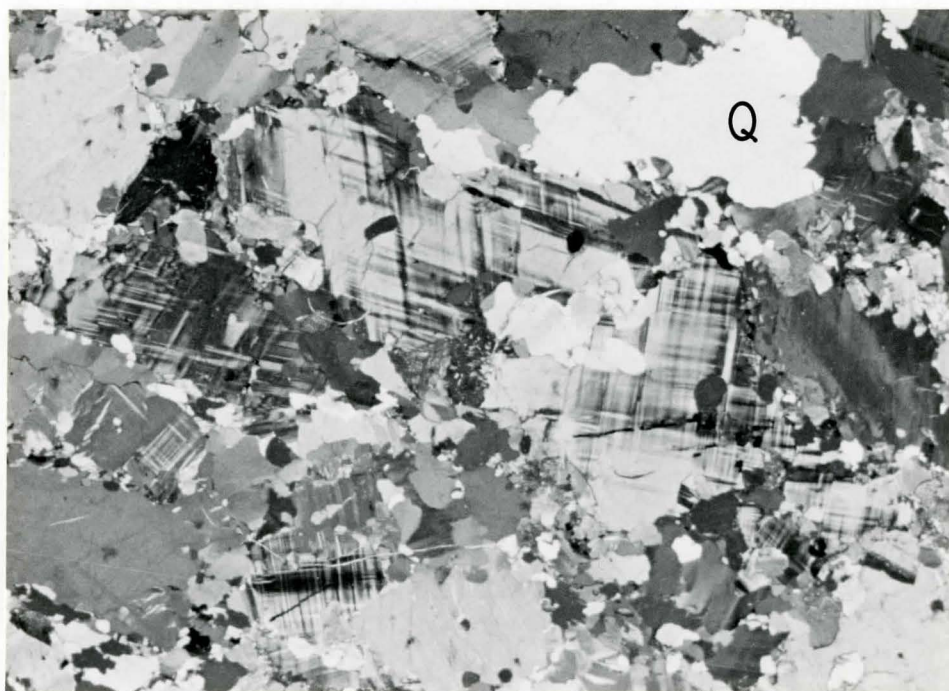


Figure 14

Photomicrograph showing the typical allotriomorphic-granular texture of an average basement granite. Notice the predominance of microcline-microperthite and quartz and the absence of distinct plagioclase grains.

(crossed nicols, magnification 8X)



Grain contacts between quartz, microcline and/or microcline-microperthite are always irregular and embayed (Figures 13-15). These felsic minerals are all essentially unaltered and fresh looking.

Invariably however, anhedral plagioclase includes and/or fringes microcline and microcline microperthite in a pseudo-Rapakivi type texture. This plagioclase is preferentially sericitized or kaolinized to finely divided micas and/or clays, and is commonly symplectically intergrown with quartz, in myrmekitic intergrowths (Figure 15). Rarely, small (1 mm or less) distinct grains of twinned plagioclase occur with polycrystalline quartz in an interstitial groundmass.

Apart from some strained quartz, most basement granites are undeformed. Two samples, BO-1 and CO-1 collected near a fault (see Figure 10) do show cataclastic textures. In these samples brecciation has crushed and milled potassium feldspar and quartz into a fine grained, to microcrystalline groundmass. Porphyroclasts (augens) of microcline (and rarely quartz) are large, and rounded from grinding, ranging in size from 3 to 18 mm.

With reference to Figure 11 and their above mineralogy, the basement granites studied are classified as Biotite Alkali-Feldspar Granites (type 2) and Leucocratic Biotite Syenogranites (type 3A).

### 3. Intrusive Plutonic Granite

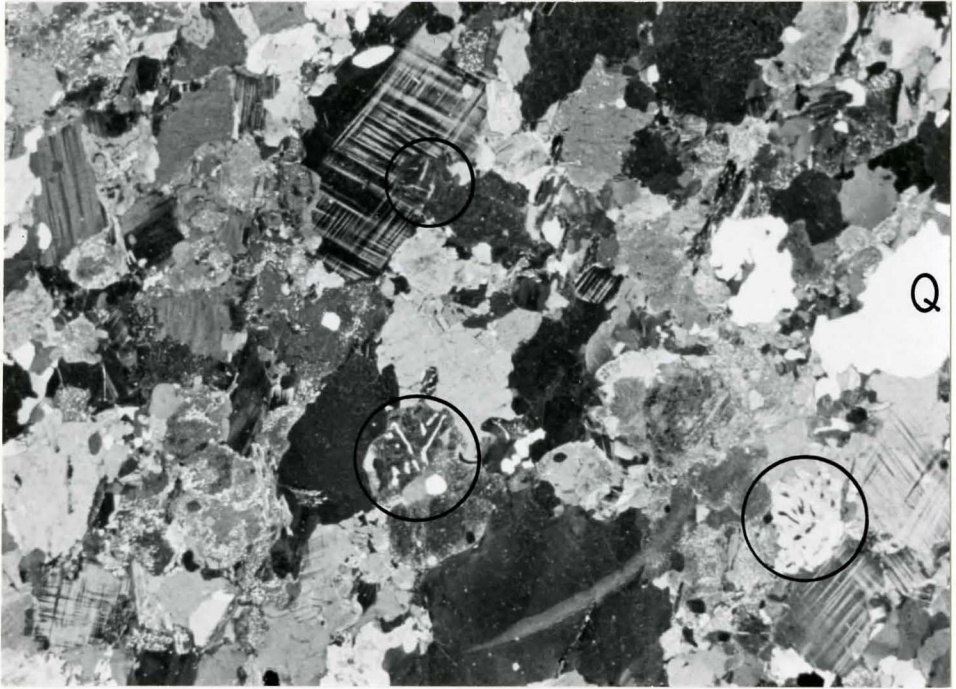
#### a) Essential Minerals

The most common constituents in order of abundance are orthoclase-microperthite, quartz, plagioclase and microcline. Potassium feldspars range from 22 and 40% of the rocks sampled but most contain between 33 and 35%. Quartz makes up 28 to 35% of the rock, and

Figure 15

Photomicrograph of a basement granite. Circled areas inclose myrmekitic intergrowths of quartz and albite growing from microcline-microperthite. Notice also the unstrained, anhedral quartz (Q).

(Crossed nicols, magnification 15X).



plagioclase 25 to 32%.

The most abundant potassium feldspar is orthoclase-microperthite, which occurs mostly in large anhedral to subhedral, equant and lath shaped grains. The predominant exsolution intergrowths are string and patch perthites. Their grain size is generally greater than 3 mm, but megacrysts up to 15 mm in size are not uncommon (Figure 16). This orthoclase-microperthite is generally untwinned but rather shows a subtle disuniform extinction pattern. However simple Carlsbad twinning is quite common (Figure 16). Microcline is much less abundant than microperthite; when present it occurs in the groundmass, in small anhedral grains displaying the characteristic grid twinning.

Quartz occurs predominately in polycrystalline, anhedral masses which are interstitial to other constituents of the mode. Less commonly quartz appears in monocrystalline, anhedral grains showing underlatory extinction. This quartz frequently contains minute fluid inclusions which are often aligned along preferred crystallographic directions.

Plagioclase is grown in subhedral laths ranging in size from 2 mm to 8 mm. Twinning according to the albite law is widespread, less commonly combined Carlsbad-Albite is seen. The plagioclase composition (Michel-Levy method) is between  $An_5$  and  $An_{20}$ .

#### b) Accessory Minerals

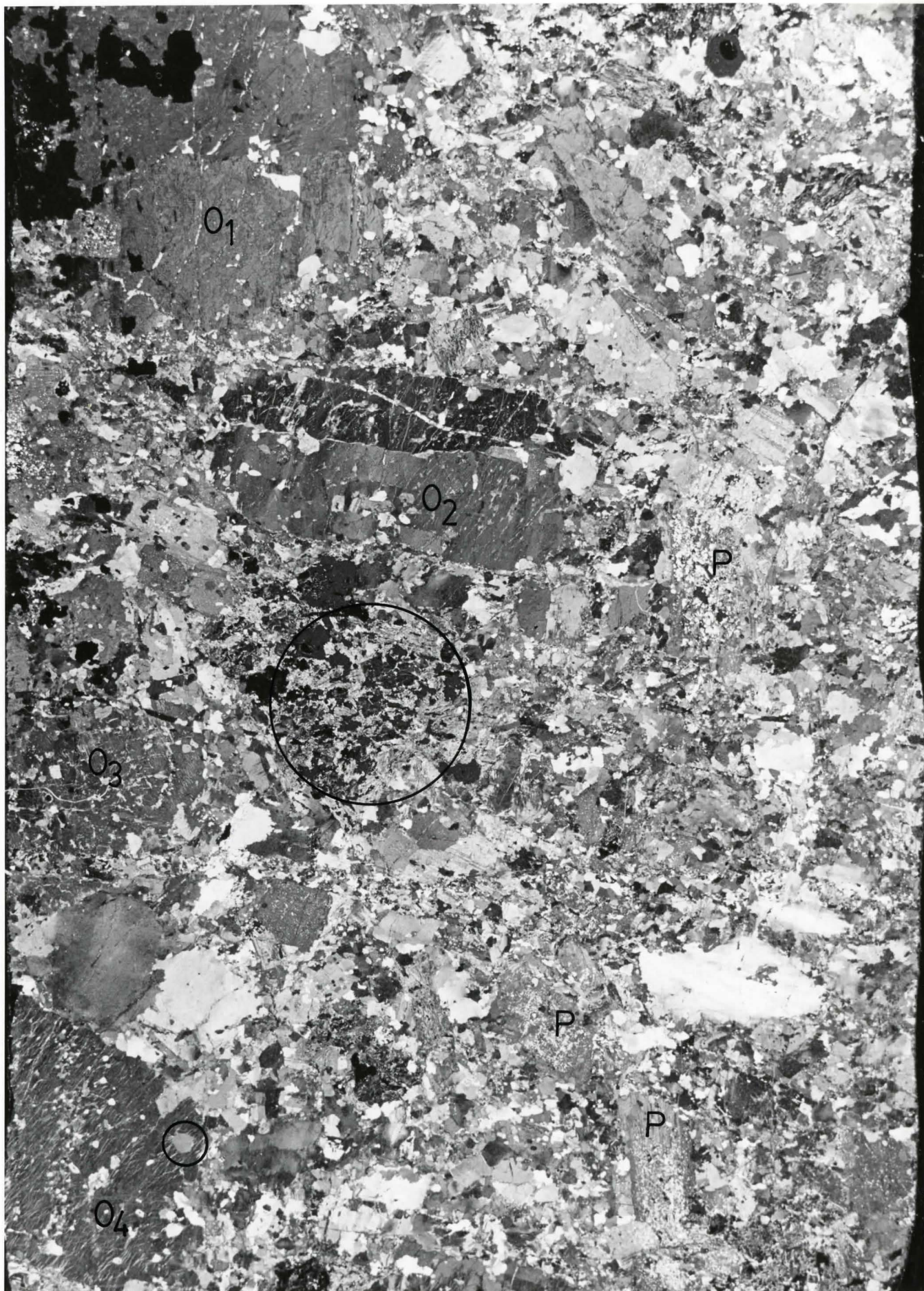
The characterising accessory mineral is biotite. Most has been completely altered to chlorite and opaques. Where unaltered, it ranges in pleochroism from a yellow to green-brown variety to a pale-dark green variety. Chlorite shows weaker pleochroism and

Figure 16

Photomicrograph showing porphyritic texture in the younger granite. Things of note in this picture:

- 1) Megacrysts of orthoclase-microperthite ( $O_1, O_2, O_3, O_4$ )
- 2) Carlsbad twinning in megacryst  $O_2$ .
- 3) Crystallographic alignment of plagioclase inclusions in  $O_2$  megacryst.
- 4) Gradational contacts between K-feldspar megacrysts and the groundmass, particularly in  $O_1, O_3$  and  $O_4$ .
- 5) Zonal nature of biotite, in discrete patches (large circle).
- 6) Pervasive deuteric alteration of plagioclase (P) to sericite.
- 7) Presence of many quartz inclusions in megacrysts, and one idiomorphic quartz inclusion in  $O_4$  (circled).

(crossed nicols, magnification 6X)



anomalous violet to "Berlin-blue" interference colours. Together biotite and chlorite compose 2 to 7% of the rock.

Trace minerals (less than 1%) which are invariably grown in close association with biotite, include iron oxides (magnetite, ilmenite and possibly hematite), pyrite and apatite (Figure 17). Some fluorite was found in a quartz vein in sample YG-5. Zircon, sphene and rutile were not observed.

### c) Textures

All samples are holocrystalline and coarse grained, with the majority of the grains greater than 3mm in size. The most common texture is hypidomorphic granular, however some samples like YG-3 and YG-8 (Figure 16) are better termed porphyritic.

Orthoclase-microperthite is ubiquitous in all sections, both as large megacrysts, and as part of a medium to coarse grained plagioclase, quartz, biotite and potassium feldspar matrix. Grain borders of the K-feldspar megacrysts are rarely distinct, rather they are diffuse and grade into adjacent matrix grains (Figure 16). Sometimes the megacryst perimeters display a symplectic intergrowth of quartz and feldspar, which resembles myrmekite. Very commonly, K-feldspar megacrysts are riddled with plagioclase and (especially) quartz inclusions (Figures 16 and 18). They are anhedral to subhedral and are commonly aligned preferentially along crystallographic directions in the host orthoclase-microperthite (Figure 16). Quartz inclusions are unstrained. Rarely one or two grains of biotite may be found as inclusions in the megacrysts.

Megacrysts twinned on the Carlsbad law are common. Grid twinning is rare and is found only in matrix crystals (microcline) and

Figure 17

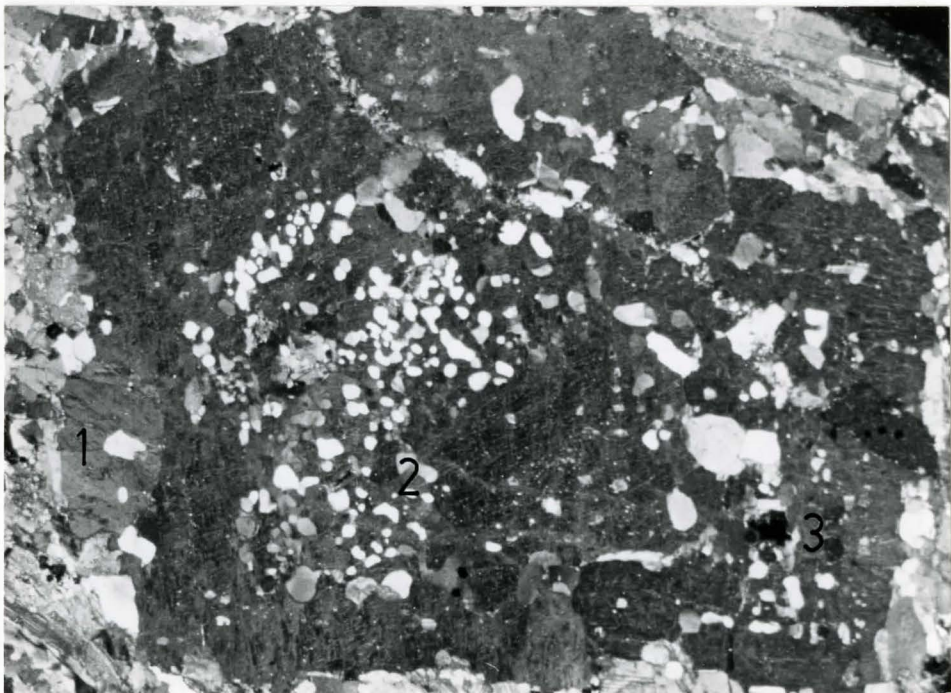
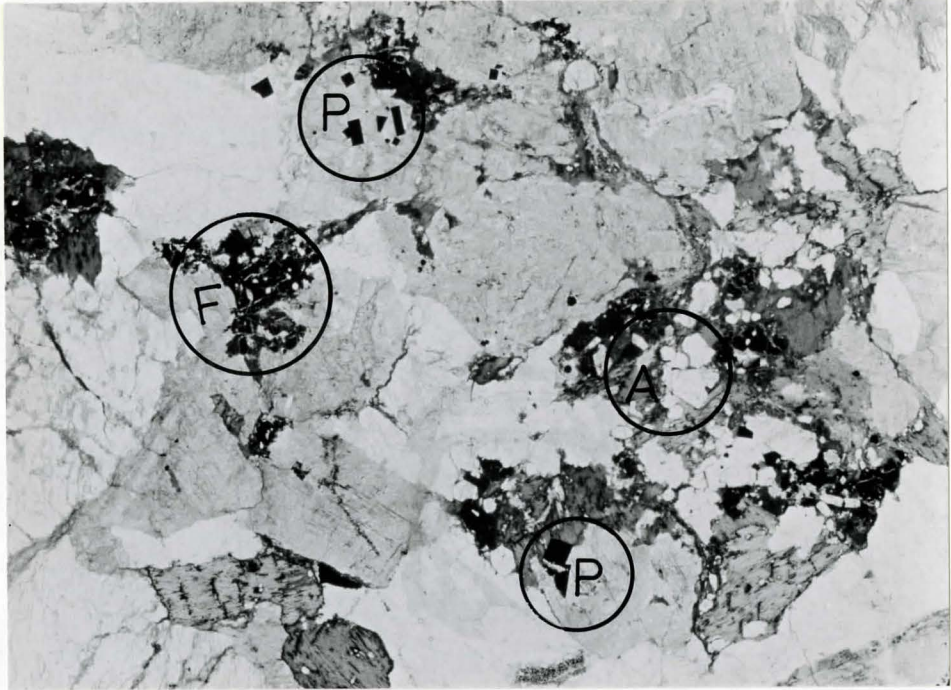
Photomicrograph of younger granite, showing a biotite zone. Notice how biotite forms both felted, tabular crystals and occupies minute veinlets between felsic crystals. Note the associated euhedral pyrite (P), apatite (A), and iron oxides (F).

(plane polars, magnification 13X).

Figure 18

Photomicrograph of an orthoclase-microperthite megacryst in younger granite. This megacryst shows syneusis structure, being a composite of 3 individual crystals (numbered) joined in parallel along prominent crystal faces. Note the high density of quartz inclusions particularly in crystal cores.

(crossed nicols, magnification 18X).



the outer portions of megacrysts. Occasionally megacrysts display a subtle oscillatory zoning marked by differential concentrations of exsolved plagioclase (which is sericitized) and/or variable extinction angles.

Plagioclase when not present as inclusions or exsolutions in alkali feldspar, occurs as a major constituent of the matrix. Groundmass plagioclase crystals are anhedral to subhedral and are sometimes as large as orthoclase-microperthite megacrysts, particularly in sections displaying the hypidiomorphic granular texture. As with K-feldspar megacrysts, plagioclase laths occasionally carry concentric optical zoning, accentuated by differential sericite alteration of zonal composition planes.

A striking textural feature commonly exhibited by the orthoclase-microperthite and plagioclase laths (operating together or separately) is synneusis structure. Vance (1969) defines synneusis as the drifting together and attachment of individual crystals to form a group or cluster of crystals (synneusis structure). The junction between individual components is not random, rather they are joined in parallel along prominent crystal faces. Synneusis structure in a K-feldspar megacryst is shown in Figure 18. A variant of synneusis structure and also seen in some sections, is synneusis twinning, which arises when crystals unite in twinned orientation (Vance, 1969). Two features which distinguish synneusis twinning from a single twinned crystal are: 1) Zoning, which may reveal composite crystal cores, and/or 2) Crystal misfit-uneven alignment and grain size differences (especially in length) of individual crystals.

Chloritized biotite and its associated trace minerals (apatite, iron oxides, and pyrite) generally occur in distinct patches throughout the rock (Figures 16 and 17). Rarely, apatite is found with interstitial polycrystalline quartz between other constituents. The biotite itself occurs both as flakes in felted masses, and in minute veinlets occupying cracks and interspaces (Figure 17). The trace constituents either include or are juxtapose to biotite and chlorite.

Sericitization and possibly kaolinization has been restricted to plagioclase feldspar(s). This alteration has affected plagioclase inclusions, and exsolutions in microperthites and particularly "free" plagioclase laths. Figure 16 shows the extent to which many plagioclase laths have altered to sericite. Deformation effects displayed in these sections include quartz straining (undulose extinction), bent twin lamellae in plagioclase, and kink banding in micas.

Table II lists the essential petrographic features of the plutonic granite and basement granites.

#### 4. Granite Dykes (Aplites)

Two granite dykes which emanate from the intrusive pluton were sampled for analysis. The Q-A-P plot in Figure 11 illustrates that the two dyke rocks are widely different with respect to the type of feldspar they contain. Sample Al-b plots as a monzogranite (3B) while YD-1 is classed as a syenogranite (3A). The former was sampled from the center of a 0.5 to 1.0 m thick dyke while the latter was taken from the margin of a 1 to 3 m wide dyke.

Although the two samples look identical in hand specimen, their

TABLE II

Salient Petrographic Features of the Granite Suites

	Basement Granites (Alkali Feldspar Granites, Syenogranites)	Plutonic Granite (Monzogranite)
Essential Minerals (in order of abundance)	Microcline-microperthite (Microcline ?) Quartz Orthoclase-microperthite Plagioclase (An <sub>0</sub> -An <sub>10</sub> )	Orthoclase-microperthite Quartz Plagioclase (An <sub>5</sub> -An <sub>20</sub> ) Microcline
Perthite Classification (after Barth, 1969)	String perthite, vein perthite	String perthite, patch perth- ite
K-feldspar Content	54-65%	22-40% (mostly 33-35%)
Quartz Content	28-35%	28-35%
Plagioclase Content	Less than 10% (mostly <5%)	25-32%
Characterising Accessory Minerals	Biotite (+Chlorite), 1-5%	Biotite (+Chlorite), 2-7%
Trace Minerals	Fe-oxides, magnetite and/or ilmenite.	Fe-oxides, magnetite and/or ilmenite (possible hematite. Apatite, pyrite.
Textures	Medium grained (1-4 mm) holocrystalline, allo- triomorphic granular.	Coarse grained (greater than 3mm), holocrystalline, hypidiomorphic granular, and porphyritic (K-feldspar megacrysts up to 15mm).
Twinning (Mineral)	Combined albite-percline (grid twinning) common (Microcline-microperth- ite), Albite twinning rare (Plagioclase).	Simple Carlsbad twinning (Orthoclase-microperthite), Albite, combined Carlsbad- albite (Plagioclase), grid twinning (Microcline). Synneusis Structures (K-feldspar, Plagioclase).
Feldspar Zoning	Absent	Not uncommon in both K-feld- spar and Plagioclase.
Myrmekite	Common, found at the junction of K-feldspar and plagioclase.	Rare, found around the margins of K-feldspar megacrysts.
Inclusions	Rare and inconspicuous, anhedral "blebs" of plagioclase in K-feld- spar. Minor amounts of quartz in K-feldspar.	Ubiquitous inclusions of anhedral to subhedral quartz (unstrained), and plagioclase in K-feldspar megacrysts. Commonly aligned crystallo- graphically.
Straining Effects	Undulatory extinction of quartz is variable. Two samples (BO-1, CO-1) are brecciated and porphyro- clastic.	Polycrystalline, interstitial quartz ubiquitous, kink banding in biotite, bent twin lamellae in plagioclase.
Alteration	Biotite chloritised with exsolved Fe-oxides. Sericitization and/or kaolinization of plagio- clase to sericite and clays. K-feldspar un- altered.	Biotite chloritised with exsolved Fe-oxides. Exsolution and free plagio- clase altered to clays and/ or sericite. K-feldspar unaltered.

petrography as outlined below is significantly different.

a) Sample Al-b (Monzogranite)

The mineralogy consists of plagioclase (40%), potassium feldspar (25%), and quartz (32%) with minor amounts of biotite, chlorite, muscovite and opaques (together make up 3%).

The section is porphyritic and in part glomeroporphyritic where phenocrysts of subhedral plagioclase laths, 2-4 mm in length, are gathered in distinct clusters. The plagioclase laths are generally zoned and highly sericitized (or kaolinized), features that have obscured twinning. Where albite twinning occurred the plagioclase composition was determined to be  $An_5$  to  $An_{20}$ . Rarely some orthoclase-microperthite crystals occur as subhedral phenocrysts in this section (Figure 19).

Quartz, alkali-feldspar and minor micaceous constituents compose an equigranular, aplitic, groundmass having a grain size from 0.1 mm to .2 mm. The alkali-feldspar is untwinned and looks identical to quartz except the former is significantly altered by sericitization (or kaolinization). Rock slab staining for K-feldspar greatly facilitated the estimation of modal abundance. Quartz and untwinned K-feldspar in the groundmass is ubiquitously strained, and displays undulatory extinction.

Due to the porphyritic texture of this rock it is better termed a porphyritic microgranite (=quartz porphyry) rather than a granite aplite.

b) Sample YD-1 (Syenogranite)

The major constituents are potassium feldspar (54%), quartz (27%), and plagioclase (17%). Trace minerals are biotite and magnetite which together compose 1 to 2%.

Figure 19

Photomicrograph of a granite dyke (Sample A1-b). The groundmass shows the typical aplitic texture, with phenocrysts of plagioclase (P) and orthoclase-microperthite (M). Note how phenocrysts grade into the groundmass, and contain numerous inclusions.

(crossed nicols, magnification 75X).



The grain size is fine to medium grained averaging 1 mm. This rock has a distinctly equigranular-aplitic texture. Feldspar, particularly the potassium feldspar, have the largest grain size, forming crystals up to 4 mm long. Orthoclase-microperthite is the predominant K-feldspar but small amounts of microcline occur as well. Inclusions of quartz and plagioclase are ubiquitous in microperthite crystals. Sericitization and/or kaolinization alteration is much more marked in plagioclase than in the K-feldspar. The plagioclase composition is  $An_{10}$  to  $An_{25}$ . Many alkali-feldspar grains closely resemble quartz, consequently slab staining was useful.

#### 5. Argillaceous Nonacho Sediments

These samples were collected from the argillaceous unit found in contact with the granite pluton along the west shore of Thekulthili Lake (Chapters I and II). Samples AR-w, AR-p, AR-g and Al-a were taken from the unit itself some distance east of the actual contact (Figures 7 and 8). While the ARG-LENS sample was collected from an argillaceous xenolith (Figure 5), in the vicinity of the YG-5 sample point (Figure 8).

The petrography of these rocks is given below.

##### a) Samples From the Argillite Proper

In the NW corner of the study area the argillite exhibits a distinct color banding, defined by thin beds (8 cm to 15 cm) alternating in color from buff to pink to grey. The samples were taken from three juxtaposed color bands to determine: 1) the extent of contact metamorphism imparted by the pluton, and 2) if the petrography varied from bed to bed. Sample nomenclature Ar-w, Ar-p, and

Ar-g denotes the color of the bed.

Sample Al-a was collected south of the others (see Figure 8), in an area of uniform color-dark grey. It was collected to compare its petrography to the samples given above.

The following is a composite petrographic description of the four argillite samples.

All samples are very fine grained (aphanitic) between 0.01 mm and 0.1 mm, and the texture is invariably granoblastic (hornfelsic), as exhibited by an equigranular, interlocking mosaic of welded quartz (invariably strained) and feldspar. Xenoblastic felsic grains are generally connected by sutured and irregular contacts. Quartz and feldspar are the major constituents, together comprising 60 to 75%. Only in samples Ar-w and Ar-p can quartz be distinguished from feldspar, as the latter is extensively altered to sericite and/or clays. Due to the aphanitic grain size and absence of twinning the type of feldspar(s) cannot be determined. Staining the rock slabs for K-feldspar did not prove useful in this regard either, since the rocks are too fine grained.

Each sample is distinct with respect to the type, and abundance of mafic and opaque minerals which it contains.

Sample Ar-w contains 15-20% chlorite and 10-15% hematite. In Ar-p there are two main mafic constituents, a yellow-green epidote (approx. 2%) and a blue-green pleochroic hornblende (5-10%, see Figure 20) plus a small amount of chlorite (1-3%). Hematite content in Ar-p is approximately 5%. Both Ar-w and Ar-p display a crude microscopic segregation banding, with turbid horizons of hematite,

Figure 20

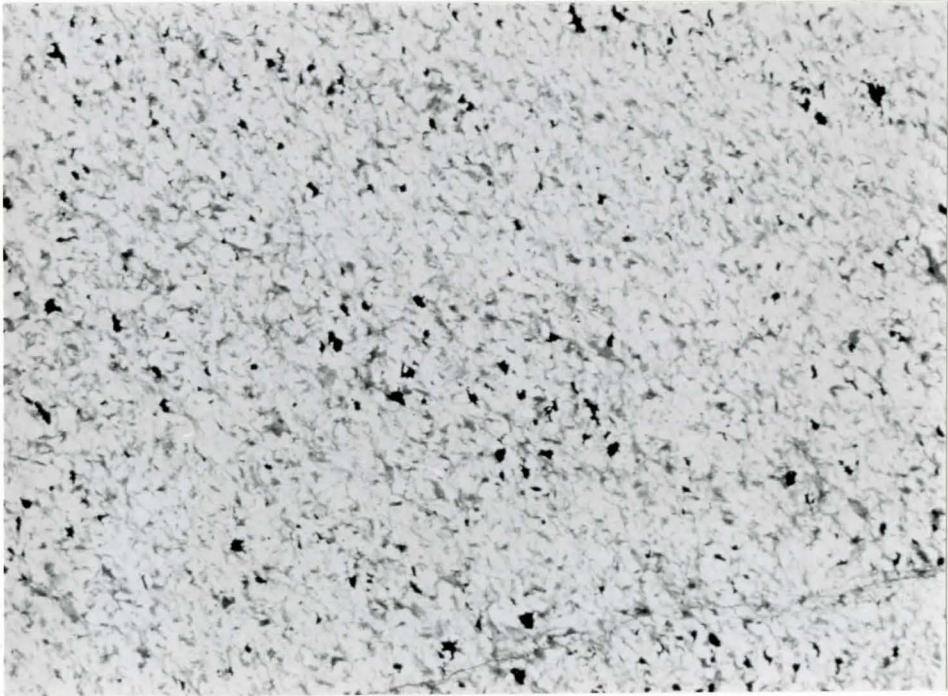
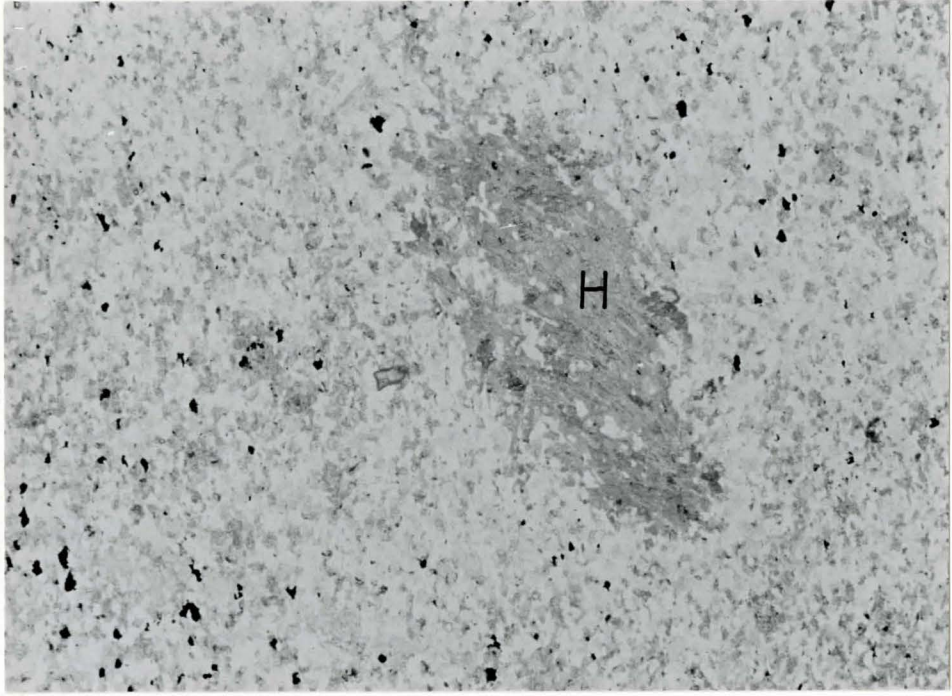
Photomicrograph of argillite sample Ar-w, showing a large grain of hornblende (H). The dark constituents are hornblende and epidote (dark grey) and opaques (black).

(plane polars, magnification 17X).

Figure 21

Photomicrograph of argillite sample Ar-g. The picture illustrates the preferred alignment of biotite grains (dark grey) and opaques (black).

(plane polars, magnification 50X).



altered feldspar, and some mafics, alternating with bands of strained and polycrystalline quartz. Both in thin section and hand specimen, this banding appears compatible with relict, primary bedding in the argillite.

Samples Ar-g and Al-a are virtually identical in hand specimen, except the latter has a discernably blacker color. Both specimens have a felsic (quartz-feldspar) content of 60 to 70%, which is fresh and unaltered, and in each, the only mafic mineral is a very fresh looking, dark brown biotite. In addition, each contains the same opaque, tentatively identified as magnetite. Section Ar-g contains 20-25% biotite and 5-10% magnetite, while Al-a has a higher biotite content (30-35%) and less magnetite (3-5%). The increased biotite content in Al-a explains its blacker color in hand specimen.

Microscopically, flakes of biotite have their long dimensions preferentially orientated, they form discontinuous stringers which crenulate between felsic constituents (see Figure 21). Upon stage rotation the whole biotite mass displays uniform pleochroism, this feature verifies their preferred orientation. Biotite alignment defines a distinct foliation which, when viewed megascopically, strongly resembles primary bedding.

Sample Al-a is truncated by several quartz-feldspar veins, one of which contains a large (0.25-0.5 mm) perfectly euhedral crystal of apatite.

b) Argillite Xenolith (sample ARG-LENS)

This section, like those above, exhibits a hornfelsic texture,

consisting of a welded equigranular mosaic of sutured quartz and feldspar. However the grain size is much coarser, from 0.1 mm to 0.5 mm. The section is cut normal to what looks like bedding. Figure 22 illustrates that this foliation is seen on a microscopic scale as well.

Microscopically, a mixed-layering (=segregation banding) is apparent. Felsic, unaltered layers consist predominantly of sutured, badly strained quartz. While turbid green and red-brown bands contain massive and finely disseminated hematite and chlorite (with trace amounts of magnetite) plus feldspars altered to clays and/or sericite. Trace apatite is scattered throughout the section.

Modal abundance of the rock constituents is difficult, due to the fine grain size and the disseminated nature of some components. Estimated modal percentages are quartz plus feldspar 80 to 90%, hematite plus chlorite 10 to 20%, and apatite plus magnetite 1-3%.

## 6. Other Nonacho Series Sediments

Initially a contact metamorphic study was to be done on Nonacho sediments sampled along profile "A" (Figure 8) using profile "B" (Figure 9) as a control line. However it was discovered, by petrographic analysis that profile "A" samples all showed some degree of brecciation. In retrospect such features are expected as the profile crosses a major fault zone running NS along the west shore of Thekulthili Lake (Figures 7 and 8).

Dynamic metamorphic effects are gradually damped out eastward of the fault zone. Cataclasis has obliterated any contact metamorphic features which may have been imparted by the western pluton in

Figure 22

Photomicrograph of argillaceous xenolith.  
Notice the foliated texture of the section.  
Dark grey horizons consist of hematite, chlorite  
and sericitized (or kaolinized) feldspar.  
Lighter "bands" consist of quartz and trace  
apatite.

(plane polars, magnification 8X).



this area of the basin.

The petrography of the 10 Nonacho sediments collected from both profiles is outlined in Appendix A.

CHAPTER IV  
GEOCHEMISTRY AND PETROGENETIC INTERPRETATIONS

1. Analytical Methods

All major and minor elements of the granitoid rocks were analysed using crushed whole rock samples. Two methods were employed. For the major elements: Si, Al, Fe, Mg, Ca, Na, K, Ti, Mn, and P the fusion method was applied. As a fluxing agent 3g of a 1:1 lithium tetraborate and lithium metaborate mixture was added to 0.5000g of rock powder. Each sample was fused at 1200°C for several minutes in a Pt/Au crucible, and then quenched into glass discs. Trace element analyses were carried out on powder pellets. Each powder sample was backed with mowoil and then pressed into a pellet under 20 tons pressure.

All elemental assays were carried out on a Philips, model PW1-450AHP, x-ray fluorescence spectrometer in the Department of Geology, McMaster University. All major elements and the trace elements Ni and S were analysed using a Cr x-ray tube. The trace elements Cr, Co, Cu, Pb, As, and Zn were determined using a Mo-tube. The remaining trace elements U, Th, Rb, Sr, Y, Zr, Nb, Ba, Ce, La, Nd, V, and Ti were assayed with a tungsten x-ray tube. Resulting Rb, Sr concentrations using this method were anomalous. These two elements were then re-analysed with a Mo-tube, which yielded more acceptable values.

XRF data was reduced on McMaster University's CDC 6400 compu-

tor. Major elements are reported as weight percentages of their respective oxides, and trace elements are given in p.p.m. (see Appendix C).

Mesonorm compositions listed in Appendix B were calculated using a computer program formulated by Birk (1978), and are based on major element cation percentages (see Chapter III). However the program included weight percent conversions of the normative components quartz (Qtz), albite (Ab), orthoclase (Or), and anorthite (An) suitable for plotting ternary petrogenetic phase diagrams (eg., Qtz -Ab-Or).

## 2. Chemical Variation Diagrams

In the study of igneous rocks many geochemical (major and trace element) variation diagrams have been produced with the underlying assumption that crystallization differentiation (fractional crystallization) controls magmatic evolution. However Krauskopf's (1979) view is that a variation diagram is by itself inconclusive proof that a rock (or group of rocks) has differentiated from a single magma. He suggests that if a group of rocks are related by differentiation then they should form a smooth trend on a variation diagram, but if the group are derived from separate intrusives then smooth curves may or may not result. Green and Poldervaart (1958) suggest that a scatter of points on a chemical variation diagram is indicative of "locally operative processes" predominating over fractionation. In this study nothing is implied about the correctness of the differentiation hypothesis except when variation diagrams are used in conjunction with other lines of evidence, be it petrographic, petrochemical or field oriented.

Perhaps the most useful function of variation diagrams is to graphically differentiate between rock types whose differences are not obvious from whole rock analyses alone.

### 3. Major Elements

Several linear and ternary variation diagrams were employed in this study. These were constructed using elemental oxide and cation weight percentages, as well as the salic components Qtz, Or, Ab, and An of the mesonorm.

#### a) Linear Variation Diagrams

The various indices utilized here in constructing linear variation diagrams are defined below:

(1) Modified Larsen Index =  $1/3 \text{ Si} + \text{K} - \text{Ca} - \text{Mg}$

Used principally to show the variation of minor elements in relation to the major components.

(Nockolds and Allen, 1953)

(2) Felsic Index = 
$$\frac{(\text{Na}_2\text{O} + \text{K}_2\text{O}) \times 100}{\text{Na}_2\text{O} + \text{K}_2\text{O} + \text{CaO}}$$

Suggested to show alkali enrichment at the expense of Ca during fractional crystallization of felsic minerals.

(Simpson, 1954)

(3) Mafic Index = 
$$\frac{(\text{FeO} + \text{Fe}_2\text{O}_3) \times 100}{\text{MgO} + \text{FeO} + \text{Fe}_2\text{O}_3}$$

To possibly illustrate how mafic fractionation leads to iron enrichment at the expense of magnesium.

(Wager and Deer, 1939; Simpson, 1954)

(4) Alkalinity Ratio = 
$$\frac{\text{Al}_2\text{O}_3 + \text{CaO} + \text{total alkalis}}{\text{Al}_2\text{O}_3 + \text{CaO} - \text{total alkalis}}$$

(When  $\text{SiO}_2$  exceeds 50% and  $\text{K}_2\text{O} : \text{Na}_2\text{O} > 1 < 2.5$ , then  $2(\text{Na}_2\text{O})$  is substituted for total alkalis)

To distinguish different degrees of alkaline or calc-alkaline affinity between a variable igneous suite.

(Wright, 1969)

To supplement the Alkalinity Ratio in determining if both alkaline and calc-alkaline granites existed in the area, several other plots were attempted. For instance the Peacock Alkali-Lime index (the weight percentage of  $\text{SiO}_2$  at which the weight percentages of  $\text{CaO}$  and  $(\text{Na}_2\text{O} + \text{K}_2\text{O})$  are equal on a  $(\text{Na}_2\text{O} + \text{K}_2\text{O})$ ,  $\text{CaO}$  vs  $\text{SiO}_2$  plot), the AFM ( $\text{Na}_2\text{O} + \text{K}_2\text{O}$ ,  $\text{Fe}_2\text{O}_3$ ,  $\text{MgO}$ ) ternary and the Differentiation Index (sum of the normative salic components quartz (Qtz), albite (Ab), orthoclase (Or), nepheline (Ne), leucite (Lc), and kalsilite (Kp) in weight percent) were discarded, as a full silica range suite (eg. the Skaergaard intrusion) is required to distinguish an alkaline or calc-alkaline trend. The granitoid as plotted using the latter three parameters showed little contrast from one another.

However, the weight percent  $\text{SiO}_2$  vs alkalinity ratio plot suggested by Wright, 1969) in Figure 23 illustrates that the younger granite has a higher calc-alkaline affinity than the more alkaline basement granites. The author stresses here a feature common to this and all subsequent variation diagrams. That is, the low degree of scatter the younger granite samples display relative to basement granites. Clearly the younger granite is more homogenous geochemically.

Binary plots of mafic index vs alkalinity ratio and felsic index vs mafic index are given in Figures 24 and 25 respectively. These serve to illustrate the possibility that, biotite in the younger granite is more fractionated (greater Fe enrichment) than that occurring in basement granites. The Fe enrichment in the young-

Figure 23

Semi-log plot of Weight% of  $\text{SiO}_2$  vs Alkalinity Ratio.  
The dashed field contains the majority of younger  
granite samples.  
Lines separating alkalinity fields after Wright,  
1969.

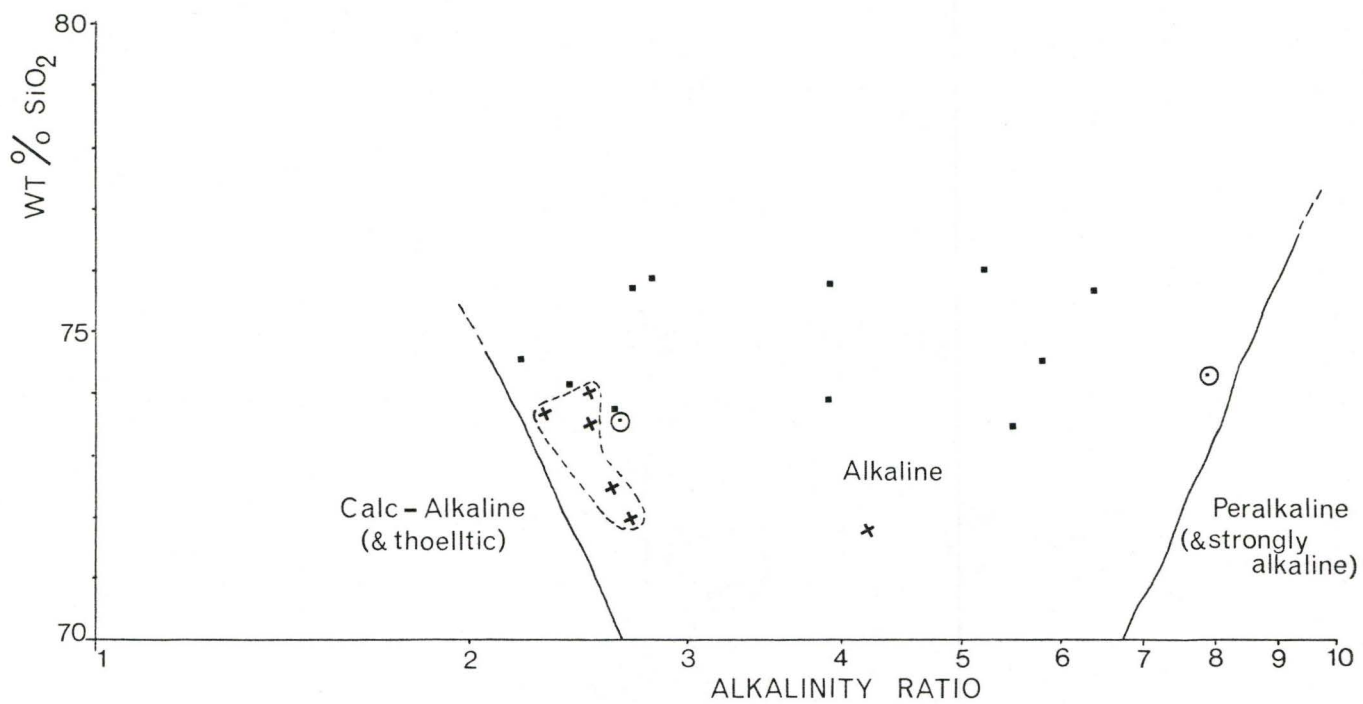


Figure 24

Mafic Index vs Alkalinity Ratio.  
Dashed lines delineate younger granite  
and basement granite fields.

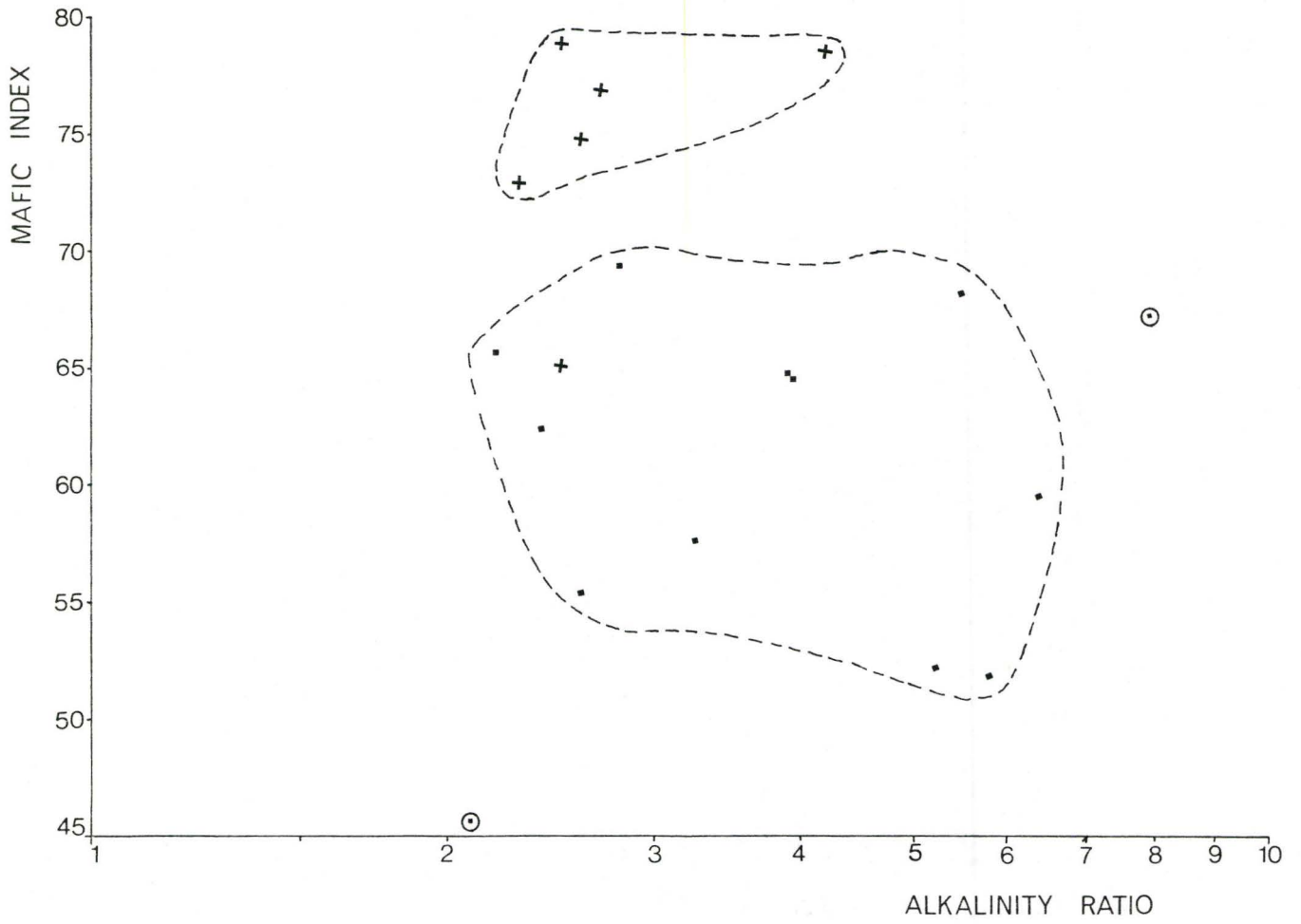
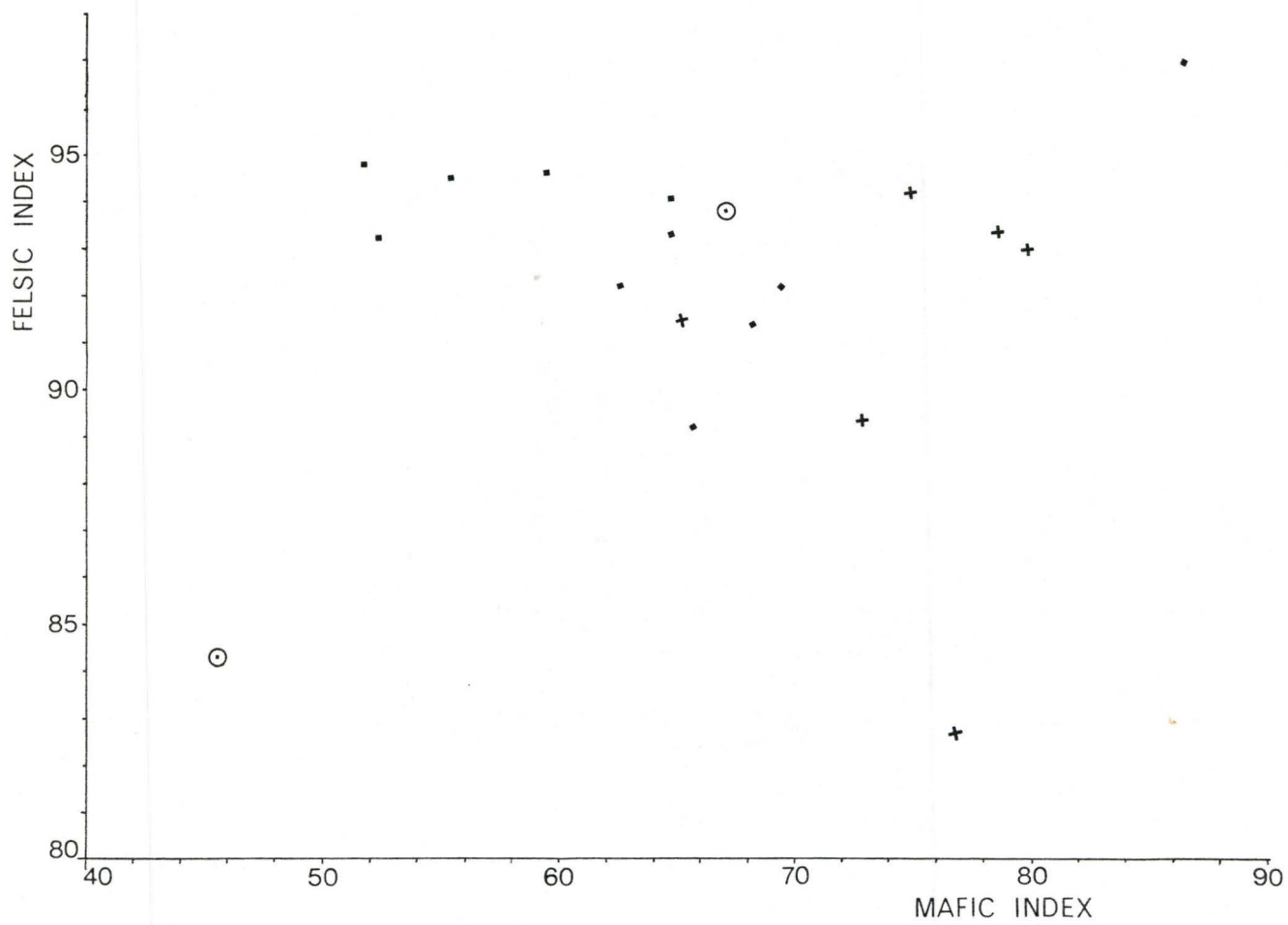


Figure 25

Felsic Index vs Mafic Index.  
(after Simpson, 1954)



er granite is exemplified by its higher biotite content. Plotting Mg/Fe percent ratio in biotite (listed in mesonorm tables, Appendix B) vs mafic index (Figure 26) appears to substantiate the hypothesis that biotites in the younger granite have undergone greater iron enrichment. This is not to say however that the two granitoids were derived from the same magma source, and that the younger granite has undergone greater mafic fractionation. On the contrary the granitoids may be totally unrelated and Figures 23 to 25 only serve to indicate the younger granite has a higher mafic index and a lower biotite Mg/Fe value.

All major elements (cation weight percentages) were plotted against the Modified Larson Index. The majority of these only illustrated that the two granitoids have approximately equivalent major element geochemistry relative to the Larson Index. However Figure 27 shows that basement granites have lower Ti and P contents, while Figure 28 indicates they have a higher Si content (average of 2 wt. % greater) relative to the younger granite. The fact that P concentrations in most basement granites is below the level of detection is reflected in their petrography by the absence of apatite.

The major oxides of Daly's (1933, p. 9) average calc-alkaline granite (546 analyses) were compared to the averages of the two granitoids. It was discovered that both granites were significantly richer in  $\text{SiO}_2$ ,  $\text{K}_2\text{O}$ , and volatiles ( $\text{H}_2\text{O}$ ,  $\text{CO}_2$  etc., detected by loss on ignition) but poorer in all other major oxides. The younger granite contains 2.7% and 1.7% more  $\text{SiO}_2$  and  $\text{K}_2\text{O}$  respectively, while basement granites are 4.6% and 2.0% richer in these oxides.

The author suspected that the granitoids were approaching alka-

Figure 26

Mesonorm biotite Mg/Fe percent ration vs Mafic Index.  
Dashed line delineates younger granite field.

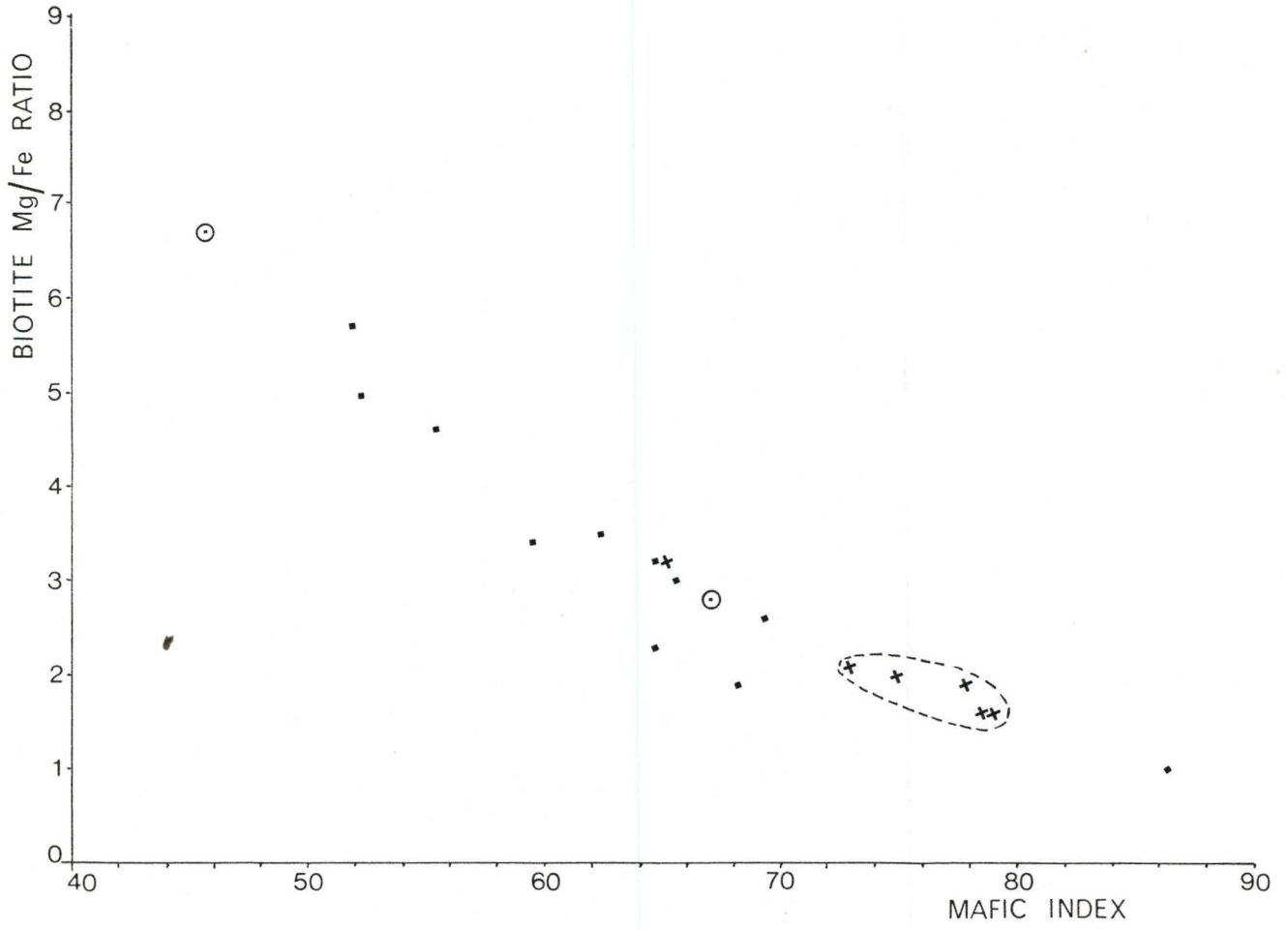


Figure 27

Weight percent Ti vs Modified Larsen Index.  
and  
Weight percent P vs Modified Larsen Index.

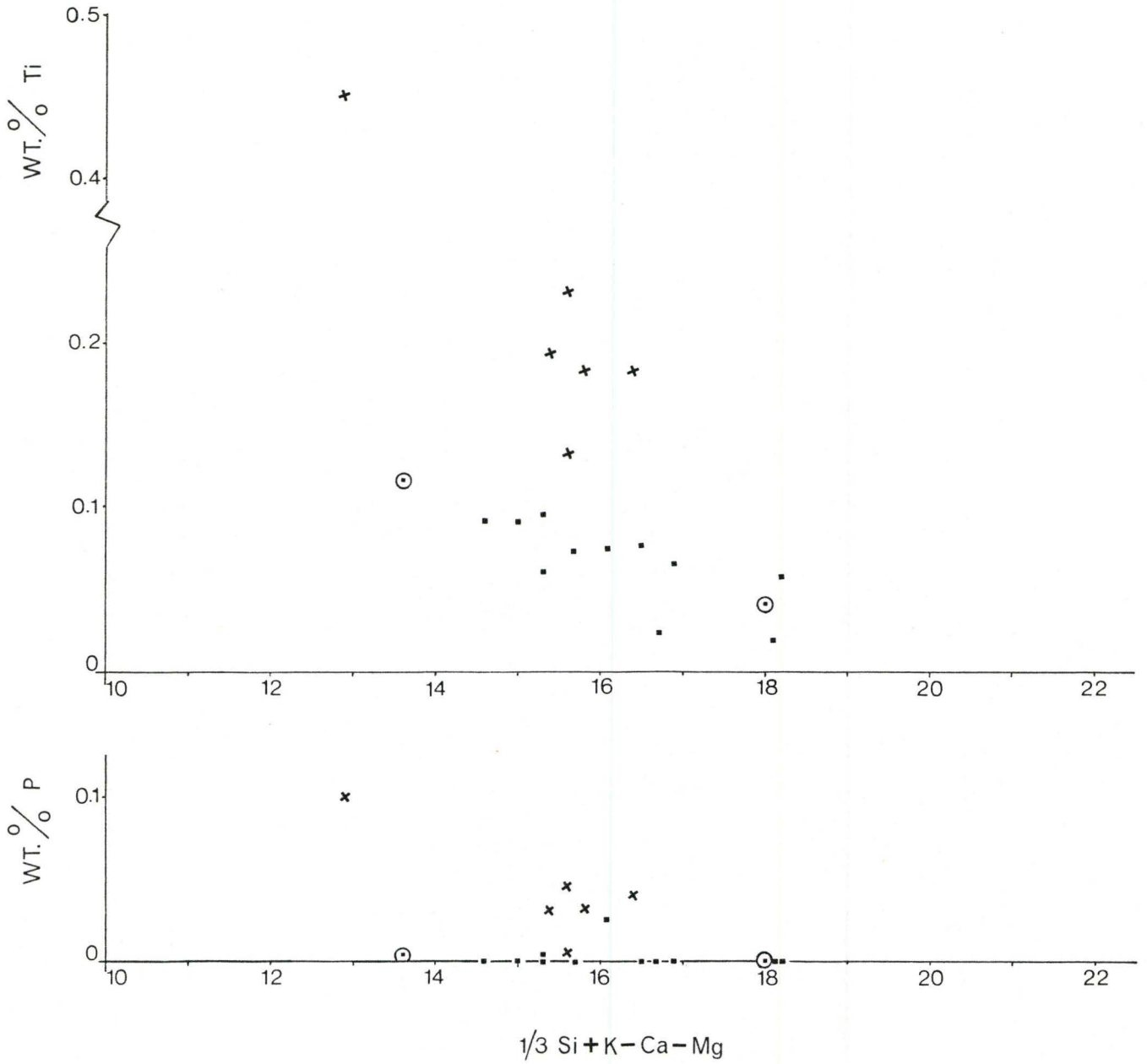
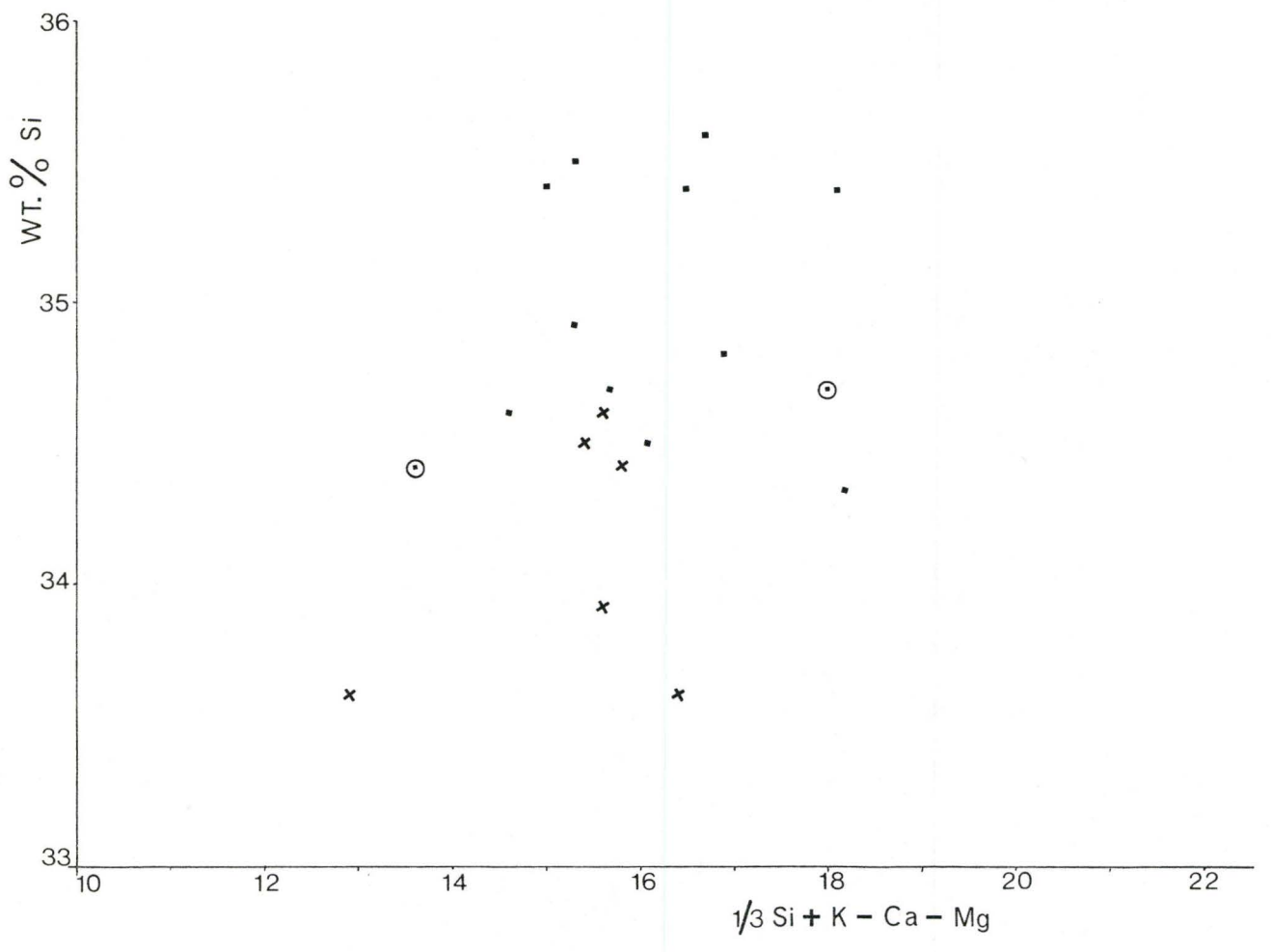


Figure 28

Weight percent Si vs Modified Larsen Index.



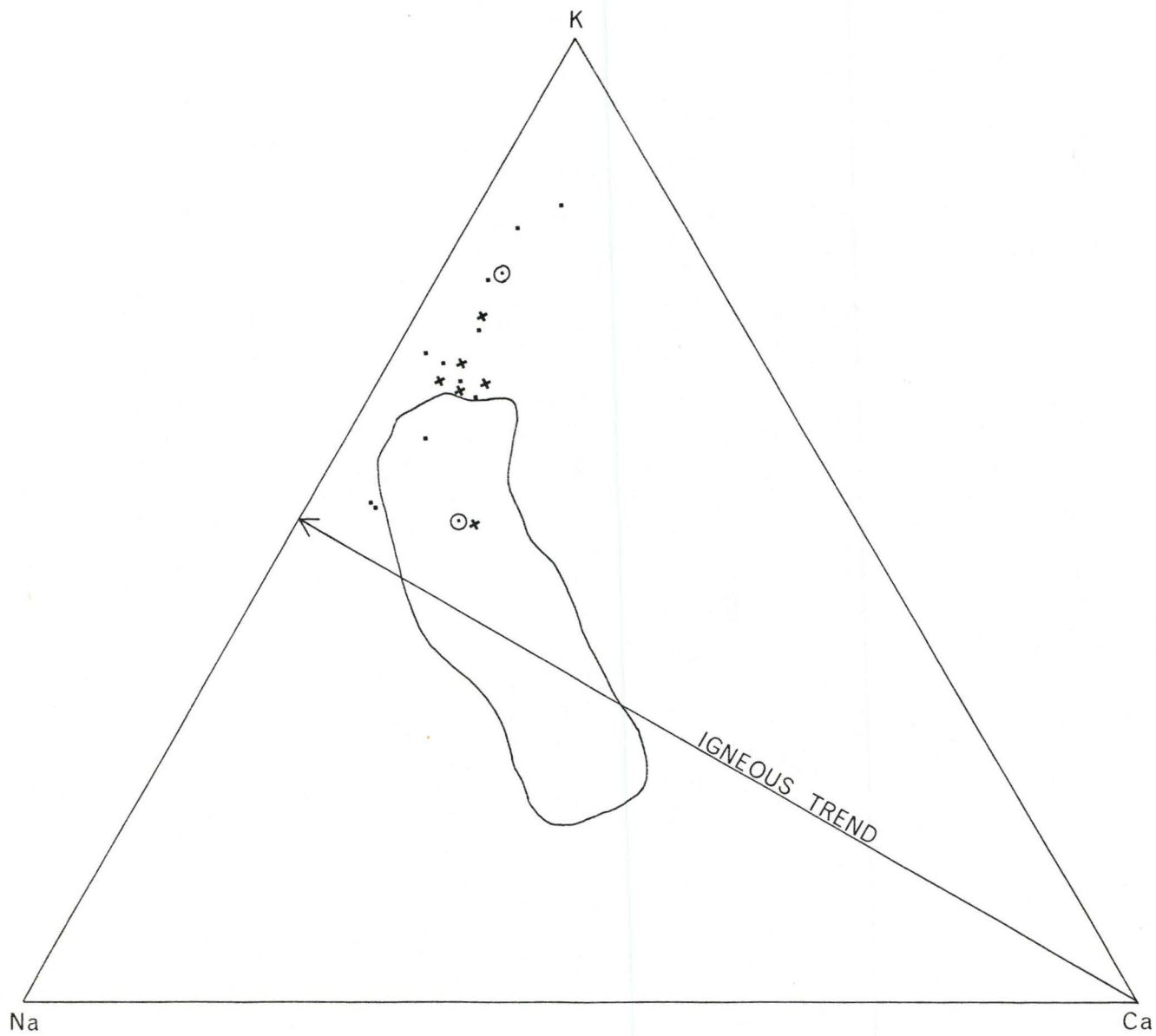
li granite composition, so they were compared to the average alkali granite (48 analyses) listed by Nockolds (1978, p.31). It was found that basement granites approximate an average alkali granite while the younger granite is intermediate between calc-alkaline and alkaline compositions. This substantiates the plot of  $\text{SiO}_2$  vs alkalinity ratio (Figure 22) as an indicator of alkaline affinity. Furthermore, petrographic analyses (Chapter III) agree with the suggestion that basement granites are alkaline while the younger granites is more calc-alkaline (refer particularly to Figure II).

#### b) Ternary Variation Diagrams

In Figure 29 the granitoids are plotted on a K-Na-Ca ionic weight percent diagram. Superimposed on the diagram is the igneous trend line of Green and Poldervaart (1958) and the delineated field for "magmatic granitic rocks" suggested by Raju and Rao (1972). In their studies a large number of analyses were utilized from different parts of the world, including the data of Daly (1933) and Nockolds (1954). Consequently the present author considers their conclusions at least statistically justified. Green and Poldervaart's (1958) igneous trend line runs from, the Ca apex to the point which bisects the K-Na side, and is meant to indicate the ideal fractionation trend from mafic to felsic rocks. The greater the deviation of plots from this line the more likely "locally operative processes" have dominated over ideal fractionation in the petrogenesis of the rock suite. Clearly, from Figure 29, processes other than simple fractional crystallization have caused the granitoid suites to plot on the potassic side of the line.

Figure 29

Plot of the K-Na-Ca ternary system.  
The irregular line delineates the field  
for magmatic granites (after Raju and Rao,  
1972). The igneous trend line of Green  
and Poldervaart (1958) separates K and Na  
fields.



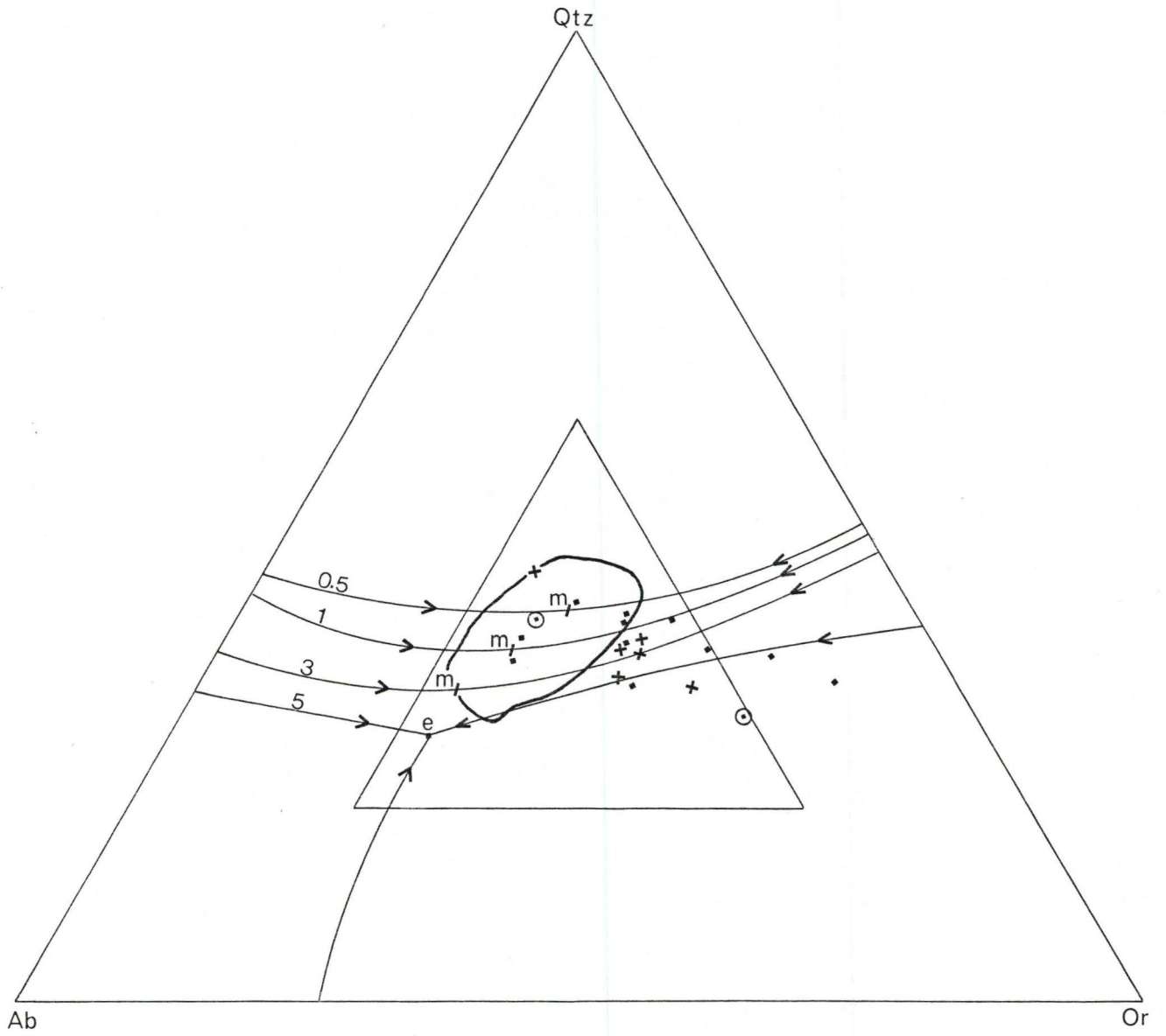
The delineated field of Raju and Rao (1972) in Figure 29 is postulated to separate "magmatic granites" from "replacement granites". The two types are of "proved origin" and presumably were initially distinguished on the basis of field relations and/or petrographic distinctions. The term "replacement" here is used in the context of metamorphic and/or metasomatic "granitization" of pre-existing rock types, and is not meant to suggest that a magmatic phase was not involved (Raju and Rao, 1972). All but three granitoid samples (over 80%) in Figure 29 would be defined as replacement granites. Further discussion of the K-Na-Ca system is reserved until later.

Extensive experimental studies by Tuttle and Bowen (1958) have been done in the quaternary system  $\text{NaAlSi}_3\text{O}_8(\text{Ab}) - \text{KAlSi}_3\text{O}_8(\text{Or}) - \text{SiO}_2(\text{Qtz}) - \text{H}_2\text{O}$ . The granitoids are plotted in Figure 29 on the approximated Qtz-Ab-Or ternary, as projected from the  $\text{H}_2\text{O}$  apex. Superimposed on this diagram are curves for water saturated liquids ( $\text{PH}_2\text{O}$  isobars) in equilibrium with quartz and alkali feldspar. These curves can be considered as cotectic boundaries (or lines of liquid descent) which separate the crystallization fields of quartz and alkali feldspar. Centered about these boundaries are thermal "troughs" into which granitic liquids move, towards the isobaric minima (m, in Figure 30, upon continued cooling and fractionation (Tuttle and Bowen, 1958). The principle effect of water in a granite system is as a fluxing agent which lowers the melting point of granitic rock (Clapeyron effect). The amount of water held in the melt is a function of pressure. On the Qtz-Ab-Or diagram increasing pressure lowers the isobaric minima and shifts it towards the Ab apex. Accor-

Figure 30

Plot of the Qtz-Ab-Or ternary, showing the curves for water saturated liquids in equilibrium with quartz and alkali feldspar at water pressures of 0.5, 1.0, 3.0, and 5.0 kb. Isobaric minima are labeled m up to 5.0 kb where a ternary eutectic, e, is generated. Arrows indicate direction of liquid descent upon cooling and fractionation. The inner triangle contains rocks with greater than 80% Qtz-Ab-Or (true granites). The oval field is the 4% contour for 571 plutonic granites listed in Washington's (1917) tables.

(Data from Tuttle and Bowen, 1958,  
and Carmichael et al, 1974).



ding to Carmichael et al (1974) at water pressures above 4 kb (or the equivalent of approximately 9 weight percent  $H_2O$ ) the liquidus surface temperature of the melt is depressed to the point where it intersects the alkali feldspar solvus and a ternary eutectic replaces the isobaric minima (see Figure 30).

The oval field delineated in Figure 30 indicates the area where the majority of 571 granites analysed in Washington's (1917) tables concentrate. The position of this field is closer to the Qtz-Ab side line than that originally shown by Tuttle and Bowen (1958). This modification follows the suggestion of Parslow (1969) that mesonorm compositions are better suited to this ternary than are CIPW norms, as the latter tend to over estimate Or (due to  $K^+$  in micas), and underestimate Qtz in granitic rocks. In any case the present position of the "maximum granite" field appears to strengthen the statement of Tuttle and Bowen (1958, p.77):

The coincidence between the maxima for granites and the thermal deep (trough) of the isobaric equilibrium diagram for lower water vapor pressures is far too strong to be fortuitous. There can be little doubt that magmatic liquids are involved in the genesis of granitic rocks, and those who propose that granites are formed primarily by solid diffusion, hydrothermal replacement, or by any other mechanism not involving a magma must demonstrate an alternative method of controlling, to such a strong degree, the composition of granites.

Assuming for the moment that this statement is valid then does this imply that most of the granites studied here (65% of which plot outside the maximum granite field in Figure 30) never crystallized from a magma? or alternatively, did they completely crystallize at temperatures significantly above the isobaric minima? Other viable explanations are those previously cited from Green and Poldervaart

(1958) and Raju and Rao (1972) for the K-Na-Ca system, i.e., these granite suites are the end result of "locally operative processes" and/or "replacements of preexisting rocks".

Before drawing any conclusions the author would like to discuss the merit of Tuttle and Bowen's (1958) Qtz-Ab-Or ternary as a petrogenetic indicator in this study. Several authors (Kleeman, 1965, Carmichael et al, 1974, Winkler, 1976, Krauskopf, 1979, among others) have criticized the validity of the diagram as it ignores the importance of anorthite (An) component in the granite system (*sensu stricto*) Qtz-Ab-Or-An-H<sub>2</sub>O. Both Winkler (1976, p.293) and Krauskopf (1979, p.329 Figure 14-4) have stressed that in granite systems where Ab/An ratios are less than about 8.0 the simple Qtz-Ab-Or system is invalid. Figure 31-a shows that as An content increases two things happen to the Qtz-Ab-Or ternary diagram (projected from the An apex): 1) the isobaric minima becomes a triple point (ternary eutectic) to the fields of quartz, plagioclase, and feldspar, and 2) the "minimum melting" temperature is increased, as evidenced by an increasing field of plagioclase.

Only four granite samples in this study have Ab/An ratios less than 8.0, thus it would appear that the Qtz-Ab-Or ternary is a viable approximation of the granite system(s) in this case. However on the suggestion of Carmichael et al (1974, p.235) that even small amounts of An are important in describing the crystallization histories of natural acid magmas, an alternative diagram was sought.

The ternary diagram of An-Ab-Or (projected from the quartz apex) suggested by Kleeman (1965, Figure 4A) is given in Figure 31-b. On this diagram the position of the low temperature trough axes

Figure 31-a

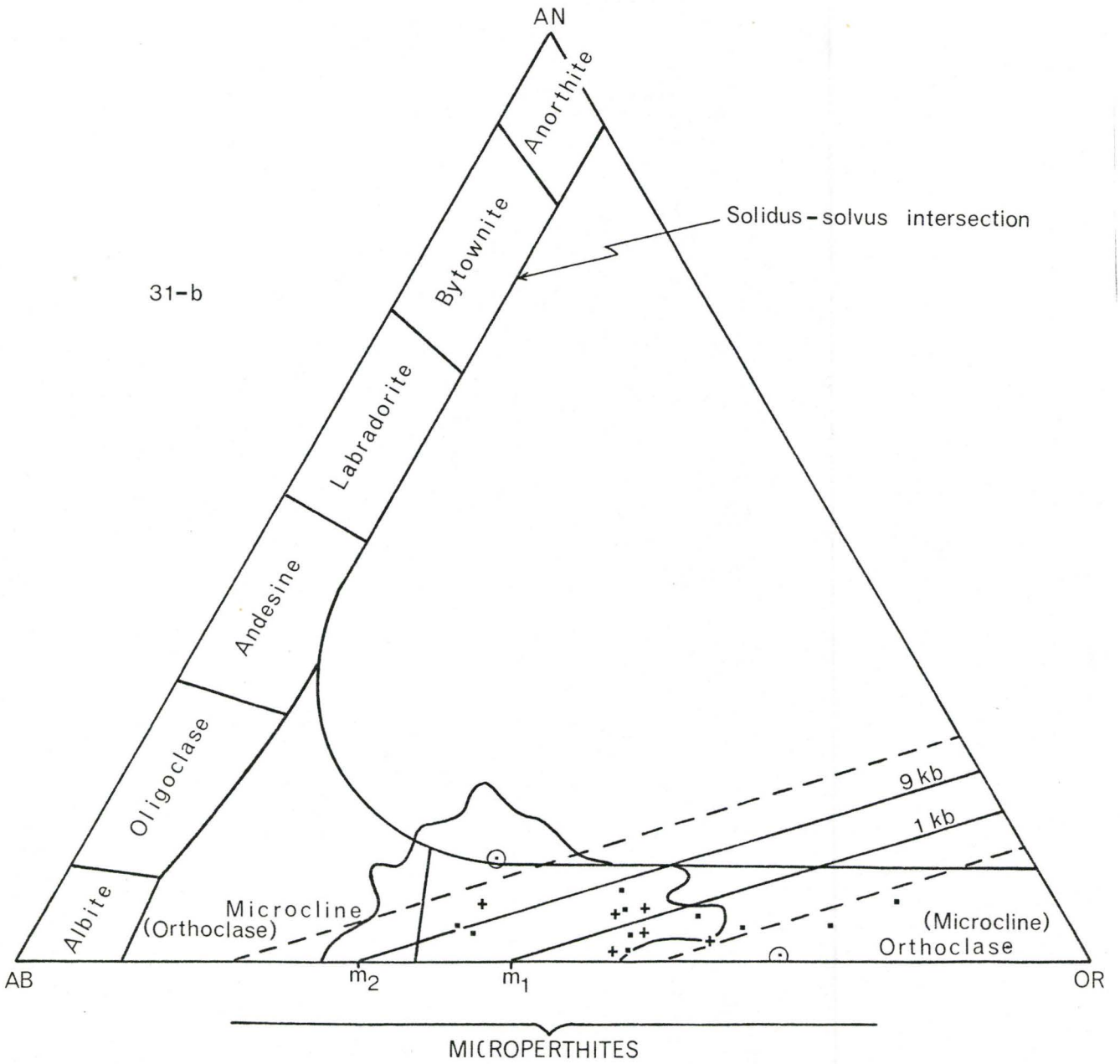
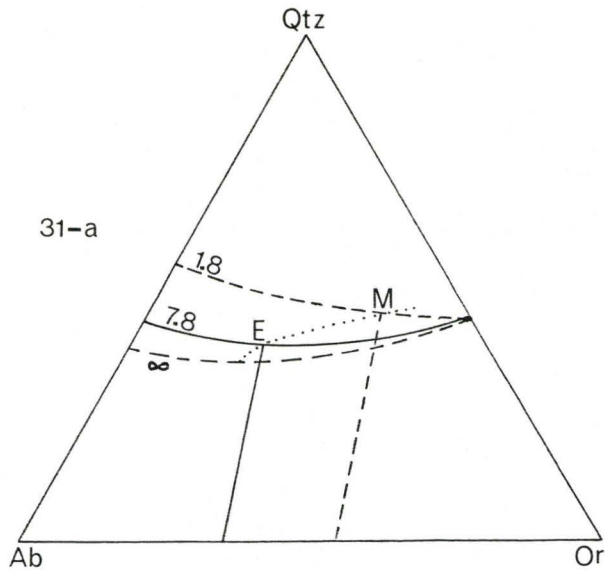
Variation in field boundaries with decreasing Ab/An ratios at 2 kb. water pressure in the Qtz-Ab-Or ternary as projected from the H<sub>2</sub>O apex. Points E and M are ternary eutectics representing the "minimum melt" composition at Ab/An = 7.8 and Ab/An = 1.8 respectively.

(after Krauskopf, 1979, p.329)

Figure 31-b

Plot of the An-Ab-Or ternary system as projected from the quartz apex. Solid straight lines are the low temperature trough axes at 1 kb and 9 kb water pressure. Dashed lines represent the  $\pm 3\%$  analytical error limits of trough positions. Irregular solid line denotes the 2% contour for 1269 rocks with greater than 80% normative Qtz + Ab + Or list in Washington's (1917) tables. Solid curved line represents the solidus-solvus intersection for the ternary feldspars. Points  $m_1$  and  $m_2$  are isobaric minima at 1 kb and 9 kb water pressures respectively.

(data from Tuttle and Bowen, 1958,  
Kleeman, 1965, and Deer et al, 1966)



(=plagioclase to K-feldspar cotectic) at 1 kb and 9 kb water pressure are superimposed upon the "average granite" field shown by Tuttle and Bowen (1958, Figure 67). Modification of the average granite field position is unnecessary in this diagram because Or is the only component which varies between mesomorms and CIPW norms, thus only a dramatic difference in calculations would change the position of data relative to the trough (Parslow, 1969).

Figure 30 illustrates that the younger granite and basement granite samples both show a strong correlation with the low temperature trough (within the  $\pm 3\%$  error limits) and the average granite composition. The majority of samples center around the 1 kb trough axis and cluster along the Or side of the average granite field. This diagram strongly suggests that both granite suites crystallized from a liquid phase. The position of the isobaric minima on the Ab-Or edge varies from  $Ab_{68}Or_{32}$  at  $PH_2O = 9$  kb to  $Ab_{55}Or_{45}$  at  $PH_2O = 1$  kb. As in Figure 30 the granitoids plot on the Or side of the minima suggesting they completely crystallized above the "minimum melt" temperature. Note also that all samples plot below the solidus-solvus intersection curve postulated for the ternary feldspar system (Deer et al, 1966) in a zone common to perthitic feldspars (Kerr, 1977, Figure 13-13).

#### 4. Trace Elements

The most extensive trace element work has been done on volcanic rather than plutonic igneous rocks (Carmichael et al, 1974). As a result much less is known about trace element distributions and their significance as petrogenetic indicators in plutonic rock evolution.

This study will be restricted predominately to the analysis of three trace elements-Rb, Sr, and Ba. These are considered to be most useful in the study of granitic systems, as they concentrate only in the major silicate phases and not in accessory minerals (McCarthy and Hasty, 1976). Rb, Sr, and Ba enter the crystal structure of silicates either as isomorphic substitutions of a major element, or as random inclusions in crystal lattice vacancies (Krauskopf, 1979). Trace elements generally substitute for major element cations according to similarities in ionic radii and ionic charge, based on the empirical "rules" of Goldschmidt (1954). Predictions based on these rules are in good agreement with observations made concerning elements comprising the first three groups of the periodic table, i.e. alkali metals, alkali earth metals, Y and rare earth elements (Krauskopf, 1979).

As it is generally assumed that magmatic differentiation controls the distribution of major element geochemistry, then it follows that the same process dictates trace element concentrations. According to Carmichael et al (1974, p.62) the chemical pattern of progressive fractionation is successive enrichment of silica and alkalis in residual liquids. Due to ionic incompatibility, elements such as Li, Na, K, Rb, Ba, Y (and rare earths), Nb, and Zr (among others) are not accommodated in early crystalline phases (Birk, 1978, Carmichael et al, 1974). The most common substitutions in residual phases are: Ba and Rb for K; and Sr with a radius intermediate to Ca and K substitutes for both. Ba tends to concentrate in early K minerals (eg. biotite) while Rb is enriched in the later K-feldspars. Sr tends to remain fairly constant during fractionation as it sub-

stitutes in early Ca minerals and later K minerals but tends to be lower in K-feldspar rich rocks (i.e. granites) than in plagioclase rich ones (Krauskopf, 1979). Zirconium due to its large ionic size and ionic charge does not enter any common mineral phases but rather is usually contained in the separate phase of zircon (Mason, 1958). However the absence of zircon in the granitoids studied here could be used as a measure of magmatic alkalinity (Birk, 1978), because under alkaline conditions Zr tends to be incorporated in mafic minerals and will not crystallize as zircon (Eowden, 1966).

The method of trace element study adopted here is the use of ratio variation of similar elements. The ratios listed in Appendix C are K/Na, K/Rb, K/Ba, Ba/Rb, Sr/Ba, Ca/Ba, Ca/Sr, Rb/Sr, and Ti/Zr. Of these Rb/Sr, Ti/Zr, Ba/Rb, and K/Rb occur in subsequent linear variation diagrams. The others are not given as such since they do not distinguish between the two granite suites.

Sixteen trace elements which were analysed but are not listed above are given in Appendix C. They were discarded from further study for one of two reasons: 1) their abundance was near the level of XRF detection and thus their concentrations are only semi-quantitative (eg. base metals, U, Th), and/or 2) they do not show appreciable substitution in residual salic phases.

However there are some important distinctions between the two granite suites based on some of these trace element averages. The younger granite has on average: 2, 2.6, 4, 2.6, 1.5, and 2.2 times more Pb, La, Ce, Nd, Nb, and Ni respectively than do basement granites. Smith (1974, p.117) found that in rocks containing coexisting plagioclase and K-feldspar, the plagioclase contains several times

more rare earth elements than K-feldspar. Since the younger granite contains much more plagioclase than basement granites this could explain its higher La, Ce, Nd, and Y contents. Alternatively contrasting rare earth contents may indicate the two granitoids were derived from different sources. Furthermore, since rare earth elements tend to preferentially concentrate in residual liquids during fractionation rather than enter crystalline phases (Carmichael et al, 1974, p.632) their greater abundance in the younger granite could indicate it is more differentiated than the basement suite. It has also been shown by Nagasawa and Schnetzler (1971) and Hanson (1978) that apatite contains high rare earth concentrations. This mineral is contained in the younger granite but is absent in basement granites. Log-log plots of Rb vs Sr, wt. % K vs Rb and Ba vs Rb for the two granite suites are given in Figures 32, 33, and 34 respectively. All three clearly indicate the younger granite has a significantly greater concentration of Rb. In addition Figure 34 shows it has higher Ba abundance.

These concentrations seem anomalous since both Rb and Ba substitute for K, yet both granitoids contain approximately equivalent amounts of K (see Figure 33). One solution to this paradox is that the granites crystallized from different source magmas, with the younger granite melt carrying more Rb than the other. Or alternatively as Carmichael et al (1974, p.361) contend, large regions of continental shields have been depleted in the radiometric elements U, Th, and Rb due to prolonged solution by high-grade metamorphic fluids. This may be true of the basement rocks studied here.

Superimposed on Figure 33 are the "R-lines" ( $R = \text{wt.}\% \text{ K} \times 10^4$ )

Figure 32

Log-log plot of Rb vs Sr based on ppm.  
Dashed lines separate younger and older granite  
fields.

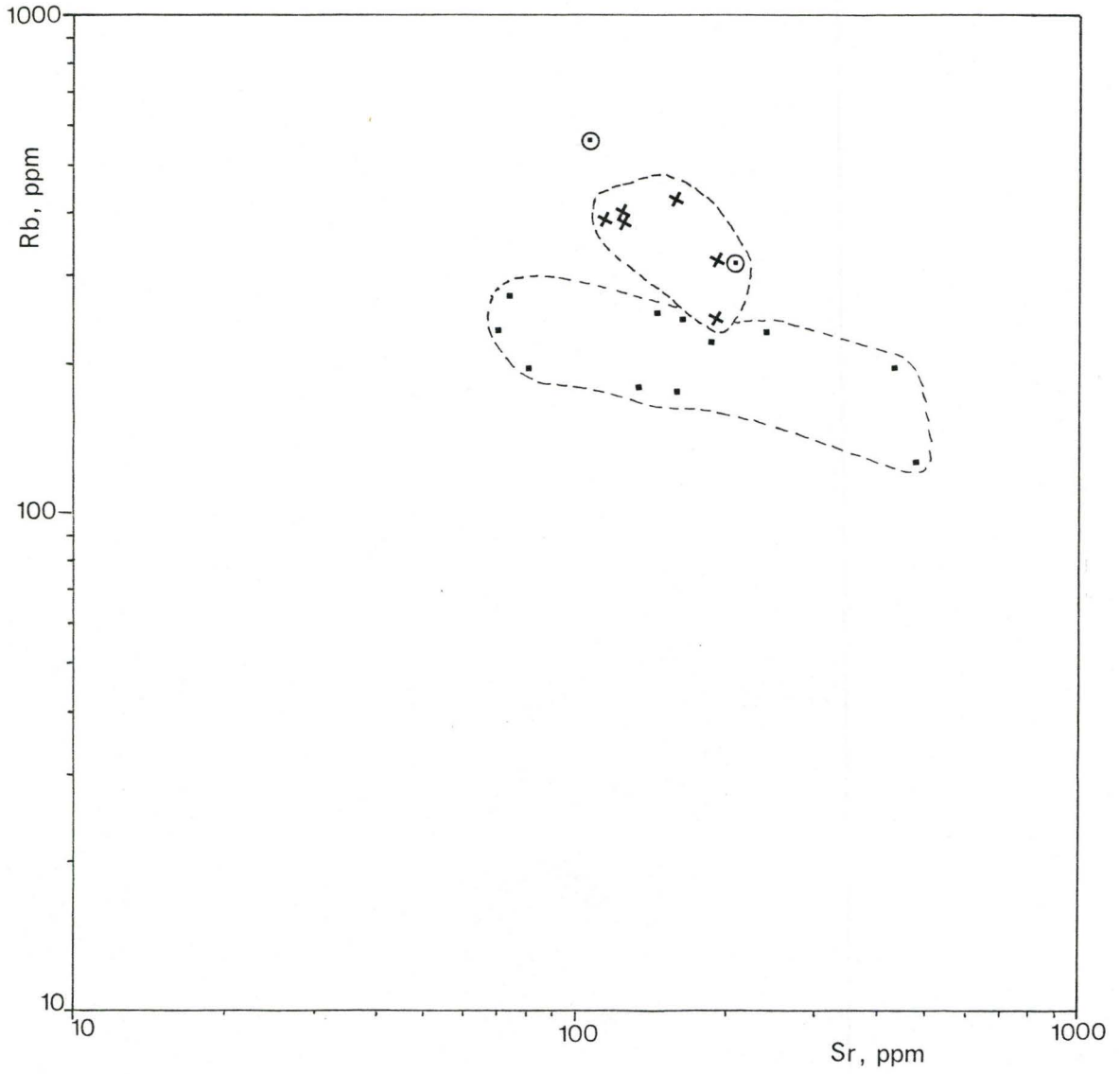


Figure 33

Log-log plot of wt. % K vs Rb ppm.  
Superimposed are the "R-lines" of Shaw (1968).

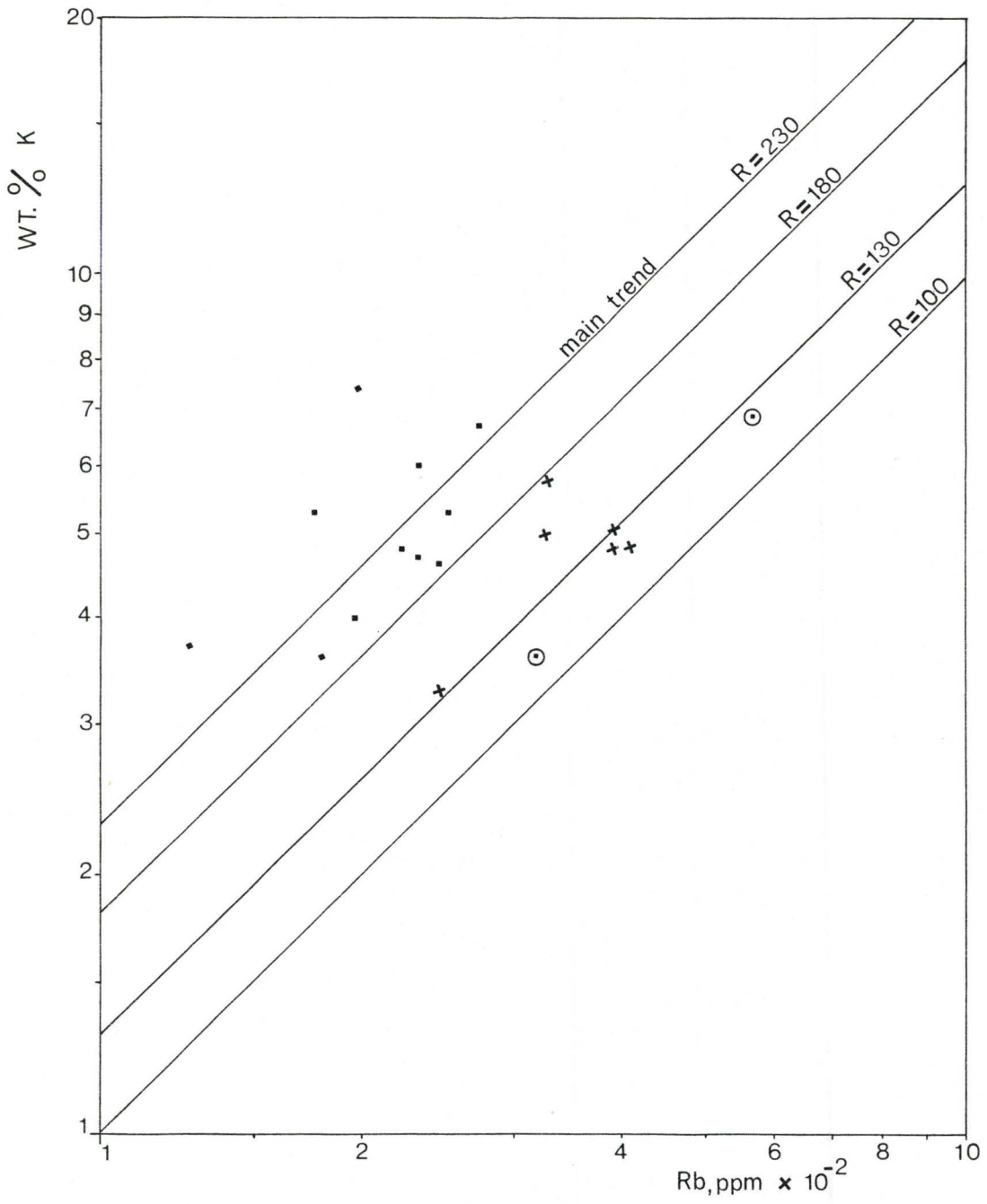
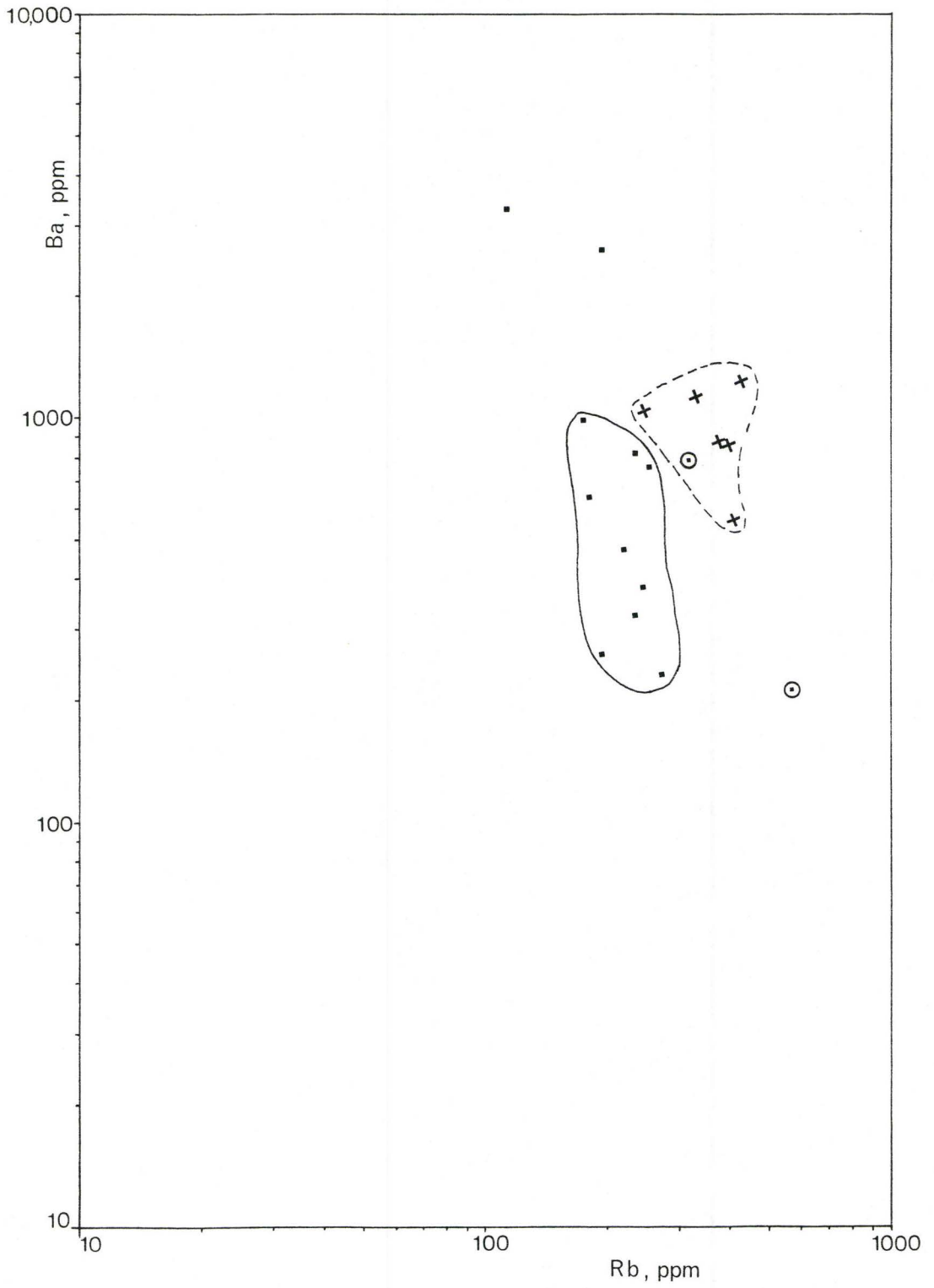


Figure 34

Log-log plot of Ba vs Rb based on ppm.  
Dashed and solid lines delineate younger granite  
and basement granite fields respectively.



p.p.m. Rb) given by Shaw (1968). The granite suite of the basement complex center about the "main trend line" ( $R=230$ ) determined for a wide variety of continental and oceanic rock types. Meanwhile most of the younger granite samples plot about the  $R=130$  line which is approaching the "pegmatite-hydrothermal trend" ( $R$  less than 100) for alkali-rich granites, syenites, pegmatites and related rocks (Shaw, 1968). The usefulness of K/Rb ratios in petrogenic studies of igneous rocks is uncertain. Many authors contend that decreasing  $R$  values are representative of increasing fractionation. Others such as Carmichael et al (1974) suggest that the widespread use of K/Rb ratios as an index of magmatic evolution is unwarranted.

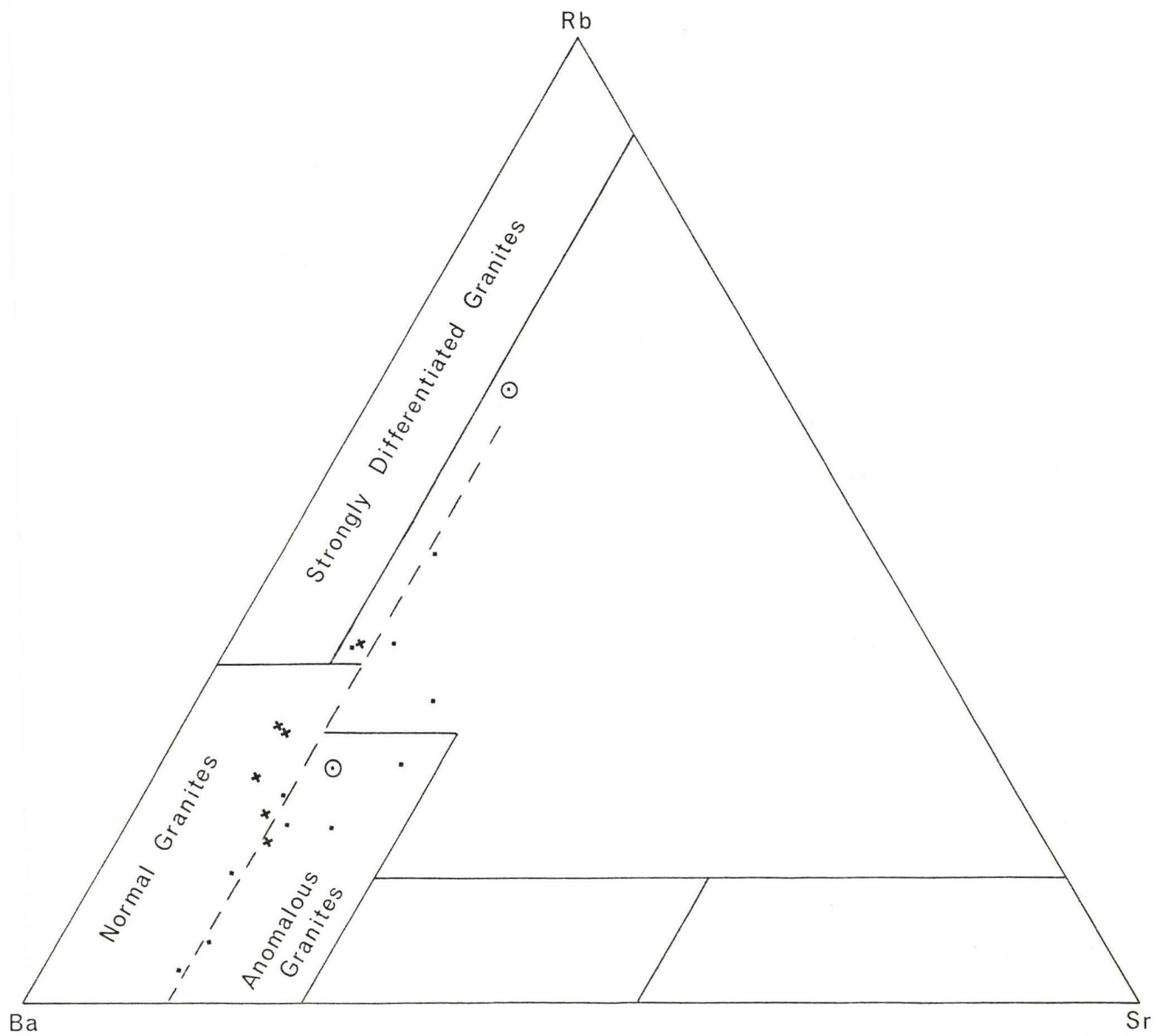
Whether or not K/Rb ratios are important petrogenetically is not the concern of this study, what is important however, is that the two granites are distinct in the concentrations of Rb they contain.

Perhaps a better method of tracing differentiation trends in granitic rocks is the Rb-Ba Sr ternary diagram proposed by Bouseily and Sokkary (1975). They claim that interpretation of fractionation trends based solely on absolute values of Rb, Ba, and Sr or on binary relations between any two of them are unreliable.

Figure 35 shows the granitoid samples as they plot on the Rb-Ba-Sr diagram. The criteria Bouseily and Sokkary (1975) used in selecting the various fields in the diagram are somewhat arbitrary and overgeneralized. Their criteria in choosing the "strongly differentiated granite" field is based on the assumption that "at the very late stages" of fractionation Rb is enriched and Ba impoverished in the residual K-minerals. In particular the merit of the "anomalous

Figure 35

Rb-Ba-Sr ternary diagram.  
Delineated fields and nomenclature after  
Bouseily and Sokkary (1975).



granite" field is questionable.

The majority of granite samples plot in the normal and anomalous granite fields, and almost all cluster about the line separating the two (dashed line in Figure 35). The line is significant in that it shows the two granite suites have near equivalent Sr contents. It also indicates that Sr plays a passive role in differentiation relative to Ba and Rb.

Figure 36 shows a plot of Ti vs Zr. This is included to illustrate that the two granites contain contrasting amounts of these two elements. The intrusive granite contains more of these elements than those of the basement complex. Ti and Zr are both large ions having high ionic charges, as such they generally do not substitute in any major silicate phase but rather form their own minerals—sphene and zircon respectively—during the latest stages of crystallization. However both sphene and zircon are absent from the petrographic analysis of the granite pluton. Thus the Ti is likely contained in ilmenite and biotite, with the latter probably hosting the majority of Zr as well, in either minute inclusions or lattice vacancies.

It was concluded earlier (major elements section) that the basement granites are alkali granites while the younger granite is more calc-alkaline. Thus if it is assumed for the moment that both granitoids derived from fractional crystallization, then it could be said the basement granites are the most fractionated. Now assuming both granite magmas were generated from the same source rock, then logically the basement granites, not the intrusive granite, would contain the greater abundance of Ti and Zr. Thus Figure 36 could be used as evidence arguing against a single magma source. Significant contrasts

Figure 36

Log-log plot of wt. % Ti vs Zr ppm.  
Solid and dashed lines delineate the basement  
granite and younger granite fields respectively.



in other trace element concentrations previously given appear to suggest the same conclusion.

##### 5. Significance of the migmatite-granite association

In Chapter II reference was made about the close association of paragneisses, migmatites and granitic rocks seen in the basement complex around Thekulthili Lake. A pertinent statement given by Winkler (1976, p.280) is worth noting here:

This world wide observation suggests that the spatial association of these rock types is due to processes occurring at similar temperature and pressure conditions in the deeper part of the crust and giving rise to high-grade metamorphic rocks, as well as to migmatites and granites. The origin of granites and migmatites in deep-seated parts of orogenic belts must be considered as directly connected with high grade metamorphism.

Based on the world wide petrographic observation that muscovite does not appear in migmatites, Winkler (1976, p.82) chooses the breakdown of muscovite in the presence of plagioclase and quartz to mark the transition from medium to high-grade metamorphism. It is therefore petrogenically significant that the migmatites and granites studied here do not contain any muscovite and are thus located in the highest temperature terrain of regional metamorphism. Assuming of course that muscovite, or the compositions necessary for its formation originally existed.

Mehnert (1968) distinguishes between two types of migmatites, injection migmatites, and "in-situ" migmatites. Of these, in-situ migmatites are the most common and are derived in-situ within a high grade metamorphic terrain. The component parts of in-situ migmatites as defined by Mehnert (1968) are:

- 1) The paleosome: the unaltered or somewhat modified parent rock, generally a paragneiss or gneissic granite.
- 2) The neosome: the portion formed during metamorphism and consisting of two parts:
  - a) The leucosome, contains mostly felsic minerals (quartz and/or feldspar), and has a fabric consistent with magmatic crystallization.
  - b) The melanosome, forms shistose layers surrounding the leucosome and is composed predominately of mafic minerals (eg. biotite, hornblende, garnet, sillimanite etc.).

Sampling in this study was restricted to leucosome layers and the scattered granitic bodies into which the migmatites graded. Rocks compatible with the paleosome are the paragneisses and granitic gneisses outcropping on the south shore of Thekulthili Lake (Figure 7). Donaghy (1977) studied the petrography of these paragneisses and found they contain a granodioritic composition with a high An ( $An_{30}$ ) plagioclase much in excess of K-feldspar. According to Winkler (1976) this is a common paragneiss composition which has derived from the high-grade metamorphism of an average shale.

#### Anatexis

Anatexis is defined as the generation of magma by the partial melting of pre-existing rocks. After many years of debate it is now generally accepted that anatexis is the predominate physico-chemical process which generates large regions of migmatic and granitic rock types. Opposing views of large scale metasomatic "granitization" of sediments are much less conclusive.

During a prograde metamorphic event paragneisses as described

above remain unchanged until a certain pressure-temperature threshold is reached and anatexis sets in. Partial melting can occur at temperatures as low as  $700^{\circ}\text{C}$  when  $\text{PH}_2\text{O}=2.0$  kb, and even lower at higher water pressures (Winkler, 1976). It must be emphasized however that since plagioclase rich gneisses are involved in anatexis, then the Ab/An ratio is also important in determining the temperature at which anatexis begins.

Assuming for the moment that the Ab/An ratio for the bulk composition of the gneissic protolith is 1.8 then at  $\text{PH}_2\text{O} = 2$  kb the "minimum melting" temperature would be  $705^{\circ}\text{C}$ , at the resulting melt composition  $\text{Qtz}_{45} - \text{Ab}_{15} - \text{Or}_{40}$  (based on experimental data listed by Winkler, 1976, p.293). This corresponds to point M in Figure 30-a. From Figure 30-a it is clear that as the Ab/An ratio decreases, there is a corresponding increase in Qtz and Or content and a decrease in Ab in the "minimum melt" composition. Furthermore, lowering the Ab/An ratio increases the minimum melting temperature for any given water pressure.

Therefore it is expected that Ab-rich gneisses are the first to begin melting during anatexis. Thus in a high grade migmatite complex the composition of leucosomes is greatly dependant on the original An content of the parent gneiss, and even anatexis of the same gneiss can produce melts of different composition, depending on the temperature reached at various places.

During anatexis a phase differentiation takes place whereby the parent gneiss is split into a melt portion of granitic composition (quartz and feldspar), and a Mg, Fe, Al and possibly Ca rich crystalline residue (Winkler, 1976). The granitic portion corresponds

to the leucosome while the mafic crystalline residue is the melanosome. The amount of water which is present is important in determining the amount of melt produced but has no effect on the temperature at which melting begins. If all available water is used up, then anatexis stops and a paleosome parent gneiss will remain, if anatexis has not gone to completion.

All granitic basement rocks studied here are very potassium feldspar rich, and carry less than 10% plagioclase. It appears at first paradoxical that such a rock can be derived from a gneiss carrying only subordinate amounts of K-feldspar. But from the previous discussion of experimental results, parent gneisses with the highest plagioclase and An contents are actually the most likely to produce K-feldspar rich leucosomes. Furthermore, if the parent gneiss contains only biotite, plagioclase, and quartz (the mineral assemblage common in high-grade paragneisses) then the only source of K is biotite (Winkler, 1976). The amount of biotite preserved during anatexis diminishes as the temperature increases, yet even at temperatures well above those at the beginning of melting; considerable biotite remains in the leucosome and continues to react with other minerals to form K-feldspar. Winkler (1976) contends that the granitic composition produced at the beginning of anatexis will be maintained even with increasing temperature. Simply more melt will be produced.

The above discussion is a viable petrologic explanation for the crystallization of the biotite alkali-feldspar granites and biotite syenogranites of the basement complex studied here. As a corollary, the anatectic interpretation explains the intimate co-

existence of migmatites, granite bodies, and high-grade gneisses.

#### 6. Hypersolvus and Subsolvus Granites and the Orthoclase to Microcline Transformation

Tuttle and Bowen (1958) define hypersolvus granites as granites in which sodium feldspar is, or was, held in solid solution with a perthitic potassium feldspar, where as in subsolvus granites a sodium-rich plagioclase coexists with the perthitic K-feldspar. Thus, it is implicit that the one feldspar hypersolvus granites crystallize as a mixed alkali feldspar at temperatures above the albite-orthoclase solvus; the maximum temperature of which was experimentally determined as approximately  $660^{\circ}$  (Tuttle and Bowen, 1958) at the composition  $Ab_{50}Or_{50}$ . Meanwhile subsolvus granites are presumed to crystallize at lower temperatures and higher water pressure in the "two-feldspar" subsolvus field.

The perthitic nature of the K-feldspar in both hypersolvus and subsolvus types is postulated to result from one of three processes: 1) unmixing of a homogeneous alkali (mixed) feldspar, 2) simultaneous crystallization of sodium rich and potassium rich feldspars, or 3) replacement of potassium by sodium feldspar (Deer et al, 1966). On the basis of experimental evidence (Tuttle and Bowen, 1958; Deer et al, 1966) the unmixing mechanism appears most viable, particularly in explaining microperthitic intergrowths. Microperthites appear to be restricted to alkali feldspars in the  $Or_{20} - Or_{85}$  compositional range (Deer et al, 1966).

From petrographic analysis (Chapter III) it is clear that the two granitoids studied have drastically different feldspar contents (see Figure II). The majority of basement granites are one feld-

spar, alkali feldspar granites, which conform to the hypersolvus classification, while the younger intrusive granite is the common two feldspar, subsolvus variety. Yet normatively the two granitoids are similar in their Ab-Or-An proportions. This means that, in the basement granites, the majority of plagioclase is held in solid solution in alkali feldspar (microcline-microperthite).

Solid solution in alkali feldspars of granites is favoured in high temperature, monoclinic orthoclase as opposed to lower temperature, triclinic microcline. Thus if the migmatites and granites of the basement complex are indeed hypersolvus one would expect the feldspar to be orthoclase rather than microcline. However, several authors (Goldsmith and Laves, 1954; Deer et al, 1966; Smith, 1974) consider the combined albite-pericline (grid) twinning, characteristic of microcline, as evidence that microcline originally crystallizes at higher temperatures as orthoclase. Deer et al (1966) and Smith (1974, p.384) contend that in the orthoclase/microcline transformation sodium feldspar is exsolved from the microcline and forms microperthite while some may rim the K-feldspar or yield myrmekite. These textural relationships are displayed by the basement granites studied here (see Chapter III).

Mehnert (1968, p.106) suggests that the idea that microcline has transformed from orthoclase is genetically significant "since granites and migmatites, especially those of Precambrian areas, typically contain cross-hatched (grid) twinning", and maybe indicative of a former high temperature stage. The conversion of monoclinic orthoclase into microcline is extremely complex, involving exsolution of albite and rearrangement of Al and Si (Smith, 1974,

p.382). The kinetics involved are very slow. For this reason, Mehnert (1968) and Mohr (1980, personal communication) suggest the transformation is favoured in slowly cooled rocks. Such a condition is conceivable in this basement complex, postulated as a remnant orogenic core, which may have taken up to 100 m.y. to cool (Mohr, 1980 personal communication).

However it is found experimentally, that in the presence of water, homogeneous alkali feldspars crystallized at hypersolvus temperatures readily unmix upon cooling. Thus if the unmixing hypothesis is accepted for the formation of perthites and subsolvus granites, it is petrogenetically significant that the basement granites studied here have maintained their hypersolvus nature, since their crystallization in the Precambrian. Tuttle and Bowen (1958, p. 139) explain:

If all the volatile materials are used, or escape, during crystallization, slow cooling will not produce complete unmixing. Unmixing will proceed to the cryptoperthite or perthite stage, but the hypersolvus character of the granite will be preserved.

This strongly suggests that the alkali feldspar phase in basement granites crystallized at high temperatures and low water pressures, and were then slowly cooled such that complete unmixing was prevented.

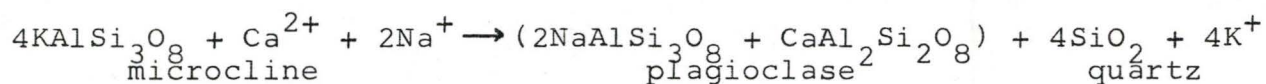
#### 7. Significance of Myrmekite in Basement Granites

In Chapter III it was noted that myrmekitic intergrowths of quartz and plagioclase are common around the embayed contacts between microcline microperthite and albite (See Figure 15).

Theories on the formation of myrmekite are numerous, and there appears to be no single origin. Most authors contend that

myrmekite grows outwards from plagioclase as it replaces K-feldspar (Smith, 1974). Many others (including Hubbard, 1967) advocate that myrmekite is developed as a result of unmixing of high temperature alkali feldspars.

The former hypothesis is discredited in this case because it is K-feldspar which has replaced plagioclase in the original gneisses. Meanwhile the second hypothesis appears most conceivable, since from the textural evidence it appears plagioclase and quartz is growing from microcline-microperthite. Nockolds (1978, p.353) suggests the following ionic exchange reaction in the formation of myrmekite from K-feldspar:



Smith (1974, p.581) concurs here, that exsolution from K-feldspar is at least a major feature for many occurrences of myrmekite.

#### 8. Significance of K-Feldspar megacrysts and Synneusis Relationships in the Younger Granite

Several petrographic features associated with the orthoclase-microperthite megacrysts strongly suggest the younger granite is of magmatic origin.

The common crystallographic orientation of subhedral plagioclase laths in the megacrysts (Figure 16) is taken as conclusive proof of magmatic origin by Vance (1969) and Hibbard (1965). They contend that these are synneusis structures formed by the joining of plagioclase and K-feldspar crystals along their broad faces, when they are suspended in a turbulent melt. The plagioclase then becomes incorporated and aligned crystallographically in the more rapidly growing K-feldspar host. Although alignment of plagioclase

and quartz is common in the megacrysts they are considered here as exceptions rather than the norm. More of the inclusions are randomly oriented (Figure 18). This may exemplify porphyroblastic growth of the alkali feldspar megacrysts during late stage deuteritic, metasomatic processes (Hibbard, 1965).

Other evidence of magmatic origin, is the occurrence of oscillatory zoning of plagioclase laths and K-feldspar megacrysts, Carlsbad twins, and the rare appearance of euhedral to subhedral quartz inclusions in the K-feldspar megacrysts. Tuttle and Bowen (1958, p.63) claim that zoning is unequivocal evidence of fractional crystallization from a melt. Euhedral quartz in K-megacrysts have been reported by Hibbard (1965, p.251) and Mehnert (1968, p.111) to suggest that idiomorphic high temp quartz crystallized previous to the host megacrysts. As well intergranular synneusis structures in alkali feldspars (Figure 18), and plagioclase of the intrusive granite support the process of drifting together, and attachment of crystals during magmatic consolidation (Vance, 1969).

In Chapter III petrographic evidence indicated that in the younger granite trace minerals of magnetite (and/or ilmenite), euhedral apatite, and euhedral pyrite all showed a marked preference for biotite "patches" as sites for accumulation (see Figure 17). Schermerhorn (1958, p.218), in his discussion on the paragenesis of accessory minerals in igneous rocks cited this common textural relationship as a "criteria for magmatic crystallization". He explains that accessory minerals crystallize early and then migrate through the magma and become successively incorporated with the early mafic constituents, such as biotite and hornblende in

granites. Once in contact the accessories tend to adhere to the growing surfaces of the mafic phases. Vance (1969, p.22) agrees with this hypothesis, and suggests this is a preferential synne-  
genesis mechanism controlling the distribution of early accessory minerals in the rock fabric.

#### 9. Deuteric Alteration and Metasomatic Relationships of the Younger Granite

From the above discussion many textural relationships indicate the younger granite crystallized from a magma. However, recall the discussion of the K-Na-Ca system (Figure 28) which indicated that processes other than simple fractional crystallization had affected the younger granite, i.e. it plotted to the K side of the magmatic field of Raju and Rao (1972) and the igneous trend line of Green and Poldervaart (1958). This high K content of the intrusive granite was further substantiated in the Qtz-Ab-Or ternary system (Figure 29), where it plotted towards the Or apex away from the minimum melt composition of the average granite.

A possible solution to this problem, and one which is well founded texturally, is that the granitoid underwent autometasomatism. Hyndman (1972, p.84) explains that during the latest stages of crystallization, magma derived hydrothermal solutions can effectively alter the rock constituents. Changes induced by deuteric solutions include: The alteration of plagioclase to sericite and/or epidote, and the chloritisation of biotite. These effects are clearly observed in the younger granite, with the alteration of plagioclase to sericite being particularly pervasive (see Chapter III and Figure 16). It is petrogenetically significant that only

the plagioclase phase is altered, all potassium feldspar contained in the groundmass or as megacrysts is completely fresh.

Metasomatism is considered to consist of two mechanisms - diffusion and infiltration (Birk, 1978), with the latter generally be most effective on a regional scale. The growth of deuteritic minerals by infiltration metasomatism is controlled by pressure and temperature gradients. Orville (1963) carried out metasomatic experiments in the system  $KAlSi_3O_8 - NaAlSi_3O_8 - NaCl - KCl - H_2O$ . He discovered that in the presence of a thermal gradient, alkali ions in a two feldspar rock migrate in response to the gradient. He concluded that at differential temperatures K will move to low temperature zones while Na moves to high temperature ones. This phenomenon he attributed to the porphyroblastic growth of K-feldspar megacrysts which are commonly found in granitic plutons. The author considers this a most viable explanation for explaining not only textural relationships of the younger granite, but also its K enrichment and Na impoverishment relative to average granites plotted in the K-Na-Ca system.

Evidence here that K-feldspar megacrysts are porphyroblastic in nature is their typically gradational contacts with groundmass constituents. In some instances a myrmekitic rim borders the megacrysts (Figure 16). Similar relationships have been studied by Phillips and Carr (1973), they suggest that myrmekite rims "may be due to an interaction between exsolution and metasomatic processes." Hyndman (1972, p.84) also contends that myrmekite is a late stage, deuteritic replacement phenomenon.

## 10. Contact Metamorphism

From the petrographic analysis of the argillaceous unit in intrusive contact with the younger granite, it is clear the unit was contact metamorphosed by the pluton (see Chapter III). All samples show a distinct hornfelsic texture. The combined silicate mineralogy of the samples is epidote, hornblende, biotite, chlorite, plagioclase, and quartz. Although the feldspar could not be positively identified as plagioclase it is assumed that the argillite is deficient in  $K_2O$  as Deer et al (1966, p.281) state that all argillaceous sediments carry predominantly non-potassic clays. This mineral assemblage is compatible with the Albite-Epidote-Amphibolite Facies given by Turner and Verhoogen (1951, p.464). This corresponds to hornblende hornfels grade of contact metamorphism, which occurs at low pressures (probably less than 2 kb) and temperatures between 500 and 650°C (Hyndman, 1972).

The fact that the argillaceous unit dips subvertically and strikes NS, parallel to the young granite pluton, is good evidence that intrusion was of a forceful nature (Pitcher, 1979). This is also indicated by the presence of angular, non-assimilated, xenoliths of argillite near the intrusive contact (Didier, 1973).

CHAPTER V  
CONCLUSIONS

Field relationships with the Nonacho Series sediments prove conclusively that two granites of different ages occur around the periphery of the Nonacho Basin. Petrographically the granitoids are distinguished on the basis of their feldspar contents. The basement granites are hypersolvus, one alkali feldspar granites, while the younger intrusive granite is a normal two feldspar, subsolvus granite. Geochemically the granitoids have similar major element contents, yet the younger granite is more homogeneous, and shows a higher calc-alkaline affinity than do the granites of the basement complex. Both granite types are enriched in potassium relative to "the average granite" but each derives this characteristic from different processes. Basement granites and migmatites have evolved from in situ anatexis (during the Kenoran Orogeny) of high grade plagioclase rich gneisses. Meanwhile the younger granite pluton was intruded (during the later phase of the Hudsonian Orogeny) into the country rocks from some depth. Late stage autometasomatism caused a depletion of Na and an enrichment of K along the margin of the pluton.

K enrichment in basement rocks is by no means restricted to the marginal basement rocks of Thekulthili Lake. Burwash and Krupicka (1969, 1970) have shown that in the broad area of the Western Canadian Shield designated as the "Athabasco Mobile Zone",

basement rocks contain "by far the highest  $K_2O$  content relative to all the present estimates for the crust, and for the Shields, as well as for the whole of the Canadian Shield and its parts."

Trace elements ratios and rare earth element concentrations suggest the two granitoids were derived from different source rocks. Younger granites appear compatible with the homogeneous late - kinematic (late tectonic) potassium rich-granites described by Marmo (1971, p.26). This chemical homogeneity is improbable in granites of anatexis origin (Pitcher, 1979, p.643). Due to its massive fabric, large size, and chemical homogeneity the young granite pluton is likely the latest stage differentiate of a magma derived from partial melting of lower crustal material. Its diapiric emplacement appears to have been controlled by deep marginal basin faults. Chemically inhomogeneous granites and migmatites of the basement complex, on the other hand, occupy a very complex geological terrain. They typify the synkinematic (syntectonic) granite description of Marmo (1971, p.26). These granites are concordant with high grade country rock gneisses and are thus postulated to represent the end result of multiple, in-situ, prograding metamorphic and anatexis events, in sedimentary supracrustal sequences.

## REFERENCES

- ABBEY, S. (1975)  
 Studies in "Standard Samples" of silicate rocks and minerals.  
 Part 4: 1974 Edition of "usable values".  
 Geological Survey Canada, Paper 74-41, 23p.
- BAADSGAARD, H. AND GODFREY, J.D. (1972)  
 "Geochronology of the Canadian Shield in Northeastern  
 Alberta, Part II: Charles-Andres-Collins Lake Area."  
 C.J.E.S., V. 9, pp.863-881
- BARTH, T.F.W. (1959)  
 Principles of classification and norm calculations of  
 metamorphic rocks;  
 J. Geol., V.67, pp. 135-152.
- BARTH, T.F.W. (1962)  
 A final proposal for calculating the mesonorm of  
 metamorphic rocks;  
 J. Geol., V.70, pp. 497-498.
- BARTH, T.F.W. (1969)  
 Feldspars;  
 John Wiley and Sons Inc., London, 261p.
- BIRK, W.D. (1978)  
 The nature and timing of granitoid plutonism in the  
 Wabigoon Volcanic Plutonic Belt, Northwestern Ontario  
 Geochemistry, Rb/Sr Geochronology, Petrography and  
 Field Investigation;  
 Dept. of Geology, McMaster Univ., PhD. thesis.
- BOUSEILY, E.A.M. AND SOKKARY, E.A.A. (1975)  
 The relationship between Rb, Ba and Sr in granitic rocks;  
 Chem. Geol., V.16, pp.207-219.
- BOWDEN, P. (1966)  
 Zirconium in younger granites of northern Nigeria;  
 Geochim. Cosmochim. Acta, V. 30, pp. 985-993.
- BURWASH, R.A. AND BAADSGAARD, H. (1962)  
 Yellowknife-Nonacho Age and Structural Relations in  
 The Tectonics of the Canadian Shield (J.S. Stevenson, Ed.)  
 Roy. Soc. Can. Spec. Public. 4, U. of Toronto Press,  
 Toronto, pp. 22-29.
- BURWASH, R.A. (1969)  
 Comparative Precambrian geochronology of the North American,  
 European and Siberian Shields;  
 Can. J. Earth Sci., V.6 pp. 357-365.
- BURWASH, R.A. AND KRUPICKA, J. (1969)  
 Cratonic Reactivation in the Precambrian Basement of  
 Western Can., Part I: Deformation and Chemistry.  
 C.J.E.S., V. 6(6), pp. 1381-1396.
- BURWASH, R.A. AND KRUPICKA, J. (1970)  
 Cratonic Reactivation in the Precambrian Basement of  
 Western Can., Part II: Metasomatism and isostasy.  
 C.J.E.S., V. 7, pp. 1275-1294.
- CARMICHAEL, I.S.E., TURNER, F.J. AND VERHOOGEN, J. (1974)  
 Igneous Petrology;  
 McGraw-Hill, Toronto, 739 p.

- CHRISTIE, A.M. (1953)  
Goldfields-Martin Lake Map Area, Sask.  
G.S.C. Mem. 269.
- DALY, R.A. (1933)  
Igneous rocks and the depths of the earth.  
McGraw-Hill, Inc., New York.
- DEER, W.A., HOWIE, R.A. AND ZUSSMAN, J. (1966)  
An introduction to the rock-forming minerals;  
Longman Group Ltd., London, 528p.
- DIDIER, J. (1973)  
Granites and Their Enclaves;  
Elsevier, New York, 393p.
- DONAGHY, T.J. (1977)  
The petrology of the Thekulthili Lake Area, N.W.T.;  
University of Alberta, MSc. Thesis (Geology).
- GOLDSMITH, J.R. AND LAVES, F. (1954a)  
The microcline-samidine stability reactions;  
Geochim. Cosmochim. Acta., V. 5, pp. 1-19.
- GREEN, J. AND POLDERVAART, A. (1958)  
Petrochemical fields and trends;  
Geochim. Cosmochim. Acta, V.13, pp. 87-122.
- HANSON, G.N. (1978)  
The application of trace elements to the petrogenesis of  
igneous rocks of granitic composition.  
Earth and Planetary Sci. Letters, V. 38, pp. 26-43.
- HENDERSON, J.F., (1937)  
Nonacho Lake Area, N.W.T.  
G.S.C. Prelim. Rept. 37-2, Dept. Mines and Resources.
- HENDERSON, J.F. (1939)  
Taltson Lake, District of Mackenzie  
G.S.C. Map 525A.
- HIBBARD, M.J. (1965)  
Origin of some alkali feldspar phenocrysts and their  
bearing on petrogenesis;  
Amer. J. Sci., V. 263, pp. 245-261.
- HIGGINS, (1971)  
Classification of cataclastic rocks;  
U.S.G.S. Prof. Paper, No. 687.
- HOFFMAN, P., DEWEY, J.F. AND BURKE, K. (1974)  
Aulacogens and their genetic relation to geocynclines,  
with a Proterozoic example from Great Slave Lake, Canada;  
S.E.P.M. Spec. Public 19, pp. 38-55.
- HUTCHISON, C.S. AND JEACOCKE, J.E. (1971)  
Fortran IV computer programme for calculation of the  
Niggli Molecular Norm;  
Geol. Soc. Malaysia, Bull. 4, pp. 91-95.
- HYNDMAN, D.W. (1972)  
Petrology of Igneous and Metamorphic Rocks;  
McGraw-Hill Book Company, 533 p.
- KERR, P.F. (1977)  
Optical mineralogy;  
McGraw-Hill, Inc., New York, 492p.

- KLEEMAN, A.W. (1965)  
Origin of Granitic Magmas.  
J. Geol. Soc. Aust., 12, pp. 35-52.
- KRAUSKOPF, K.B. (1979)  
Introduction to Geochemistry;  
McGraw-Hill, Inc., New York, 617 p.
- KRUPICKA, J. AND SASSANO, G.P., (1972)  
Multiple deformation of crystalline rocks in the  
Tazin Group, Eldorado Fay Mine, NW. Sask.  
C.J.E.S., V. 1, pp. 422-432.
- MARMO, V. (1971)  
Granite Petrology and the Granite Problem;  
Elsevier, Amsterdam, 244 p.
- MASON, B. (1952)  
Principles of geochemistry;  
John Wiley & Sons Inc., 310p.
- MCCARTHY, T.S. AND HASTY, R.A. (1976)  
Trace element distribution patterns and their relationship  
to the crystallization of granitic melts;  
Geochim. Cosmochim. Acta, V. 40, pp. 1351-1358.
- McGLYNN, J.F. (1966)  
Thekulthili Lake Area;  
GSC Paper 66-1A, pp. 32-33.
- McGLYNN, J.C. (1970)  
Study of the Nonacho Gp. of Sedimentary Rocks, Nonacho Lake,  
Taltson and Reliance Areas, District of MacKenzie;  
G.S.C. Paper 70-1A, (Parts of E,F,K.) pp. 154-155.
- McGLYNN, J.C. (1970)  
Churchill Province;  
In: R.J.W. Douglas, ed., Geology and Economic Minerals  
of Canada;  
Geol. Survey Canada, Econ. Geol. Report No. 1, 838 p.
- McGLYNN, J.C. (1971)  
Stratigraphy, Sedimentology and Correlation of the  
Nonacho Gp., District of Mackenzie.  
G.S.C. Paper 71-1A, pp. 140-142.
- McGLYNN, J.C., HANSON, G.N. AND IRVING, E. AND PARK, J.K. (1974)  
Paleomagnetism and Age of Nonacho Group sandstones and  
associated Sparrow dikes, District of Mackenzie;  
Can. J. Earth Sci., V. 11, pp. 30-42.
- McGLYNN, J.C. (1978)  
Geologic Map of Nonacho Basin;  
GSC open file 543.
- MEHNERT, K.R. (1968)  
Migmatites;  
Elsevier Publishing Company, Amsterdam, 393p.
- MOHR, D. (1980)  
Dept. of Geology, McMaster Univ., Professor.
- MULLIGAN, R. AND TAYLOR, F.C. (1969)  
Hill Island Lake, District of Mackenzie;  
GSC Map 1203A.

- NAGASAWA, H. AND SCHNETZLER, C. (1971)  
Partitioning of rare earth, alkali and alkaline earth elements between phenocrysts and acidic igneous magma; *Geochim. Cosmochim. Acta*, V. 35, pp. 953-968.
- NOCHOLDS, S.E. (1954)  
Average chemical compositions of some igneous rocks; *Geol. Soc. Amer., Bull.* V. 65, pp. 1007-1032.
- NOCKOLDS, S.R. AND ALLEN, R. (1953)  
The geochemistry of some igneous rock series; *Geochim. Cosmochim. Acta*, V. 4 pp. 105-142.
- NOCKOLDS, S.R., KNOX, R.W. O'B. AND CHIMMER, G.A. (1978)  
*Petrology for students*;  
Cambridge University Press, London, 435p.
- ORVILLE, P.M. (1963)  
Alkali ion exchange between vapor and feldspar phases; *Amer. J. Sci.*, V. 261, pp. 201-237.
- PARSLOW, G.R. (1969)  
Mesonorms of granitic rock analyses; *Min. Mag.*, V. 37, No. 286, pp. 262-269.
- PHILLIPS, E.R. AND CARR, G.R. (1973)  
Myrmekite associated with alkali feldspar megacrysts in felsic rocks from New South Wales; *Lithos*, V. 6, pp. 245-260.
- PITCHER, W.S. (1979)  
The nature, ascent and emplacement of granitic magmas. *Jour. Geol. Soc. Lon.*, V. 136, pp. 627-662.
- RAJU, D.R. AND RAO, J.R.K. (1972)  
Chemical distinction between replacement and magmatic granitic rocks; *Contr. Min. Petrol.*, V. 35, pp. 169-172.
- SCHERMERHORN, L.J.G. (1958)b  
The paragenesis of accessory minerals in igneous rocks; *Econ. Geol.*, V. 53, pp. 215-218.
- SHAW, D.M. (1968)  
A review of K-Rb fractionation trends by covariance analysis; *Geochim. Cosmochim. Acta*, V. 32, pp. 573-601.
- SIMPSON, E.S.W. (1954)  
On the graphical representation of differentiation trends in igneous rocks; *Geol. Mag.*, V. 91, pp. 238-244.
- SMITH, J.V. (1974)  
*Feldspar minerals, part two: chemical and textural properties*;  
Springer-Verlag, Berlin, 690p.
- STOCKWELL, C.H. (1972)  
Revised Precambrian time scale for the Canadian Shield; *Geol. Survey Canada, paper 72-52*, 4 p.
- STRECKEISON, A.L. (1973)  
Plutonic rock, classification and nomenclature recommended by the I.U.G.S. subcommission on the systematics of igneous rock. *Geotimes*, October, pp. 26-30.

- TUTTLE, O.F. AND BOWEN, N.L. (1958)  
Origin of granite in the light of experimental studies  
in the system  $\text{NaAlSi}_3\text{O}_8$ - $\text{KAlSi}_3\text{O}_8$ - $\text{SiO}_2$ - $\text{H}_2\text{O}$ .  
Geol. Soc. Am., Memoir 74, 153p.
- TURNER, F.J. AND VERHOOGEN, J. (1951)  
Igneous and metamorphic petrology;  
McGraw-Hill book Company, Inc.
- VANCE, J.A. (1969)  
On synneusis;  
Contr. Min. Petrol., V.24, pp. 7-29.
- WANLESS, R.K., STEVENS, R.D., LACHANCE, G.R. AND  
RIMSAITE, R.Y.H., (1967)  
Age Determinations and Geologic Studies;  
G.S.C. Paper 67-2
- WASHINGTON, H.S. (1917)  
Chemical analyses of igneous rocks;  
U.S.G.S. Prof. Paper 99, 1201p.
- WILLIAMS, H., TURNER, F.J. AND GILBERT, C.M. (1954)  
Petrography: an introduction to the study of rocks in thin  
section;  
Freeman and Company, Inc., San Francisco, 406p.
- WILSON, J.T. (1941)  
Fort Smith, District of Mackenzie.  
G.S.C. Map 607A.
- WINKLER, H.G.F. (1976)  
Petrogenesis of metamorphic rocks; 4 ed.,  
Springer-Verlag, New York, 334p.
- WRIGHT, J.B. (1969)  
A simple alkalinity ratio and its application to  
questions of non-orogenic granite genesis;  
Geol. Mag., V. 106, pp. 370-384.

## APPENDIX A

Petrographic descriptions of ten Nonacho Gp. sediments sampled from Profile "A" (Figure B) and Profile "B" (Figure 9).

Unit descriptions are outlined in Chapter II and are given on the regional geology map in Figure 7.

#### Profile "A" Samples

##### A-2 (Unit Ps)

An extremely deformed rock with a micro to cryptocrystalline grain size. Although the sections shows signs of intense granulation, the texture shows no preferred orientation. Polycrystalline aggregates (porphyroclasts) of quartz and feldspar are set in massive quartzofeldspathic matrix. The proportion of matrix in the mode is 50-70%, and thus the rock is classed as a cataclastic "B", according to the Higgins (1971) classification for cataclastic rocks used in this study. The absence of fluxion and foliated structures indicate the rock has not reached a mylonitic state of dynamic metamorphism.

Trace amounts of epidote and hematite are disseminated throughout the section.

##### A-3 (Unit Ps)

This sample was taken from a mafic band found on a small island which predominantly consisted of metag quartzite. The rock has a very fine grain size and a schistose texture. The mafic phases chlorite and epidote compose 60-70% of the mode with the remainder consisting of xenoblastic quartz and plagioclase. The mafic minerals define the schistosity, forming stringers which braid across the slide around zones of quartzofeldspathic material. This mineral assemblage and texture is compatible with greenschist facies metamorphism (Williams et al, 1954).

A-4 (Unit Ps)

This rock displays a marked deformation texture. Chlorite and epidote (together = 15-20%) are segregated into discontinuous bands which weave about porphyroclasts of quartzofeldspathic material. Then porphyroclasts reach several millimeters in size, commonly show flaser structures, and are invariably polycrystalline. Slab staining indicates porphyroclasts consist predominantly of K-feldspar, which is marked petrographically by its extensive alteration to clays and/or sericite. Rarely grains of plagioclase occur which have lost their distinctive lath shape and/or have bent twin lamellae. Quartzofeldspathic material makes up 70-80% of the mode. Substantial amounts of muscovite occur (3-5%), as well as some trace apatite (less than 1%).

A-5 (Unit C)

This is a poorly sorted sandstone with a clastic texture consisting of subrounded to rounded particles (0.1-0.5 mm size) set in a fine grained (0.01-0.1 mm) matrix of felsic and micaceous material. The rock contains little or no cement. Particle sized material is predominantly feldspar (40-45%) and quartz (35-40%), with some epidote and an opaque mineral (magnetite or ilmenite) occurring in minor amounts. There are no rock particles contained in the slide.

All quartz particles are strained and many are polycrystalline indicating possibly a metamorphic source rock. However the section itself is essentially undeformed.

By Williams et al (1954, p.292) classification for impure sandstones, this rock is classed as an Arkosic Wacke; owing to its: 1) poor sorting, 2) matrix content of great than 10% argillaceous sized

material, and 3) feldspar particle content of more than 25%.

#### A-6 (Unit C)

Mineralogically this section is much the same as A-5, but it contains some rock particles and some calcite cement. Texturally however A-6 shows evidence of deformation and it also contains some pebble sized particles. In hand specimen the rock is best described as a polymictic, pebble conglomerate. In thin section the larger particles are usually identified as polycrystalline quartz. Other pebbles which are fractured and have pseud-fluxion structures associated with them are better termed porphyroclasts.

It is the matrix between pebble clasts which resembles the A-5 sandstone, but the former shows deformation effects and a higher particle density.

#### A-7 (Unit Ps)

Petrographic analysis indicates this section has been dynamically metamorphosed. The texture is strongly cataclastic, consisting of a massive, very fine grained felsic matrix surrounding porphyroclasts of quartz and feldspar. The distinction between porphyroclasts and matrix can only be made under crossed polarized light, which shows that the two are both polycrystalline, yet the former is less so.

Chlorite, hematite, and epidote occur in trace amounts, together they compose less than 1% of the mode.

The 50-70% content of the matrix classifies this rock as a cataclasite "B" according to Higgins (1971) scheme.

#### Profile "B" Samples

##### B-1 (Unit C)

This section looks similar to A-5 in most respects. It has a clastic texture consisting of subrounded to rounded sand sized (0.1-0.5mm) particles of quartz (65-70%) and feldspar (30-35%) in a fine grained (0.05-0.1mm) quartzofeldspathic and micaceous (sericite, clays) matrix. The particle density and clay content is greater in this section than in A-5. Furthermore, unlike A-5, the quartz particles are all monocrystalline and the majority show uniform extinction.

A foliation is defined in the argillaceous matrix by the subparallel alignment of micas and clays.

The mode contains trace amounts of granular chlorite, hematite, and epidote. Some (less than 1%) authigenic calcite cement is present as well.

Like A-5 this sandstone is classified as an Arkosic Wacke.

#### B-2a (Unit E)

This sample was collected from a sandy layer of Unit E which is composed of polymictic conglomerate and interbedded sandstones.

The section displays a well sorted clastic texture consisting of subrounded to rounded felsic particles (0.5-1.0mm in size) set in a fine grained micaceous matrix. Particle grains are almost exclusively quartz (80-90%) with feldspar and lithic fragments forming the remainder. This quartz generally is unstrained, but some polycrystalline quartz does occur. Particles of feldspar generally have diffuse, gradational contacts with the sericitic and clay matrix. As in B-1 the constituents of the micaceous matrix displays a preferred orientation.

Chlorite and epidote granules occur in trace amounts. Min-

ute veins and vugs of authigenic calcite and euhedral quartz are common cementing features.

This sandstone is classified as something between a Quartz Wacke and a Feldspathic Wacke (see Williams et al, 1954, p.292).

#### B-2b(Unit E)

This sample was taken from a polymictic conglomerate interbed. Megascopically the thin section consists of two large pebble clasts and numerous smaller ones. Microscopically, one of the large pebbles consists of quartz and feldspar displaying a granitic (hypidiomorphic) texture, while the other is essentially polycrystalline quartz. Sample B-2a resembles the matrix of the section, but here there is more lithic fragments and a more abundant micaceous matrix. Authigenic calcite and quartz cement is common.

Substantial amounts of chlorite (and to a lesser extent epidote) occur in the matrix, and is particularly prevalent around pebble clast perimeters.

Undulose extinction in quartz is ubiquitous in this section.

#### B-3 (Unit C)

This section is essentially identical to B-1. However particles are more angular, and much more abundant than in the latter. Particle density is such that point contacts between particles are common. In thin section the absence of twinning indicates there is little or no feldspar. However a stained slab study discovered a 30 to 40% alkali feldspar content, the remaining 60-70% of particles are quartz.

Unlike many of the other sandstones studied here B-3 lacks

any preferred orientation, due to its high particle density in conjunction with a reduced micaceous matrix content.

This sandstone is classified as an Arkosic Wacke.

APPENDIX B  
MESONORM TABLES

NORMATIVE MINERAL	ABBREVIATION
Quartz	Qtz
Orthoclase	Or
Albite	Ab
Anorthite	An
Corundum	Cor
Biotite	Bi
Wollastonite	Wo
Magnetite	Mt
Titanite	Tn
Apatite	Ap

D.I. = Mesonorm Differentiation Index

Only the normative minerals listed above were calculated to be in these rocks.

TABLE III

## MESONORMS

SAMPLE	Qtz	Or	Ab	An	Cor	Bi	Wo	Mt	Tn	Ap	D.I.	Biotite % Mg/Fe Ratio
BASEMENT GRANITES												
KULT-13	29.79	24.07	37.61	2.54	0.98	3.90	--	0.78	0.33	--	91.5	77/23
AO-2	32.75	24.82	36.52	2.12	1.02	2.06	--	0.40	0.32	--	94.1	76/24
BO-1	29.06	53.43	10.90	4.51	0.50	1.14	--	0.25	0.21	--	93.4	72/28
BO-2	32.26	48.15	15.52	2.72	0.33	0.82	--	0.13	0.06	--	95.9	77/23
BO-3	35.37	32.64	26.13	0.89	1.36	2.31	--	1.03	0.27	--	94.1	50/50
CO-1	31.39	40.65	20.19	2.20	0.67	4.13	--	0.54	0.23	--	92.2	85/15
CO-2	34.49	36.82	22.45	3.10	0.36	2.40	--	0.31	0.08	--	93.8	83/17
CO-4	35.34	27.01	29.08	2.79	1.46	3.22	--	0.74	0.33	0.02	91.4	72/28
DO-1	33.10	31.33	25.54	4.74	1.40	3.07	--	0.62	0.21	--	90.0	75/25
DO-2	31.34	32.76	26.65	3.37	1.27	3.70	--	0.68	0.23	--	90.7	78/22
EO-1	28.13	36.17	28.51	1.94	0.86	3.49	--	0.51	0.27	0.13	92.8	82/18
YOUNGER GRANITE												
YG-3	30.85	32.75	27.37	3.30	0.55	3.90	--	0.79	0.48	0.02	91.0	76/24
YG-4	30.77	35.15	26.37	1.87	0.86	3.14	--	1.03	0.66	0.15	92.3	62/38
YG-5	35.05	20.39	28.95	3.35	1.42	6.66	--	2.04	1.62	0.51	84.4	65/35
YG-6	27.86	40.41	23.15	1.65	2.69	2.56	--	0.83	0.65	0.21	91.4	62/38
YG-7	31.72	33.82	25.02	3.61	0.95	3.20	--	0.85	0.68	0.15	90.6	69/31
YG-8	28.54	34.04	29.12	0.76	1.72	3.70	--	1.06	0.82	0.23	91.7	67/33
GRANITE DYKES (APLITES)												
YD-1	26.72	48.66	21.25	0.52	--	1.30	1.09	0.28	0.17	--	96.6	74/26
Al-b	31.71	23.22	31.65	6.59	1.51	4.45	--	0.46	0.40	0.02	86.6	87/13

APPENDIX C  
GEOCHEMICAL WHOLE ROCK DATA

## Accuracy of XRF Determinations

1. Major Oxides (Fusion Method)

The accuracy of XRF determinations was checked by running standards as unknowns and comparing them to recommended literature values (Abbey, 1975). The four international standards used in this analysis were: NIM-S, SY-3, NIM-G, and G-1.

The following results were obtained from running the standards NIM-S and SY-3 as unknowns.

OXIDES	STANDARD, WT. %			
	NIM-S (recommended)	NIM-S (unknown)	SY-3 (recommended)	SY-3 (unknown)
SiO <sub>2</sub>	63.65	64.53	59.68	59.94
Al <sub>2</sub> O <sub>3</sub>	17.35	17.72	11.80	11.12
Fe <sub>2</sub> O <sub>3</sub>	1.40	1.23	6.44	6.22
MgO	0.46	0.51	2.64	2.50
CaO	0.66	0.67	8.26	8.22
Na <sub>2</sub> O	0.42	0.51	4.15	3.93
K <sub>2</sub> O	15.38	15.50	4.24	4.16
TiO <sub>2</sub>	0.04	0.05	0.15	0.15
MnO	0.01	0.01	0.38	0.32
P <sub>2</sub> O <sub>5</sub>	0.12	0.11	0.54	0.56

This data indicates the errors involved using the XRF fusion method are negligible in this study.

2. Trace Elements (Powder Method)

The principle of running standards as unknowns was employed to check the accuracy the trace element analyses. Again they were compared to literature values listed by Abbey(1975).

a) For the trace elements Rb, Sr, Y, Zr, and Nb, the standards NIM-G, GSP-1, NIM-S, SY-1, BCR-1, W-1, NIM-L, JG-1, QLO-1, AGV-1, STM-1, SDC-1, MAG-1, G-2, and BHVO-1 were run as unknowns. The results for two of these are below.

ELEMENTS	STANDARDS, PPM			
	GSP-1 (recommended)	GSP-1 (unknown)	BCR-1 (recommended)	BCR-1 (unknown)
Rb	250	252	47	49
Sr	230	231	330	333
Y	32	28	46	39
Zr	500	517	not given	196
Nb	29	30	14	12

Errors are negligible.

b) For the trace elements Cr, Co, Pb, Cu, Zn, and As the standards GSP-1, W-1, BCR-1, AGV-1, NIM-G, NIM-L, JB-1, JG-1, NIM-D, SY-1, SY-2, and SY-3 were ran as unknowns. The following results were obtained for standards JB-1 and NIM-D.

ELEMENTS	STANDARDS, PPM			
	JB-1 (recommended)	JB-1 (unknown)	NIM-D (recommended)	NIM-D (unknown)
Cr	400	402	2900	2900
Co	39	35	210	210
Pb	12	17	2	10
Cu	56	41	10	20
Zn	84	84	91	93
As	1	0	1	0

A high degree of accuracy resulted from these standards. Greater errors resulted from most of the other standards, as their base metal contents were near the level of XRF detection.

c) For the trace elements Ce, Nd, V, La, and Ba the following standards were run as unknowns: NIM-D, W-1, BCR-1, AGV-1, GSP-1, NIM-S, and G-2. The standards AGV-1 and GSP-1 gave the following results for Ba and Ce.

ELEMENTS	STANDARDS, PPM			
	AGV-1 (recommended)	AGV-1 (unknown)	GSP-1 (recommended)	GSP-1 (unknown)
Ba	1200	1154	1300	1398
Ce	63	63	390	382

Error is not significant.

d) With the trace elements Ni and S the standards NIM-P, BR, NIM-N, W-1, SY-1, BCR-1, NIM-D, MRG-1, BHVO-1, and QLO-1 were used as unknowns. Of these BR and NIM-N yielded the following results for Ni.

ELEMENT	STANDARDS, PPM			
	BR (recommended)	BR (unknown)	NIM-N (recommended)	NIM-N (unknown)
Ni	270	284	120	96

Similar results were obtained with the other standards. Error here suggests these results may be only semi-quantitative.

e) U and Th were analysed with the standards STM-1, SDC-1, MAG-1, BHVO-1, SY-3, SY-2, NIM-L, GSP-1, NIM-G, JG-1, G-2, and W-1 used as unknowns. Standards STM-1 and G-2 gave the below results.

ELEMENTS	STANDARDS, PPM			
	STM-1 (recommended)	STM-1 (unknown)	G-2 (recommended)	G-2 (unknown)
U	9	20	11	8
Th	26	9	24	2

The errors involved here are extreme. These results should not be considered as strictly quantitative. Three pellets of an homogeneous aplite (sample YD-1) were run in this XRF analysis with the following results.

PELLET	U	Th
YD-1(A)	28	66
YD-1(B)	14	29
YD-1(C)	9	46

This variability substantiates the inaccuracy of these results. In conclusion, U and Th concentrations are at or below the level of detection, of this XRF technique, i.e. concentrations are reasonably assumed to be less than 15 ppm.

## BIOTITE ALKALI-FELDSPAR GRANITE/SYENOGRANITE (BASEMENT GRANITE)

SAMPLE	SiO <sub>2</sub>	Al <sub>2</sub> O <sub>3</sub>	Fe <sub>2</sub> O <sub>3</sub> <sup>1</sup>	MgO	CaO	Na <sub>2</sub> O	K <sub>2</sub> O	TiO <sub>2</sub>	MnO	P <sub>2</sub> O <sub>5</sub>	L.O.I. <sup>2</sup>
KULT-13	73.88	13.9	1.47	0.80	0.61	4.13	4.43	0.15	0.03	n.d.	1.11
AO-2	75.77	12.98	0.76	0.41	0.53	4.00	4.35	0.15	0.03	n.d.	1.01
BO-1	73.44	13.63	0.47	0.22	0.95	1.18	8.91	0.10	0.02	n.d.	1.09
BO-2	75.64	12.72	0.25	0.16	0.55	1.69	8.03	0.03	0.02	n.d.	0.91
BO-3	75.75	12.29	1.93	0.30	0.26	2.84	5.63	0.13	0.02	n.d.	0.84
CO-1	74.50	12.78	1.00	0.93	0.51	2.20	7.17	0.11	0.02	n.d.	0.76
CO-2	76.03	12.29	0.58	0.52	0.63	2.44	6.33	0.04	0.03	n.d.	1.11
CO-4	75.84	12.79	1.40	0.62	0.68	3.18	4.84	0.16	0.05	0.01	0.44
DO-1	74.56	13.54	1.16	0.61	1.01	2.79	5.53	0.10	0.05	n.d.	0.65
<sup>3</sup> DO-2	74.13	13.50	1.29	0.53	0.75	2.85	5.78	0.12	0.04	n.d.	1.02
EO-1	73.71	13.58	0.96	0.78	0.55	3.14	6.41	0.13	0.02	0.06	0.66
AVERAGE	74.8	13.1	1.0	0.5	0.6	2.8	6.1	0.1	0.03	0.0	0.9

## BIOTITE LEUCOCRATIC MONZOGANITE (INTRUSIVE PLUTON GRANITE)

SAMPLE	SiO <sub>2</sub>	Al <sub>2</sub> O <sub>3</sub>	Fe <sub>2</sub> O <sub>3</sub>	MgO	CaO	Na <sub>2</sub> O	K <sub>2</sub> O	TiO <sub>2</sub>	MnO	P <sub>2</sub> O <sub>5</sub>	L.O.I.
YG-3	73.99	12.92	1.48	0.79	0.83	2.99	5.84	0.22	0.03	0.01	0.90
YG-4	73.50	12.78	1.93	0.52	0.68	2.87	6.12	0.31	0.03	0.07	1.20
YG-5	71.93	11.91	3.76	1.14	1.49	3.11	4.01	0.75	0.05	0.23	1.61
YG-6	71.81	14.72	1.55	0.43	0.67	2.53	6.97	0.31	0.03	0.09	0.89
<sup>3</sup> YG-7	73.69	13.03	1.60	0.52	0.99	2.88	5.84	0.32	0.04	0.07	1.03
YG-8	72.48	13.59	1.98	0.66	0.56	3.19	6.04	0.39	0.03	0.11	0.97
AVERAGE	72.9	13.2	2.0	0.7	0.9	2.1	5.8	0.4	0.04	0.10	1.1

## GRANITE DYKES (APLITES)

YD-1	74.23	12.92	0.52	0.25	0.70	2.33	8.23	0.07	0.02	n.d.	0.72
Al-b	73.58	14.16	0.87	1.04	1.46	3.47	4.35	0.19	0.03	0.01	0.83

<sup>1</sup> Total Fe expressed as Fe<sub>2</sub>O<sub>3</sub><sup>2</sup> Loss on Ignition

n.d. Not detected

<sup>3</sup> Mean of 3 fusion discs

TABLE V

## TRACE ELEMENT ANALYSES (P.P.M.)

## BASEMENT GRANITES

SAMPLE	Rb	Sr	Y	Zr	Nb	U	Th
Kult-13	126	489	21	137	21	12	6
AO-2	180 <sup>2</sup>	136 <sup>2</sup>	24	100	31	2 <sup>2</sup>	20 <sup>2</sup>
BO-1	198	438	18	36	22	3	n.d.
BO-2	274 <sup>2</sup>	75 <sup>2</sup>	23	36	31	1 <sup>2</sup>	n.d. <sup>2</sup>
BO-3	232 <sup>2</sup>	72 <sup>2</sup>	29	134	32	3 <sup>2</sup>	32 <sup>2</sup>
CO-1	233 <sup>2</sup>	243 <sup>2</sup>	23	80	24	10 <sup>2</sup>	101 <sup>2</sup>
CO-2	176	162	23	93	20	--	--
CO-4	197	82	25	146	31	n.d.	6
DO-1	247	166	29	101	31	6	29
DO-2	223	190	28	104	26	n.d.	n.d.
EO-1	252 <sup>3</sup>	148 <sup>3</sup>	28 <sup>2</sup>	94 <sup>2</sup>	28 <sup>2</sup>	n.d. <sup>3</sup>	3.4 <sup>3</sup>

## YOUNGER GRANITE

SAMPLE	Rb	Sr	Y	Zr	Nb	U	Th
YG-3	409	126	28	206	40	1	144
YG-4	392	127	29	231	41	n.d. <sup>2</sup>	92 <sup>2</sup>
YG-5	247	195	40	378	49	n.d.	65
YG-6	428	167	31	211	40	15	102
YG-7	392	117	31	235	40	15	99
YG-8	326	198	30	248	37	1	84

## APLITES

<sup>3</sup> YD-1	569	109	39	76	65	17	47
Al-b	319	212	23	155	33	n.d.	30

<sup>2</sup> Average of 2 powder pellets      <sup>3</sup> Average of 3 powder pellets

TABLE VI  
TRACE ELEMENT ANALYSES (P.P.M.)  
BASEMENT GRANITES

SAMPLE	As	V	Cr	Co	Ni	Cu	Zn	S
Kult-13	7	19	6	45	1	n.d.	26	39
AO-2	12	34	2	49	7	n.d.	20	n.d.
BO-1	14	20	6	65	5	n.d.	18	n.d.
BO-2	25	18	5	63	10	n.d.	16	n.d.
BO-3	14	38	7	104	13	n.d.	18	122
CO-1	5	37	1	43	8	n.d.	20	72
CO-2	7	24	7	56	4	n.d.	14	n.d.
CO-4	9	22	8	66	6	n.d.	31	n.d.
DO-1	n.d.	35	8	45	12	n.d.	28	n.d.
DO-2	10	40	3	50	10	n.d.	36	n.d.
<sup>2</sup> EO-1	5	28	7	56	10	n.d.	26	n.d.

## YOUNGER GRANITE

SAMPLE	As	V	Cr	Co	Ni	Cu	Zn	S
YG-3	2	21	8	29	19	n.d.	30	5
YG-4	5	29	11	51	19	20	34	67
YG-5	1	64	12	50	15	n.d.	76	70
YG-6	n.d.	31	5	17	18	n.d.	33	n.d.
YG-7	n.d.	27	7	34	17	n.d.	38	25
YG-8	n.d.	34	9	36	15	n.d.	43	77

## APLITES

<sup>3</sup> YD-1	6	8	9	45	30	n.d.	16	n.d.
Al-b	24	19	3	33	15	n.d.	21	n.d.

<sup>2</sup> Average of 2 powder pellets

<sup>3</sup> Average of 3 powder pellets

TABLE VII  
TRACE ELEMENT ANALYSES (P.P.M.)  
BASEMENT GRANITES

SAMPLE	Ba	Pb	La	Ce	Nd
Kult-13	3273	13	66	38	19
AO-2	646	23	108	90	34
BO-1	2614	54	57	30	20
BO-2	230	30	62	23	18
BO-3	324	16	90	94	38
CO-1	803	39	106	98	37
CO-2	993	25	60	52	24
CO-4	259	18	69	49	22
DO-1	380	27	90	--	35
DO-2	477	25	101	87	40
<sup>2</sup> EO-1	761	25	84	66	28

## YOUNGER GRANITE

SAMPLE	Ba	Pb	La	Ce	Nd
YG-3	564	59	167	189	55
YG-4	865	60	212	238	69
YG-5	1035	32	345	451	130
YG-6	1226	46	161	181	57
YG-7	858	49	181	216	66
YG-8	1143	39	198	236	75

## APLITES

<sup>3</sup> YD-1	221	59	84	66	26
Al-b	795	30	88	78	28

<sup>2</sup> Average of 2 pellets

<sup>3</sup> Average of 3 pellets

TABLE VIII

## ELEMENT RATIOS BASED ON P.P.M.

## BASEMENT GRANITES

SAMPLE	K/Na	K/Rb	K/Ba	Ba/Rb	Sr/Ba	Ca/Ba	Ca/Sr	Rb/Sr	Ti/Zr
Kult-13	1.2	283	11	25.9	0.15	1.3	9.0	0.26	6.6
AO-2	1.2	200	56	3.6	0.21	5.9	27.1	1.32	9.0
BO-1	8.4	370	28	13.2	0.17	2.6	15.5	0.45	16.7
BO-2	5.4	248	290	0.8	0.33	17.1	48.8	3.66	5.0
BO-3	2.2	203	144	1.4	0.22	5.7	27.1	3.24	5.8
CO-1	3.7	259	74	3.4	0.30	4.5	15.0	0.96	8.2
CO-2	2.9	292	53	5.6	0.16	4.5	28.1	1.09	2.6
CO-4	1.7	201	155	1.3	0.32	18.8	60.8	2.39	6.6
DO-1	2.2	184	121	1.5	0.44	19.0	42.5	1.49	5.9
DO-2	2.3	218	101	2.1	0.40	11.2	28.2	1.17	6.9
EO-1	2.3	213	70	3.0	0.20	5.2	26.0	1.70	8.3

## YOUNGER GRANITES

SAMPLE	K/Na	K/Rb	K/Ba	Ba/Rb	Sr/Ba	Ca/Ba	Ca/Sr	Rb/Sr	Ti/Zr
YG-3	2.2	118	86	1.4	0.22	10.5	45.4	3.24	6.4
YG-4	2.4	130	59	2.2	0.15	5.6	37.4	3.10	8.0
YG-5	1.4	133	32	4.2	0.19	10.3	53.0	1.27	11.9
YG-6	3.1	135	47	2.9	0.14	3.9	28.2	2.57	8.8
YG-7	2.2	124	56	2.2	0.14	8.2	59.2	3.36	8.2
YG-8	2.1	152	44	3.5	0.17	3.5	20.0	1.65	9.4

## APLITES

YD-1	3.9	120	309	0.4	0.49	22.6	45.4	5.24	5.5
Al-b	1.4	113	45	2.5	0.27	13.1	49.5	1.50	7.4